UNIWERSYTET RZESZOWSKI

AUTOREFERAT PRACY DOKTORSKIEJ

mgr inż. Monika Pichla

Ocena potencjalnych substancji terapeutycznych na modelu komórkowym w chorobach wieku podeszłego

Promotor: **prof. dr hab. Izabela Sadowska-Bartosz**

Dziedzina: nauk ścisłych i przyrodniczych

Dyscyplina naukowa: nauki biologiczne

RZESZÓW 2021

SPIS TREŚCI

INFORMACJE WPROWADZAJĄCE

Źródła finansowania:

Badania wykonano we współpracy z:

– Katedrą Biofizyki Molekularnej Uniwersytetu Łódzkiego

– Pracownią Regulacji Transkrypcyjnej Instytutu Biologii Medycznej PAN

– Centrum Dydaktyczno-Naukowym Mikroelektroniki i Nanotechnologii Uniwersytetu Rzeszowskiego

STRESZCZENIE

Na rozprawę doktorską składa się cykl czterech prac opublikowanych w czasopismach *Oxidative Medicine and Cellular Longevity, Molecules* oraz *Analytical Biochemistry,* w których skupiono się na (i) analizie współczesnych trendów dotyczących zastosowania nanocząstek w terapii chorób neurodegeneracyjnych, (ii) ocenie neuroprotekcyjnych właściwości nanocząstek redoks zawierających nitroksydy (NRNP) oraz (iii) walidacji metod badawczych przy określaniu biologicznych właściwości badanych nanocząstek.

Za komórkowy model choroby Parkinsona posłużyły komórki linii SH-SY5Y traktowane 6-hydroksydopaminą (6-OHDA), jako jedną z najczęściej stosowanych neurotoksyn do indukcji modelu tej choroby. Na podstawie badań *in vitro* wykazano, że neuroprotekcyjny charakter nanocząstek zawierających nitroksydy oraz zdolność ich przenikania przez barierę krew-mózg były wyższe w odniesieniu do nitroksydów *per se*. W oparciu o pozyskane wyniki analiz, toksyczność 6-OHDA polega w dużej mierze na uszkodzeniu mitochondriów, które może prowadzić do depolaryzacji wewnętrznej błony mitochondrialnej, obniżenia masy mitochondrialnej oraz spadku poziomu ATP. Wśród szeregu przebadanych substancji, nanocząstki będące kopolimerem opartym na poli(bezwodniku styrenowo-ko-maleinowym) (NRNP1) oraz nanocząstki zależne od pH, zaprojektowane z wykorzystaniem samoorganizującego się amfifilowego kopolimeru blokowego, składającego się z segmentu hydrofilowego złożonego z poli(tlenku etylenu) oraz segmentu hydrofobowego złożonego z poli(chlorometylostyrenu) w którym grupy chlorometylowe zostały zastąpione nitroksydem TEMPO (2,2,6,6-tetrametylopiperydyno-1-oksyl) (NRNP2/NRNP [pH]) chroniły mitochondria przed niszczącym działaniem reaktywnych form tlenu (RFT), po ekspozycji na 6-OHDA, co potwierdza ich ochronne właściwości.

Co więcej, zarówno nitroksydy oraz nanocząstki je zawierające mogą powodować zmianę w równowadze redoks komórek za pośrednictwem utleniania wewnątrzkomórkowych antyoksydantów. Otrzymane wyniki badań wskazują, że zarówno NRNP oraz nitroksydy *per se* zwiększają szybkość utleniania trzech najbardziej popularnych sond fluorescencyjnych stosowanych do pomiaru RFT, przez co należy zachować ostrożność przy interpretacji wyników otrzymanych z ich wykorzystaniem.

Z uwagi na fakt, że badania *in vitro* są jedynie wstępem do poznania właściwości badanych związków, bardziej szczegółowe informacje na temat ich działania przyniosą badania *in vivo.*

ABSTRACT

The doctoral dissertation consists of four articles published in the *Oxidative Medicine and Cellular Longevity, Molecules* and *Analytical Biochemistry*, that focus on (i) the review of contemporary trends in the use of nanoparticles as therapeutics for neurodegenerative diseases, (ii) the assessment of the neuroprotective properties of nitroxide-containing redox nanoparticles (NRNPs); and (iii) a validation of methods used to determine the biological properties of the selected nanoparticles.

Cells of the SH-SY5Y cell line were treated with 6-hydroxydopamine (6-OHDA) – as one of the most common neurotoxins used to induce a model of Parkinson's disease. Based on our research, it was shown that the neuroprotective nature of NRNPs and their ability to cross the blood-brain barrier was superior in relation to nitroxides *per se*. In accordance with the obtained results, 6-OHDA toxicity mostly depends on damaging the mitochondria, which can lead to depolarization of the inner mitochondrial membrane, a decrease in the mitochondrial mass and a decrease in ATP levels.

Among an array of tested compounds, two of them: the NRNP1 – a copolymer based on poly(styrene-co-malein anhydride) and NRNP2/NRNP ^{pH} – a pH-sensitive radical-containing nanoparticle that was designed and developed using a self-assembling amphiphilic block copolymer (PEG-*b*-PCTEMPO) composed of a hydrophilic poly(ethylene glycol) (PEG) segment and a hydrophobic poly(chloromethylstyrene) (PCMS) segment in which the chloromethyl groups were converted to 2,2,6,6-tetramethylpiperidinyloxys (TEMPOs), protected mitochondria from the damage of reactive oxygen species, after exposure to 6-OHDA, so the that we were able to confirm the protective properties of NRNPs.

Moreover, both nitroxides and NRNPs can alter the redox balance of cells through the oxidation of intracellular antioxidants. The results indicate that both NRNPs and nitroxides *per se* increase the oxidation rate of the three most popular fluorescent probes used for the reactive oxygen species measurement, therefore the interpretation of the results obtained using these probes should be approached with particular care.

Nonetheless, *in vitro* studies are only an introduction to understanding the properties of NRNPs and more detailed information about their properties might be provided by *in vivo* studies.

WYKAZ SKRÓTÓW

4-amino-TEMPO – 4-amino-2,2,6,6-tetrametyl-piperydyno-l-oksyl

6-OHDA – 6-hydroksydopamina

DAPI – 4′,6-diamidyno-2-fenyloindol

DHE – dihydroetydyna

DHR123 – dihydrorodamina 123

DMEM F12 – modyfikowane medium Eagle'a F12 (ang. *Dulbecco's Modified Eagle Medium)*

EPR – elektronowy rezonans paramagnetyczny

FBS – bydlęca surowica płodowa (ang. *Fetal Bovine Serum)*

GSH – zredukowany glutation

H₂DCF-DA – dioctan 2′,7′-dichlorohydrofluoresceiny

IC₅₀ – stężenie hamujące wzrost komórek w 50% (ang. *inhibitory concentration*)

MTT – bromek 3-(4,5-dimetylotiazol-2-ilo)-2,5-difenylotetrazoliowy, formazan błękitu triazolowego

NRNP – nanocząstki redoks zawierające nitroksydy

PCMS – poli(chlorometylostyren)

PEG – poli(tlenek etylenu)

RFT – reaktywne formy tlenu

TEMPO – 2,2,6,6-tetrametylopiperydyno-1-oksyl

WSTĘP

Niewątpliwie postęp nauk medycznych i biologicznych doprowadził do polepszenia jakości życia społecznego oraz wydłużenia życia człowieka. Co więcej, zaobserwowano również spadek płodności społeczeństwa, a te dwa czynniki przyczyniają się do jego ogólnego starzenia się, a proces ten najprawdopodobniej przyspieszy. Według Światowej Organizacji Zdrowia, niewykluczone jest, że liczba osób po 65 roku życia wzrośnie z 524 milionów (dane na rok 2010) do prawie 1,5 miliarda do roku 2050. Wzrost długości życia wiąże się z narastającą liczbą przypadków chorób przewlekłych i degeneracyjnych. Szacuje się, że w ciągu kolejnych 10-15 lat, ludzkość będzie coraz bardziej cierpieć z powodu chorób takich jak choroby serca, choroby nowotworowe czy cukrzyca [1].

Wśród chorób neurodegeneracyjnych, współczynniki: zachorowalności na chorobę Parkinsona, niepełnosprawności oraz śmiertelności charakteryzują się najwyższym wzrostem. Na całym świecie, zachorowalność na tę chorobę zwiększyła się o ponad połowę – z 2,5 mln przypadków w roku 1990 do 6,1 mln w roku 2016 [2]. W związku z powyższym, szacuje się, że do około 2050 roku, na świecie będzie ponad 12 milionów osób cierpiących na chorobę Parkinsona. Ponadto, jeśli populacja ludzka nadal będzie się starzeć, postęp medycyny podnosił przeżywalność, a czynniki środowiskowe przyczyniające się do indukcji choroby pozostaną na tym samym poziomie lub wzrosną, wówczas można spodziewać się jeszcze większej liczby przypadków choroby Parkinsona [3]. W związku z szacowanym szybkim przyrostem liczby osób dotkniętych chorobami związanymi z wiekiem, należy skupić się odpowiednio wcześniej na rozwoju terapii przeciwko chorobom neurodegeneracyjnym, dlatego w nawiązaniu do powyższych statystyk, skupiliśmy się na poszukiwaniu nowych związków, które w przyszłości po badaniach klinicznych mogłyby się okazać pomocne w łagodzeniu objawów chorobie Parkinsona.

Związki niskocząsteczkowe (o masie cząsteczkowej ≤500 Da) cechuje prosta struktura, ich właściwości farmakokinetyczne i farmakodynamiczne są z reguły łatwiejsze do przewidzenia, a następnie ich eksperymentalnego potwierdzenia niż w przypadku leków biologicznych, czyli ściśle związanych z endogennymi cząsteczkami biologicznie czynnymi np. przeciwciała monoklonalne. Związki niskocząsteczkowe, ze względu na swój niewielki rozmiar mogą z reguły łatwo przechodzić przez błony komórkowe i wchodzić w interakcje z innymi organellami komórkowymi. Ponadto, wiele związków niskocząsteczkowych cechuje się wysoką stabilnością oraz możliwością przyjmowania ich doustnie [4].

Dokładna patogeneza choroby Parkinsona nie została do końca poznana, niemniej jednak charakteryzuje się ona szeregiem cech neuropatologicznych na poziomie komórkowym m.in. śmiercią głównie neuronów dopaminergicznych istoty czarnej, występowaniem ciałek Lewy'ego oraz podwyższonym poziomem reaktywnych form tlenu (RFT) w centralnym układzie nerwowym. Zarówno w badaniach przedklinicznych, jak i klinicznych wykazano, że brak równowagi redoks komórek odgrywa ważną rolę w patogenezie chorób neurodegeneracyjnych, a obniżenie poziomu RFT może być obiecującym podejściem w leczeniu tych schorzeń. W związku z tym, oprócz głównego zastosowania związków niskocząsteczkowych w onkologii, patologii ogólnej, a w szczególności w leczeniu procesów zapalnych, wiele z tych substancji wykazuje również potencjał w terapii schorzeń psychiatrycznych i neurodegeneracyjnych, ze względu na możliwość regulowania stanu redoks komórek układu nerwowego [5,6].

Przewaga nitroksydów będących syntetycznymi antyoksydantami nad naturalnymi przejawia się poprzez ich złożoność działania – oprócz standardowego działania antyoksydacyjnego, związki te mogą hamować agregację białek oraz niepożądane reakcje enzymatyczne. Mają aktywność pseudoenzymatyczną podobną do dysmutazy ponadtlenkowej [7] mogą hamować reakcję Fentona poprzez zdolność do utleniania jonów metali przejściowych oraz terminować rodnikowe reakcje łańcuchowe na drodze rekombinacji rodnikowej [8,9]. Wadą tych związków jest niestety ich krótki czas trwania *in vivo* oraz cytotoksyczność, dlatego zastosowanie polimerowego nośnika może poprawić właściwości farmakologiczne nitroksydów [10].

Ponadto, istnieje wiele przeszkód zarówno chemicznych jak i biologicznych, które wpływają na efektywność terapii m.in. niespecyficzność leku, niedostateczna akumulacja, opsonizacja i wydalanie leków przez szereg komórkowych systemów sekwestracji [11]. Aby przeciwdziałać tym mechanizmom, nowoczesna nanomedycyna oferuje zastosowanie nośników leków celem polepszenia ich właściwości terapeutycznych. Nanoterapeutyki wykazują duży potencjał w poprawieniu bezpieczeństwa i efektywności konwencjonalnych terapeutyków. Poza koniugatami lek-nanocząstka, nanomedycyna znajduje zastosowanie w terapii genowej czy obrazowaniu *in vivo* [12].

Aby przeciwdziałać stresowi oksydacyjnemu, w niniejszej pracy, analizie poddano nanocząstki o właściwościach antyoksydacyjnych. Główną zaletą nanocząstek jest łatwość modyfikowania ich struktury już na etapie syntezy, tak aby mogły one reagować na różne

bodźce, zarówno wewnątrz- jak i/lub zewnątrzkomórkowe, np. pH, równowaga redoks [13,14,15], aktywność enzymatyczna [16], temperatura, pole magnetyczne lub elektryczne, ultradźwięki czy nawet światło [17].

Substancje wrażliwe na pH zaczęły zyskiwać zainteresowanie badawcze, ponieważ można je wykorzystać na trzech poziomach, a mianowicie na poziomie (i) narządu, (ii) tkanki i (iii) komórki, w celu zwiększenia i poprawy wychwytu leku, kolejno przez (i) przewód pokarmowy, (ii) wykorzystanie mikrośrodowisko guza celem zwiększenia specyficzności leku, czy też skorzystanie z (iii) efektu „gąbki protonowej" w celu internalizacji terapeutyku [18]. Istnieje wiele różnych strategii, aby zaprojektować nanocząstki, w sposób, aby zmieniały swój rozmiar, kształt czy właściwości powierzchniowe w odpowiedzi na bodźce wewnątrz- i/lub zewnątrzkomórkowe (Ryc.1).
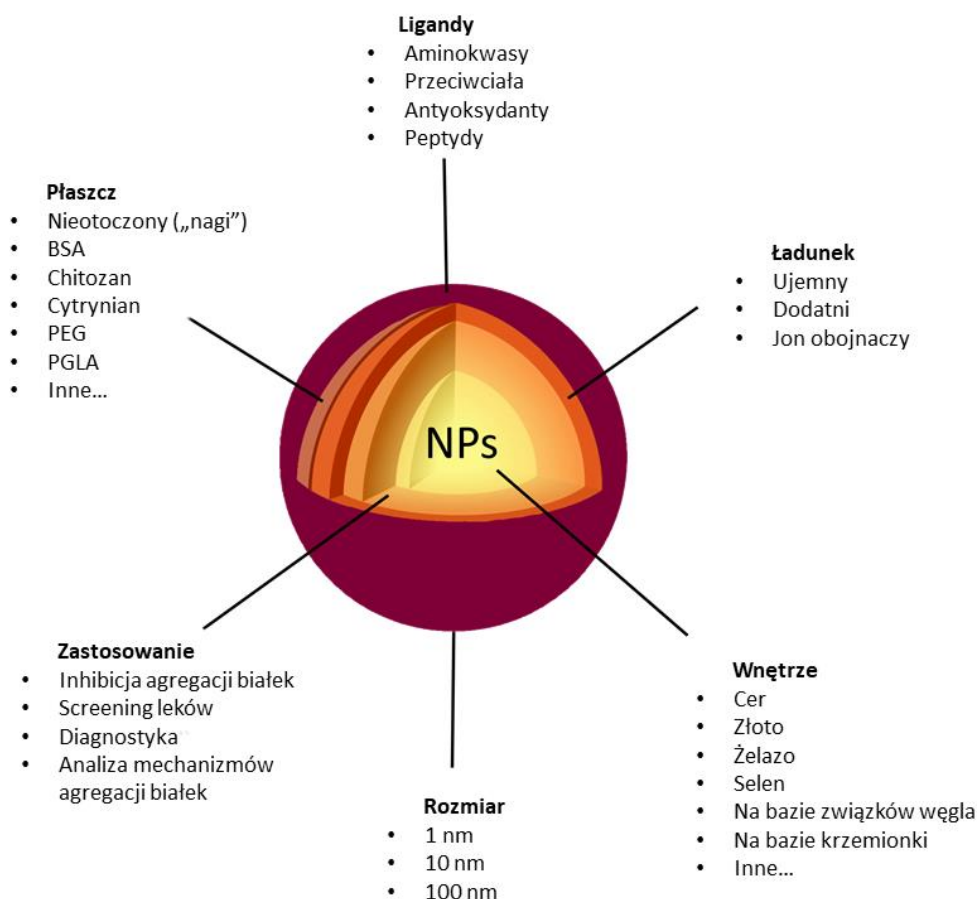
Rycina 1. Możliwe modyfikacje struktury nanocząstek. Opracowanie własne.

CEL I ZAKRES PRACY

Głównym celem badań była analiza właściwości wybranych nanocząstek o potencjale antyoksydacyjnym jako potencjalnie użytecznych w terapii chorób neurodegeneracyjnych, na modelu komórkowym choroby Parkinsona.

Hipoteza niniejszej rozprawy doktorskiej dotyczyła nanocząsteczek redoks zawierających nitroksydy. Postulowała, że związki te mogą okazać się bardziej skuteczne w łagodzeniu stresu oksydacyjnego i nitracyjnego oraz będą wykazywać lepsze działanie antyneurodegeneracyjne niż niskocząsteczkowe nitroksydy *per se*.

STRUKTURA ROZPRAWY DOKTORSKIEJ

Rozprawa doktorska obejmuje cykl czterech publikacji naukowych, których sumaryczny **Impact Factor** w roku opublikowania jest równy **16.296**, a liczba punktów MNiSW wynosi **370**.

1. **Pichla M.,** Bartosz G., Sadowska-Barotsz I., *The anti-aggregative and anti-amyloidogenic properties of nanoparticles: a promising tool for the treatment and diagnostics of neurodegenerative diseases*. Oxidative Medicine and Cellular Longevity, 2020, 3534570.
   IF$_{2020}$: 5.076; MNiSW: 100

2. **Pichla M.,** Pułaski Ł., Kania KD., Stefaniuk I., Cieniek B., Pieńkowska N., Bartosz G., & Sadowska-Bartosz I. *Nitroxide Radical-Containing Redox Nanoparticles Protect Neuroblastoma SH-SY5Y Cells against 6-Hydroxydopamine Toxicity*. Oxidative Medicine and Cellular Longevity, 2020, 9260748.
   IF$_{2020}$: **5.076**; **MNiSW: 100**

3. **Pichla, M.**; Bartosz, G.; Stefaniuk, I.; Sadowska-Bartosz, I. *pH-Responsive Redox Nanoparticles Protect SH-SY5Y Cells at Lowered pH in a Cellular Model of Parkinson Disease*. Molecules 2021, 26, 543.
   IF$_{2020}$: 3.267; MNiSW: 100

4. **Pichla M,** Bartosz G, Pieńkowska N, Sadowska-Bartosz I. *Possible artefacts of antioxidant assays performed in the presence of nitroxides and nitroxide-containing nanoparticles*. Analytical Biochemistry 2020; 597:113698.
   IF$_{2020}$: 2.877; **MNiSW: 70**

MATERIAŁY I METODY

Jako komórkowy model choroby Parkinsona posłużyła często stosowana do celów badań nad chorobami neurodegeneracyjnymi, linia komórkowa SH-SY5Y, która została poddana ekspozycji na 6-OHDA. Linia ta wywodzi się z linii komórkowej SK-N-SH, która została wyizolowana w 1970 roku i pochodzi z biopsji szpiku kostnego 4-letniej dziewczynki, u której zdiagnozowano nerwiaka zarodkowego. Komórki linii SH-SY5Y są częścią zarówno układu dopaminergicznego i noradrenergicznego, ponieważ komórki te mogą syntetyzować zarówno dopaminę jak i noradrenalinę. Pomimo jej nowotworowego pochodzenia i licznych aberracji genetycznych, linia ta zachowuje w stanie niezmienionym większość zaburzeń szlaków sygnałowych typowych dla choroby Parkinsona [19]. Komórki linii SH-SY5Y hodowano w kompletnym medium DMEM F12 z dodatkiem 10% FBS i 1% roztworu penicyliny i streptomycyny, w warunkach 95% wilgotności, 5% CO_2, 37 °C.

W badaniach ewaluacji poddano trzy różne nanocząstki zawierające nitroksydy (NRNP), roboczo nazywane: NRNP1, NRNP2 (NRNP ^{pH}) i NRNP3. NRNP1 jest kopolimerem opartym na poli(bezwodniku styrenowo-ko-maleinowym) (Ryc. 2).
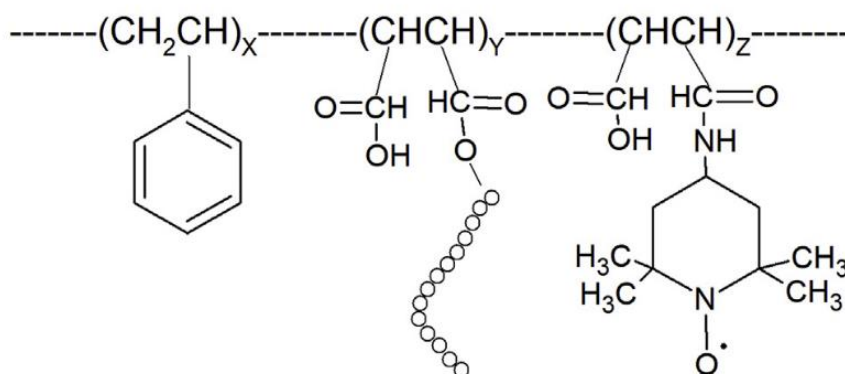
Rycina 2. Struktura nanocząstki NRNP1.

NRNP2 (NRNP ^{pH}) jest nanocząstką zależną od pH, zaprojektowaną z wykorzystaniem samoorganizującego się amfifilowego kopolimeru blokowego (PEG-*b*-PCTEMPO) składającego się z segmentu hydrofilowego złożonego z poli(tlenku etylenu) (PEG) oraz segmentu hydrofobowego złożonego z poli(chlorometylostyrenu) (PCMS), w którym grupy chlorometylowe zostały zastąpione TEMPO (2,2,6,6-tetrametylopiperydyno-1-oksyl) (Ryc. 3).

$(CH_3O-(CH_2CH_2O)_m-CH_2CH_2S-(CH_2CH)_2-H$

pH-sensitive site

NH

MeO-PEG-*b*-PCTEMPO

O•
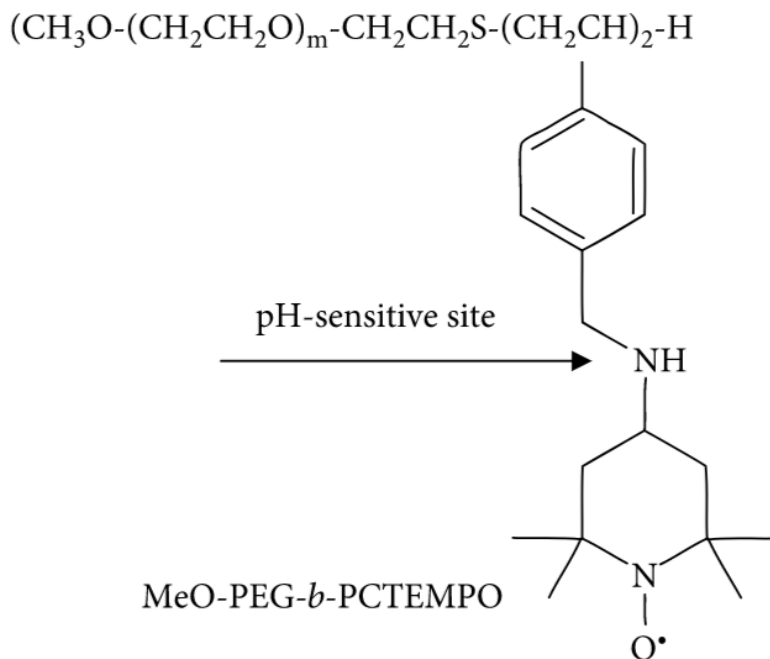
Rycina 3. Struktura NRNP2 (NRNP ^{pH}).

NRNP3 jest kopolimerem składającym się z estrów sorbitanu z kwasami tłuszczowymi i 4-amino-TEMPO (4-amino-2,2,6,6-tetrametylopiperydyno-1-oksyl) (Ryc. 4).
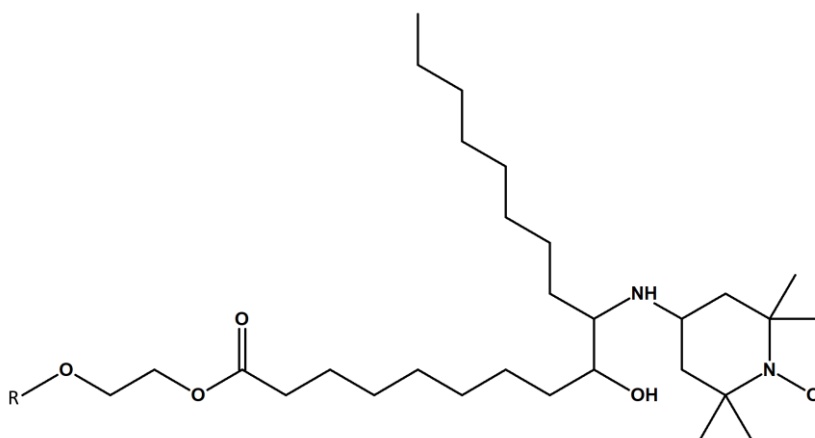
Rycina 4. Struktura NRNP3.

W aspekcie modelu choroby Parkinsona, w pierwszej kolejności przeprowadzono wstępne testy cytotoksyczności 6-OHDA. 6-Hydroksydopamina jest najczęściej używaną neurotoksyną do indukcji modelu choroby Parkinsona *in vitro*. Celem doboru odpowiednich warunków hodowli komórek oraz optymalizacji metod badawczych, cytotoksyczność oceniano za pomocą trzech różnych testów: z czerwienią obojętną, testu z solami tetrazolowymi (MTT) oraz testu opartego na resazurynie.

Najbardziej odpowiednią metodą badań oraz najczęściej stosowaną w literaturze naukowej w określaniu cytotoksyczności różnych substancji wobec linii SH-SY5Y okazał się test MTT. Po ustaleniu metod hodowlanych w **Publikacji nr 2** sprawdzono również cytotoksyczność nanocząstek zawierających nitroksydy oraz wolnych nitroksydów wchodzących w skład badanych nanocząstek – TEMPO oraz 4-amino-TEMPO.

Następnie analizie poddano potencjalne działanie antyneurodegeneracyjne badanych nanocząstek w trzech wariantach:

- komórki traktowane równocześnie 6-OHDA w stężeniu IC_{50} oraz wybranymi stężeniami antyoksydantów syntetycznych oraz nanocząstek zawierających nitroksydy przez 24 godziny,
- komórki preinkubowane z antyoksydantami i NRNP przez 2 godziny, a następnie traktowane 6-OHDA w stężeniu odpowiadającym IC_{50} przez 24 godziny,
- komórki preinkubowane z 6-OHDA w stężeniu odpowiadającym IC_{50} przez 24 godziny, a następnie inkubowane z antyoksydantami i NRNP przez 24 godziny.

Wariant, zgodnie z którym komórki były preinkubowane z antyoksydantami, a następnie poddane działaniu neurotoksyny okazał się posiadać najbardziej korzystny efekt neuroprotekcyjny, dlatego został on wykorzystany w kolejnych analizach. Badania zostały przeprowadzone w dwóch punktach czasowych – po jednej i 24 godzinach od dodania 6-OHDA.

W celu analizy stresu oksydacyjnego komórek, dokonano pomiaru poziomu: zredukowanego glutationu (GSH), RFT z wykorzystaniem dihydroetydyny (DHE) oraz mitochondrialnego rodnika ponadtlenkowego z użyciem testu Cell Meter™ Fluorimetric Mitochondrial Superoxide Activity Assay Kit. Poziom ATP w komórkach oznaczano z wykorzystaniem testu luminescencyjnego opartego na reakcji enzymatycznego przekształcenia lucyferyny do oksylucyferyny przez rekombinowaną lucyferazę [20]. Uszkodzenia w obrębie mitochondriów spowodowane działaniem 6-OHDA oszacowano na podstawie zmian potencjału mitochondrialnego z wykorzystaniem fluorescencyjnego barwnika JC-1 oraz oceny masy mitochondrialnej używając fluorescencyjnej sondy *N*-nonyl-oranżu akrydyny. Zmiany w obrębie struktur komórkowych zobrazowano za pomocą barwień – do tego celu wykorzystano barwniki fluorescencyjne takie jak MitoTracker Deep Red FM, falloidynę sprzężoną z Atto-488 oraz DAPI, do wizualizacji kolejno mitochondriów, cytoszkieletu aktynowego oraz jąder komórkowych.

Ponadto, dokonano analizy zdolności badanych substancji, do przenikania bariery krew-mózg, na modelu komórkowym z wykorzystaniem komórek hCMEC/D3 oraz techniki elektronowego rezonansu paramagnetycznego (EPR). Linia komórkowa hCMEC/D3 jest najlepiej poznanym modelem ludzkiej bariery krew-mózg, która została wyizolowana z mikronaczyń płata skroniowego i jest linią często stosowaną do badań dotyczących transportu leków w odniesieniu do centralnego układu nerwowego [21].

W **Publikacji nr 3** przeanalizowano wpływ pH na profil wnikania NRNP ^{pH} do komórek linii SH-SY5Y z wykorzystaniem techniki EPR oraz ich potencjał antyneurodegeneracyjny w różnych warunkach pH. Badania przeprowadzono po 24h inkubacji z NRNP ^{pH}. Model badawczy wykorzystano w oparciu o dane pozyskane w **Publikacji nr 2.** Podobnie jak poprzednio, zbadano poziom ATP, RFT, GSH oraz parametry mitochondrialne (potencjał mitochondrialny i masa mitochondriów) komórek po zastosowaniu NRNP ^{pH}. Ponadto dokonano analizy profilu śmierci komórkowej z wykorzystaniem testu RealTime-Glo™ Annexin V Apoptosis and Necrosis Assay (Promega), występującej w modelu neurodegeneracyjnym indukowanym 6-OHDA oraz jaki wpływ na jej rodzaj ma terapia NRNP ^{pH}.

W **Publikacji nr 4** dokonano walidacji metod badawczych związanych z analizą poziomu RFT, z wykorzystaniem popularnych sond fluorescencyjnych. Wykazano indukcję artefaktów w pomiarach RFT otrzymanych przy zastosowaniu dioctanu 2',7'-dichlorohydrofluoresceiny ($H_2DCF-DA$), DHE i dihydrorodaminy 123 (DHR123) w układach bezkomórkowych i komórkowych.

Analizy statystyczne wykonano przy użyciu oprogramowania STATISTICA 13.3. Istotność statystyczną obserwowanych różnic oceniano stosując test Kruskala-Wallisa, test U-Mann-Whitney oraz w niektórych przypadkach dokonywano analizy statystycznej testem *t*-Studenta. Przyjęto poziom istotności $p < 0,05$.

WYNIKI BADAŃ

Pierwsza praca wchodząca w skład cyklu ma charakter poglądowy i jest ona uzupełnieniem treści dotyczącej zastosowania nanocząstek w terapii chorób neurodegeneracyjnych **[Publikacja 1].** Stanowi ona również rozszerzenie informacji dotyczących dotychczas poznanych mechanizmów trzech najbardziej popularnych chorób neurodegeneracyjnych oraz ich współczesnej terapii.

W kolejnej pracy wykazano neuroprotekcyjne działanie nanocząstek redoks zawierających nitroksydy jako potencjalny lek przeciwko chorobie Parkinsona **[Publikacja nr 2].** Celem scharakteryzowania badanych nanocząstek wyznaczono przy wykorzystaniu techniki EPR zawartość reszt nitroksylowych przypadających na jedną cząsteczkę polimeru. Wyniki wskazują, że badane nanocząstki NRNP1, NRNP2 oraz NRNP3 zawierają kolejno 27,6 (MW 7500 Da); 7,7 (MW 8300 Da); i 8,4 (MW 2246-2417 Da) reszt rodnika. W układzie bezkomórkowym wykazano wyższą zdolność antyoksydacyjną badanych nanocząstek w porównaniu z 4-amino-TEMPO *per se*.

6-Hydroksydopamina wykazała zależną od dawki toksyczność wobec komórek linii SH-SY5Y. Stężenie IC_{50} po 24 godzinach inkubacji z neurotoksyną wynosiło 64 µM. Wszystkie badane antyoksydanty wykazywały cytotoksyczność w zakresie stężeń 75-150 µM (odpowiednio dla 4-amino-TEMPO oraz nanocząstek) i 100-150 µM dla TEMPO po 24 godzinach inkubacji. Jednak NRNP1 wykazały znaczny efekt neuroprotekcyjny przed działaniem 6-OHDA w stężeniach 75-150 µM. Pozostałe przebadane nanocząstki NRNP2 i NRNP3 nie oferowały tak znacznej poprawy żywotności.

Wykazano, że NRNP1 wnikają do komórek linii SH-SY5Y z wydajnością 34% już po 2h inkubacji. Co więcej, udowodniono, że zarówno NRNP1 oraz badane nitroksydy są zdolne do penetracji bariery krew-mózg, której model stanowiły komórki hCMEC/D3. Zaobserwowano obustronny transport na podobnym poziomie szybkości przenikania oraz nie wykazano obecności aktywnego transportera jako czynnika pośredniczącego w transporcie tych związków przez model bariery krew-mózg.

Badane antyoksydanty wykazują nieznaczną protekcję przeciwko działaniu 6-OHDA w modelu krótkotrwałym (1h). Natomiast 24-godzinna ekspozycja komórek na działanie 6-OHDA powoduje obniżenie poziomu ATP komórek do 65% względem kontroli negatywnej (komórki nie poddane działaniu 6-OHDA). Badane nanocząstki oraz 4-amino-

TEMPO wykazały podobne działanie ochronne, dając poprawę stanu energetycznego komórek o około 20% względem kontroli pozytywnej.

Istotny efekt zaobserwowano w odniesieniu do stresu oksydacyjnego komórek. Po 24-godzinach inkubacji z neurotoksyną odnotowano najprawdopodobniej kompensacyjny wzrost poziomu GSH w kontroli pozytywnej. Analizowane nanocząstki znacznie przeciwdziałały temu zjawisku, wręcz obniżając poziom GSH względem kontroli negatywnej.

Po 24-godzinnej inkubacji z 6-OHDA obserwowano dwukrotny wzrost poziomu RFT w teście z DHE, gdzie jedynie TEMPO w stężeniu 150 μM istotnie obniżało ich poziom, a nanocząstki wręcz podnosiły poziom RFT.

Jak wykazano w **Publikacji nr 4,** będącej częścią niniejszej rozprawy doktorskiej należy ostrożnie interpretować wyniki pomiarów RFT. Jest to spowodowane faktem, że najprawdopodobniej nitroksydy oraz nanocząstki je zawierające zwiększają szybkość utleniania trzech najbardziej popularnych sond fluorescencyjnych stosowanych do pomiaru RFT, takich jak $H_2DCF-DA$, DHE i DHR123. Bezpośrednia oksydacja tych sond została już wcześniej udokumentowana w literaturze – dla przykładu, $H_2DCF-DA$ jest utleniany przez hemoglobinę, mioglobinę czy też cytochrom *c*, bez pośrednictwa ze strony RFT [22]. W efekcie przeprowadzonych badań, zaobserwowano zwiększenie utleniania w przypadku $H_2DCF-DA$ i DHE przez TEMPO i NRNP1 oraz DHR123 przez TEMPO, gdzie 4-amino-TEMPO i NRNP1 hamowało utlenianie DHR123. Wykazano, że nitroksydy mogą wykazywać zarówno właściwości anty- jak i prooksydacyjne, a w zależności od systemu i warunków reakcji jeden charakter może przeważać nad drugim. W związku z powyższymi wynikami należy z rozwagą podchodzić do interpretacji wyników pomiarów RFT z użyciem sond fluorescencyjnych w obecności nitroksydów lub cząstek je zawierających. Co więcej, przeprowadzone eksperymenty wykazały, że zarówno nitroksydy jak i NRNP1 są zdolne do utleniania GSH, a efekt ten jest zależny od czasu i stężenia, dlatego również należy brać ten aspekt pod uwagę przy interpretacji wyników.

W świetle powyższych obserwacji, celem bardziej miarodajnego i precyzyjnego określenia RFT, zbadano poziom mitochondrialnego rodnika ponadtlenkowego, z wykorzystaniem specyficznej dla niego sondy. Wyniki te niepodważalnie pokazują wzrost poziomu rodnika ponadtlenkowego już po jednej godzinie inkubacji z neurotoksyną oraz fakt, że jedynie badane nanocząstki są zdolne do zahamowania generacji rodnika ponadtlenkowego w tak

krótkim czasie. W modelu długotrwałym, wszystkie badane antyoksydanty są zdolne do obniżania poziomu rodnika ponadtlenkowego, niemniej jednak nanocząstki wykazują co najmniej o połowę lepsze działanie antyoksydacyjne.

Uszkodzenia mitochondriów spowodowane działaniem 6-OHDA oszacowano na podstawie potencjału mitochondrialnego oraz zmian w masie mitochondrialnej. Wartość potencjału mitochondrialnego została istotnie obniżona już po 1h inkubacji z neurotoksyną, a badane nanocząstki niestety nie wykazały działania ochronnego w tym aspekcie, w przeciwieństwie do pozostałych nitroksydów – 4-amino-TEMPO w stężeniu 100 μM i TEMPO w stężeniu 150 μM. Jednakże po dobowej inkubacji, obserwuje się istotne, jednak nieznaczne w porównaniu do kontroli negatywnej działanie ochronne ze strony badanych związków. Masa mitochondriów szacowana po 24h inkubacji z 6-OHDA (kontrola pozytywna), maleje o połowę, a nanocząstki NRNP1 w stężeniu 150 μM oraz TEMPO w stężeniu 100 μM cechują się około 30% działaniem ochronnym.

Analiza mikroskopowa wykazała równomierne rozproszenie mitochondriów w komórkach kontroli pozytywnej (komórek traktowanych 6-OHDA) w porównaniu do kontroli negatywnej (komórek nietraktowanych 6-OHDA). W komórkach traktowanych badanymi nanocząstkami zaobserwowano podobne rozmieszczenie mitochondriów w obrębie komórek, jednak obecne są również skupiska mitochondriów, tak jak w przypadku komórek nietraktowanych 6-OHDA. W pozostałych przypadkach mitochondria były skoncentrowane wokół błony komórkowej. Wykorzystując program komputerowy ImageJ wyznaczono stosunek intensywności fluorescencji mitochondriów do intensywności fluorescencji cytoszkieletu. Analiza wykazała spadek intensywności o około 20% pomiędzy kontrolą pozytywną a negatywną. Parametr ten w komórkach traktowanych nanocząstkami w stężeniu 150 μM jest o 20% wyższy i o 20% niższy w komórkach traktowanych 150 μM 4-amino-TEMPO w porównaniu do kontroli pozytywnej. Wyniki te korelują z analizą masy mitochondrialnej odnośnie zmian w obrębie stanu mitochondriów – sugerują wpływ nanocząstek na ich biogenezę.

W **Publikacji nr 3**, na podstawie danych eksperymentalnych świadczących o obniżonym pH (~pH 6.5) tkanki mózgowej dotkniętej chorobą Parkinsona, dokonano analizy neuroprotekcyjnych właściwości nanocząstek redoks w różnych warunkach pH. Wykazano, że wnikanie NRNP ^{pH} do komórek silnie zależało od pH. Najprawdopodobniej jest to związane z otwarciem się struktury nanocząstki w niższym pH i ekspozycją dodatniego

ładunku na jej powierzchni [23], dzięki czemu możliwa jest ich adsorpcja na ujemnie naładowanej powierzchni komórek, a następnie dalsze wnikanie do komórek. Analiza wykazała, że NRNP [pH] posiadają znacznie lepszy efekt neuroprotekcyjny w pH niższym niż fizjologiczne. Ponadto, spadek masy mitochondrialnej był lepiej hamowany w niższym pH, a efekt ten był zależny od stężenia nanocząstek.

Mitochondria odgrywają kilka ważnych ról w komórce. Oprócz tego, że są głównym źródłem ATP i RFT, biorą udział m.in. w kontroli cyklu komórkowego, apoptozy, syntezie hemu i steroidów. 6-OHDA może wpływać na wszystkie te procesy, i w zależności od stopnia uszkodzenia, może mieć kluczowe znaczenie dla przeżywalności komórki. Chociaż dokładny mechanizm ochrony komórek SH-SY5Y przed cytotoksycznością ze strony 6-OHDA nie może zostać wyjaśniony na podstawie tego badania; uzyskane wyniki wskazują, że stymulacja biogenezy mitochondriów przez NRNP [pH] może zapobiegać skutkom uszkodzenia komórek.

PODSUMOWANIE

W świetle przeprowadzonych badań podczas realizacji pracy doktorskiej, wykazano potencjał terapeutyczny wybranych substancji w chorobach wieku podeszłego.

W przypadku komórkowego modelu choroby Parkinsona, na podstawie przeprowadzonych analiz, udało się wykazać silniejsze działanie ochronne nanocząstek zawierających nitroksydy w porównaniu z nitroksydami *per se*. Nanocząstki redoks lepiej chroniły komórki linii SH-SY5Y przed toksycznością ze strony 6-OHDA służącej do modelowania patofizjologii choroby Parkinsona niż wolne nitroksydy. Co więcej, zdolność nanocząstek do przenikania przez model bariery krew-mózg była większa niż nitroksydów *per se*. W oparciu o uzyskane wyniki, toksyczność 6-OHDA przejawia się głównie poprzez uszkodzenie mitochondriów, które może prowadzić do depolaryzacji wewnętrznej błony mitochondrialnej, obniżenia masy mitochondrialnej oraz spadku poziomu ATP. Badane nanocząstki chroniły mitochondria przed niszczącym działaniem reaktywnych form tlenu, po ekspozycji na 6-OHDA, przez co w świetle uzyskanych wyników potwierdzono antyneurodegeneracyjne właściwości nanocząstek NRNP1 i NRNP ^{pH}. Ponadto, NRNP1 wnikają do komórek linii SH-SY5Y z wydajnością 34% już po 2h inkubacji oraz są zdolne do penetracji bariery krew-mózg bez obecności aktywnego transportera jako czynnika pośredniczącego w ich transporcie.

Na podstawie przeprowadzonych analiz, należy też zauważyć, że zarówno nitroksydy jak i nanocząstki je zawierające mogą zmieniać równowagę redoks komórek poprzez utlenianie wewnątrzkomórkowych antyoksydantów jak np. GSH oraz indukować artefakty w oznaczeniach markerów stresu oksydacyjnego.

Wymagane są dalsze badania nad związkami przytoczonymi w niniejszej rozprawie doktorskiej, aby w pełni poznać ich działanie terapeutyczne. Niestety badania *in vitro* są jedynie wstępem do poznania właściwości badanych związków, a bardziej dokładne informacje na temat ich działania przynoszą badania *in vivo*.

LITERATURA

1. *Global health and ageing*. World Health Organization. 2011. Dostęp on-line [maj 2020]: https://www.who.int/ageing/publications/global_health/en/

2. *GBD 2016 Parkinson's Disease Collaborators. Global, regional, and national burden of Parkinson's disease, 1990-2016: a systematic analysis for the Global Burden of Disease Study 2016*. Lancet Neurol. 2018;17(11):939-953

3. Rocca WA. *The burden of Parkinson's disease: a worldwide perspective*. Lancet Neurol. 2018;17(11):928-929.

4. Laurence L. Burton, John S. Lazo, Keith L. Parker. *Gilman's Manual of Pharmacology and Therapeutics*, 11th edition, p.1-7, 2006. ISBN: 0071422803

5. Olanow CW, Tatton WG. *Etiology and pathogenesis of Parkinson's disease*. Annu Rev Neurosci. 1999;22:123-144

6. Schiavone S, Trabace L. Small Molecules: Therapeutic Application in Neuropsychiatric and Neurodegenerative Disorders. Molecules. 2018;23(2):411.

7. Soule BP, Hyodo F, Matsumoto K, Simone NL, Cook JA, Krishna MC, Mitchell JB. *The chemistry and biology of nitroxide compounds*. Free Radic Biol Med. 2007 Jun 1;42(11):1632-50

8. Wilcox CS. *Effects of tempol and redox-cycling nitroxides in models of oxidative stress*. Pharmacol Ther. 2010;126(2):119-145

9. Liang Q, Smith AD, Pan S, et al. *Neuroprotective effects of TEMPOL in central and peripheral nervous system models of Parkinson's disease*. Biochem Pharmacol. 2005;70(9):1371-1381

10. Sadowska-Bartosz I, Bartosz G. Redox nanoparticles: synthesis, properties and perspectives of use for treatment of neurodegenerative diseases. J Nanobiotechnology. 2018 Nov 3;16(1):87

11. Blanco E, Shen H, Ferrari M. *Principles of nanoparticle design for overcoming biological barriers to drug delivery*. Nat. Biotechnol. 2015; 33:941-951

12. Prasad M, Lambe UP, Brar B, et al. *Nanotherapeutics: An insight into healthcare and multi-dimensional applications in medical sector of the modern world*. Biomed Pharmacother. 2018;97:1521-1537

13. Guo X, Cheng Y, Zhao X, Luo Y, Chen J, Yuan WE. *Advances in redox-responsive drug delivery systems of tumor microenvironment*. J Nanobiotechnology. 2018 Sep;22;16(1):74.

14. Jiang Z, Thayumanava S. *Disulfide-Containing Macromolecules for Therapeutic Delivery*. Israel J. Chem. 2020;60:132-139,

15. Yang DS, Yang YH, Zhou Y, Yu LL, Wang RH, Di B, Niu MM. *A Redox-Triggered Bispecific Supramolecular Nanomedicine Based on Peptide Self-Assembly for High-Efficacy and Low-Toxic Cancer Therapy*. Adv. Funct. Mater. 2020 30:1904969

16. Hu Q, Katti PS, Gu Z. *Enzyme-responsive nanomaterials for controlled drug delivery*. Nanoscale 2014;6:12273-12286

17. Sahle FF, Gulfam M, Lowe TL. *Design strategies for physical-stimuli-responsive programmable nanotherapeutics.* Drug Discov Today. 2018 May;23(5):992-1006

18. Gao W, Chan JM, Farokhzad OC. *pH-Responsive nanoparticles for drug delivery*. Mol Pharm. 2010 Dec 6;7(6):1913-20

19. Xicoy H, Wieringa B, Martens GJ. *The SH-SY5Y cell line in Parkinson's disease research: a systematic review*. Mol Neurodegener. 2017;12(1):10

20. https://pl.promega.com/-/media/files/resources/protocols/technical-bulletins/0/celltiter-glo-luminescent-cell-viability-assay-protocol.pdf?la=en Dostęp on-line: 10.02.2021]

21. Weksler B, Romero IA, Couraud PO. *The hCMEC/D3 cell line as a model of the human blood brain barrier. Fluids Barriers CNS*. 2013 Mar 26;10(1):16.

22. Ohashi T, Mizutani A, Murakami A, Kojo S, Ishii T, Taketani S. *Rapid oxidation of dichlorodihydrofluorescin with heme and hemoproteins: formation of the fluorescein is independent of the generation of reactive oxygen species*. FEBS Lett. 2002;511(1-3):21-27

23. Yoshitomi T, Suzuki R, Mamiya T, Matsui H, Hirayama A, Nagasaki Y. *pH-sensitive radical-containing-nanoparticle (RNP) for the L-band-EPR imaging of low pH circumstances*. Bioconjug Chem. 2009 Sep;20(9):1792-8

DOROBEK NAUKOWY

Pozostałe publikacje

1. Pieńkowska N., Bartosz G., **Pichla M.**, Grzesik-Pietrasiewicz M., Gruchala M, Sadowska-Bartosz I. *Effect of antioxidants on the H_2O_2-induced premature senescence of human fibroblasts*. Aging (Albany NY). 2020;12(2):1910-1927.
   IF_{2020}: 4.831; MNiSW: 140

2. Uram Ł., Misiorek M., **Pichla M.**, Filipowicz-Rachwał A., Markowicz J., Wołowiec S., Wałajtys-Rode E. *The Effect of Biotinylated PAMAM G3 Dendrimers Conjugated with COX-2 Inhibitor (celecoxib) and PPARγ Agonist (Fmoc-L-Leucine) on Human Normal Fibroblasts, Immortalized Keratinocytes and Glioma Cells in Vitro*. Molecules. 2019;24(20):3801.
   IF_{2019}: 3.267; MNiSW: 100

3. Grzesik M., Bartosz G., Stefaniuk I., **Pichla M.**, Namieśnik J., Sadowska-Bartosz I. *Dietary antioxidants as a source of hydrogen peroxide*. Food Chemistry. 2019;278:692-699.
   IF_{2019}: 6.306; MNiSW: 200

4. **Pichla, M.,** Sroka, J., Pieńkowska, N., Piwowarczyk, K., Madeja, Z., Bartosz, G., & Sadowska-Bartosz, I. *Metastatic prostate cancer cells are highly sensitive to 3-bromopyruvic acid*. Life Sci. 2019 Jun 15;227:212-223.
   IF_{2019}: 3.448; MNiSW: 70

Sumaryczna wartość współczynnika **Impact Factor** dorobku publikacyjnego łącznie z publikacjami wchodzącymi w skład rozprawy doktorskiej (wg opublikowania) wynosi **34.148 (880 punktów MNiSW).**

Liczba cytowań według bazy Scopus: 40; h-index = 3

Staże

Department of Cellular and Molecular Medicine, Katholieke Universiteit Leuven
w okresie 02.03.2020 – 30.06.2020; staż naukowy w ramach programu Erasmus+

Udział w grancie Narodowego Centrum Nauki

Konkurs SONATA BIS „Antyoksydanty nanocząsteczkowe: biologiczne podstawy potencjalnej terapii celowanej chorób neurodegeneracyjnych". Numer grantu: NCN 2016/22/E/NZ7/00641. Kierownik projektu: prof. dr hab. Izabela Sadowska-Bartosz

Komunikaty zjazdowe

The FEBS Congress (Kraków) 6-11.07.2019

Prezentacja posterowa: "Redox nanoparticles protect neuroblastoma SH-SY5Y cells against 6-hydroxydopamine toxicity". **Pichla M**., Pieńkowska N., Bartosz G., Nagasaki Y., Sadowska-Bartosz I.

3rd BIO Congress (Gdańsk) 18-21.09.2018

Wygłoszenie prezentacji w języku angielskim: „3-Bromopyruvic acid: a small molecule with strong anti-tumor potency". **Pichla M**., Sadowska-Bartosz I., Bartosz G.

Prezentacja posterowa: "3-Bromopyruvic acid affects the mobility and redox balance of metastatic cells". **Pichla M**., Pieńkowska N., Sroka J., Piwowarczyk K., Madeja Z., Bartosz G., Sadowska-Bartosz I.

Ogólnopolskie Sympozjum Biomedyczne ESKULAP (Lublin) 2-3.12.2017

Prezentacja posterowa: "Właściwości przeciwnowotworowe biotynylowanego dendrymeru PAMAM G3, sprzężonego z inhibitorem COX-2 i agonistą receptorów PPARγ". **Pichla M**., Uram Ł.

III Podkarpacka Konferencja Młodych Naukowców (Rzeszów) 12-14.10.2017

Prezentacja posterowa: "Właściwości przeciwnowotworowe biotynylowanego dendrymeru PAMAM G3, sprzężonego z inhibitorem COX-2 i agonistą receptorów PPARγ wobec linii raka płaskonabłonkowego (SCC-15) i glejaka (U-118 MG)". **Pichla M.**, Uram Ł.

OŚWIADCZENIA WSPÓŁAUTORÓW

Rzeszów, dnia 18.02.2021

mgr inż. Monika Pichla

Jednostka: Pracownia Biochemii Analitycznej

Instytut Technologii Żywności i Żywienia

Promotor: prof. dr hab. Izabela Sadowska-Bartosz

Promotor pomocniczy: nie dotyczy

OŚWIADCZENIE

W związku z przygotowywaniem przeze mnie rozprawy doktorskiej w formie spójnego tematycznie zbioru artykułów, oświadczam niniejszym, że wkład mojej pracy naukowej, a tym samym pracy pozostałych współautorów w opublikowaniu poniższych artykułów, które zamierzam przedstawić jako własną dysertację doktorską jest następujący:

1. Pichla, M., Bartosz, G., & Sadowska-Bartosz, I. (2020). *The Antiaggregative and Antiamyloidogenic Properties of Nanoparticles: A Promising Tool for the Treatment and Diagnostics of Neurodegenerative Diseases*. Oxidative Medicine and Cellular Longevity, 2020, 3534570.

   - koncepcja badań: **70%** - określenie problemu badawczego oraz jego znaczenia
   - metodyka: <u>nie dotyczy</u>
   - praca terenowa: <u>nie dotyczy</u>
   - praca laboratoryjna: <u>nie dotyczy</u>
   - analiza i zestawienie wyników: <u>nie dotyczy</u>
   - interpretacja wyników i dyskusja: <u>nie dotyczy</u>
   - prace nad manuskryptem (draft, wersja końcowa): **90%**
   - analiza bibliograficzna: **100%**
   - proces publikacji (autor korespondencyjny): **0%**

   Zatem mój wkład pracy naukowej w opublikowanie manuskryptu wynosił w sumie **70%**.

   Jako współautor akceptuję przedstawiony przez Panią mgr inż. Monikę Pichla udział w przygotowaniu powyżej publikacji naukowej, która stanowić będzie część Jej dysertacji doktorskiej:

1. Izabela Sadowska-Bartosz (udział 25%) ....

2. Grzegorz Bartosz (udział 5%) ....

2. Pichla, M., Pulaski, Ł., Kania, K. D., Stefaniuk, I., Cieniek, B., Pieńkowska, N., Bartosz, G., & Sadowska-Bartosz, I. (2020). Nitroxide Radical-Containing Redox Nanoparticles Protect Neuroblastoma SH-SY5Y Cells against 6-Hydroxydopamine Toxicity. Oxidative medicine and cellular longevity, 2020, 9260748.

- koncepcja badań: **10%** – wyznaczenie celów
- metodyka: **80%** – udział w adaptacji metod do oznaczeń
- praca terenowa: nie dotyczy
- praca laboratoryjna:**80%** – wykonywanie oznaczeń
- analiza i zestawienie wyników:**80%**
- interpretacja wyników i dyskusja:**20%**
- prace nad manuskryptem (draft, wersja końcowa): **50%**
- analiza bibliograficzna:**10%**
- proces publikacji (autor korespondencyjny):**0%**

Zatem mój wkład pracy naukowej w opublikowanie manuskryptu wynosił w sumie **50%**.

Jako współautor akceptuję przedstawiony przez Panią mgr inz. Monikę Pichla udział w przygotowaniu powyżej publikacji naukowej, która stanowić będzie część Jej dysertacji doktorskiej:

1. Łukasz Pułaski (udział 3%) ....Ł. Pułaski..........

2. Katarzyna Dominika Kania (udział 10%) ....

3. Ireneusz Stefaniuk (udział 3%) ....

4. Bogumił Cieniek (udział 2%) ....

5. Natalia Pieńkowska (udział 4%) ....

6. Grzegorz Bartosz (udział 3%) ....

7. Izabela Sadowska-Bartosz (udział 25%) ....

3. Pichla, M.; Bartosz, G.; Stefaniuk, I.; Sadowska-Bartosz, I. pH-Responsive Redox Nanoparticles Protect SH-SY5Y Cells at Lowered pH in a Cellular Model of Parkinson Disease. Molecules 2021, 26, 543.

- koncepcja badań: **10%** – wyznaczenie celów
- metodyka: **80%** – udział w adaptacji metod do oznaczeń
- praca terenowa: nie dotyczy
- praca laboratoryjna: **90%** – wykonywanie oznaczeń laboratoryjnych
- analiza i zestawienie wyników: **80%**
- interpretacja wyników i dyskusja: **50%**
- prace nad manuskryptem (draft, wersja końcowa): **50%**
- analiza bibliograficzna: **80%**
- proces publikacji (autor korespondencyjny): **0%**

Zatem mój wkład pracy naukowej w opublikowanie manuskryptu wynosił w sumie **60%**.

2. Pichla, M., Pulaski, Ł., Kania, K. D., Stefaniuk, I., Cieniek, B., Pieńkowska, N., Bartosz, G., & Sadowska-Bartosz, I. (2020). Nitroxide Radical-Containing Redox Nanoparticles Protect Neuroblastoma SH-SY5Y Cells against 6-Hydroxydopamine Toxicity. Oxidative medicine and cellular longevity, 2020, 9260748.

- koncepcja badań: **10%** - wyznaczenie celów
- metodyka: **80% -** udział w adaptacji metod do oznaczeń
- praca terenowa: nie dotyczy
- praca laboratoryjna:**80% -** wykonywanie oznaczeń
- analiza i zestawienie wyników:**80%**
- interpretacja wyników i dyskusja:**20%**
- prace nad manuskryptem (draft, wersja końcowa): **50%**
- analiza bibliograficzna:**10%**
- proces publikacji (autor korespondencyjny):**0%**

Zatem mój wkład pracy naukowej w opublikowanie manuskryptu wynosił w sumie **50%**.

Jako współautor akceptuję przedstawiony przez Panią mgr inż. Monikę Pichla udział w przygotowaniu powyżej publikacji naukowej, która stanowić będzie część Jej dysertacji doktorskiej:

1. Łukasz Pułaski (udział 3%) ....

2. Katarzyna Dominika Kania (udział 10%) ...._Katarzyna Kania_....

3. Ireneusz Stefaniuk (udział 3%) ....

4. Bogumił Cieniek (udział 2%) ....

5. Natalia Pieńkowska (udział 4%) ....

6. Grzegorz Bartosz (udział 3%) ....

7. Izabela Sadowska-Bartosz (udział 25%) ....

3. Pichla, M.; Bartosz, G.; Stefaniuk, I.; Sadowska-Bartosz, I. pH-Responsive Redox Nanoparticles Protect SH-SY5Y Cells at Lowered pH in a Cellular Model of Parkinson Disease. Molecules 2021, 26, 543.

- koncepcja badań: **10%** - wyznaczenie celów
- metodyka: **80% -** udział w adaptacji metod do oznaczeń
- praca terenowa: nie dotyczy
- praca laboratoryjna: **90% -** wykonywanie oznaczeń laboratoryjnych
- analiza i zestawienie wyników: **80%**
- interpretacja wyników i dyskusja: **50%**
- prace nad manuskryptem (draft, wersja końcowa): **50%**
- analiza bibliograficzna: **80%**
- proces publikacji (autor korespondencyjny): **0%**

Zatem mój wkład pracy naukowej w opublikowanie manuskryptu wynosił w sumie **60%**.

2. Pichla, M., Pulaski, Ł., Kania, K. D., Stefaniuk, I., Cieniek, B., Pieńkowska, N., Bartosz, G., & Sadowska-Bartosz, I. (2020). Nitroxide Radical-Containing Redox Nanoparticles Protect Neuroblastoma SH-SY5Y Cells against 6-Hydroxydopamine Toxicity. Oxidative medicine and cellular longevity, 2020, 9260748.

- koncepcja badań: **10%** - wyznaczenie celów
- metodyka: **80%** - udział w adaptacji metod do oznaczeń
- praca terenowa: <u>nie dotyczy</u>
- praca laboratoryjna:**80%** - wykonywanie oznaczeń
- analiza i zestawienie wyników:**80%**
- interpretacja wyników i dyskusja:**20%**
- prace nad manuskryptem (draft, wersja końcowa): **50%**
- analiza bibliograficzna:**10%**
- proces publikacji (autor korespondencyjny):**0%**

Zatem mój wkład pracy naukowej w opublikowanie manuskryptu wynosił w sumie **50%**.

Jako współautor akceptuję przedstawiony przez Panią mgr inż. Monikę Pichla udział w przygotowaniu powyżej publikacji naukowej, która stanowić będzie część Jej dysertacji doktorskiej:

1. Łukasz Pułaski (udział 3%) ....

2. Katarzyna Dominika Kania (udział 10%) ....

3. Ireneusz Stefaniuk (udział 3%) .... *Ireneusz Stefaniuk* ....

4. Bogumił Cieniek (udział 2%) ....

5. Natalia Pieńkowska (udział 4%) ....

6. Grzegorz Bartosz (udział 3%) ....

7. Izabela Sadowska-Bartosz (udział 25%) ....

3. Pichla, M.; Bartosz, G.; Stefaniuk, I.; Sadowska-Bartosz, I. pH-Responsive Redox Nanoparticles Protect SH-SY5Y Cells at Lowered pH in a Cellular Model of Parkinson Disease. Molecules 2021, 26, 543.

- koncepcja badań: **10%** - wyznaczenie celów
- metodyka: **80%** - udział w adaptacji metod do oznaczeń
- praca terenowa: <u>nie dotyczy</u>
- praca laboratoryjna: **90%** - wykonywanie oznaczeń laboratoryjnych
- analiza i zestawienie wyników: **80%**
- interpretacja wyników i dyskusja: **50%**
- prace nad manuskryptem (draft, wersja końcowa): **50%**
- analiza bibliograficzna: **80%**
- proces publikacji (autor korespondencyjny): **0%**

Zatem mój wkład pracy naukowej w opublikowanie manuskryptu wynosił w sumie **60%**.

2. Pichla, M., Pulaski, Ł., Kania, K. D., Stefaniuk, I., Cieniek, B., Pieńkowska, N., Bartosz, G., & Sadowska-Bartosz, I. (2020). Nitroxide Radical-Containing Redox Nanoparticles Protect Neuroblastoma SH-SY5Y Cells against 6-Hydroxydopamine Toxicity. Oxidative medicine and cellular longevity, 2020, 9260748.

- koncepcja badań: **10%** - wyznaczenie celów
- metodyka: **80%** - udział w adaptacji metod do oznaczeń
- praca terenowa: <u>nie dotyczy</u>
- praca laboratoryjna: **80%** - wykonywanie oznaczeń
- analiza i zestawienie wyników: **80%**
- interpretacja wyników i dyskusja: **20%**
- prace nad manuskryptem (draft, wersja końcowa): **50%**
- analiza bibliograficzna: **10%**
- proces publikacji (autor korespondencyjny): **0%**

Zatem mój wkład pracy naukowej w opublikowanie manuskryptu wynosił w sumie **50%**.

Jako współautor akceptuję przedstawiony przez Panią mgr inż. Monikę Pichla udział w przygotowaniu powyżej publikacji naukowej, która stanowić będzie część Jej dysertacji doktorskiej:

1. Łukasz Pułaski (udział 3%) ....

2. Katarzyna Dominika Kania (udział 10%) ....

3. Ireneusz Stefaniuk (udział 3%) ....

4. Bogumił Cieniek (udział 2%) ......*Bogumił Cieniek*...........................

5. Natalia Pieńkowska (udział 4%) ....

6. Grzegorz Bartosz (udział 3%) ....

7. Izabela Sadowska-Bartosz (udział 25%) ....

3. Pichla, M.; Bartosz, G.; Stefaniuk, I.; Sadowska-Bartosz, I. pH-Responsive Redox Nanoparticles Protect SH-SY5Y Cells at Lowered pH in a Cellular Model of Parkinson Disease. Molecules 2021, 26, 543.

- koncepcja badań: **10%** - wyznaczenie celów
- metodyka: **80%** - udział w adaptacji metod do oznaczeń
- praca terenowa: <u>nie dotyczy</u>
- praca laboratoryjna: **90%** - wykonywanie oznaczeń laboratoryjnych
- analiza i zestawienie wyników: **80%**
- interpretacja wyników i dyskusja: **50%**
- prace nad manuskryptem (draft, wersja końcowa): **50%**
- analiza bibliograficzna: **80%**
- proces publikacji (autor korespondencyjny): **0%**

Zatem mój wkład pracy naukowej w opublikowanie manuskryptu wynosił w sumie **60%**.

2. Pichla, M., Pulaski, Ł., Kania, K. D., Stefaniuk, I., Cieniek, B., Pieńkowska, N., Bartosz, G., & Sadowska-Bartosz, I. (2020). Nitroxide Radical-Containing Redox Nanoparticles Protect Neuroblastoma SH-SY5Y Cells against 6-Hydroxydopamine Toxicity. Oxidative medicine and cellular longevity, 2020, 9260748.

- koncepcja badań: **10%** - wyznaczenie celów
- metodyka: **80%** - udział w adaptacji metod do oznaczeń
- praca terenowa: <u>nie dotyczy</u>
- praca laboratoryjna:**80%** - wykonywanie oznaczeń
- analiza i zestawienie wyników:**80%**
- interpretacja wyników i dyskusja:**20%**
- prace nad manuskryptem (draft, wersja końcowa): **50%**
- analiza bibliograficzna:**10%**
- proces publikacji (autor korespondencyjny):**0%**

Zatem mój wkład pracy naukowej w opublikowanie manuskryptu wynosił w sumie **50%**.

Jako współautor akceptuję przedstawiony przez Panią mgr inż. Monikę Pichla udział w przygotowaniu powyżej publikacji naukowej, która stanowić będzie część Jej dysertacji doktorskiej:

1. Łukasz Pułaski (udział 3%) ....

2. Katarzyna Dominika Kania (udział 10%) ....

3. Ireneusz Stefaniuk (udział 3%) ....

4. Bogumił Cieniek (udział 2%) ....

5. Natalia Pieńkowska (udział 4%) ...... *Natalia   Pieńkowska* ....

6. Grzegorz Bartosz (udział 3%) ....

7. Izabela Sadowska-Bartosz (udział 25%) ....

3. Pichla, M.; Bartosz, G.; Stefaniuk, I.; Sadowska-Bartosz, I. pH-Responsive Redox Nanoparticles Protect SH-SY5Y Cells at Lowered pH in a Cellular Model of Parkinson Disease. Molecules 2021, 26, 543.

- koncepcja badań: **10%** - wyznaczenie celów
- metodyka: **80%** - udział w adaptacji metod do oznaczeń
- praca terenowa: <u>nie dotyczy</u>
- praca laboratoryjna: **90%** - wykonywanie oznaczeń laboratoryjnych
- analiza i zestawienie wyników: **80%**
- interpretacja wyników i dyskusja: **50%**
- prace nad manuskryptem (draft, wersja końcowa): **50%**
- analiza bibliograficzna: **80%**
- proces publikacji (autor korespondencyjny): **0%**

Zatem mój wkład pracy naukowej w opublikowanie manuskryptu wynosił w sumie **60%**.

2. Pichla, M., Pulaski, Ł., Kania, K. D., Stefaniuk, I., Cieniek, B., Pieńkowska, N., Bartosz, G., & Sadowska-Bartosz, I. (2020). Nitroxide Radical-Containing Redox Nanoparticles Protect Neuroblastoma SH-SY5Y Cells against 6-Hydroxydopamine Toxicity. Oxidative medicine and cellular longevity, 2020, 9260748.

- koncepcja badań: **10%** - wyznaczenie celów
- metodyka: **80%** - udział w adaptacji metod do oznaczeń
- praca terenowa: <u>nie dotyczy</u>
- praca laboratoryjna: **80%** - wykonywanie oznaczeń
- analiza i zestawienie wyników: **80%**
- interpretacja wyników i dyskusja: **20%**
- prace nad manuskryptem (draft, wersja końcowa): **50%**
- analiza bibliograficzna: **10%**
- proces publikacji (autor korespondencyjny): **0%**

Zatem mój wkład pracy naukowej w opublikowanie manuskryptu wynosił w sumie **50%**.

Jako współautor akceptuję przedstawiony przez Panią mgr inż. Monikę Pichla udział w przygotowaniu powyżej publikacji naukowej, która stanowić będzie część Jej dysertacji doktorskiej:

1. Łukasz Pułaski (udział 3%) ....

2. Katarzyna Dominika Kania (udział 10%) ....

3. Ireneusz Stefaniuk (udział 3%) ....

4. Bogumił Cieniek (udział 2%) ....

5. Natalia Pieńkowska (udział 4%) ....

6. Grzegorz Bartosz (udział 3%) ....*G. Bartosz*..

7. Izabela Sadowska-Bartosz (udział 25%) ....*I. Sadowska-Bartosz*.....................

3. Pichla, M.; Bartosz, G.; Stefaniuk, I.; Sadowska-Bartosz, I. pH-Responsive Redox Nanoparticles Protect SH-SY5Y Cells at Lowered pH in a Cellular Model of Parkinson Disease. Molecules 2021, 26, 543.

- koncepcja badań: **10%** - wyznaczenie celów
- metodyka: **80%** - udział w adaptacji metod do oznaczeń
- praca terenowa: <u>nie dotyczy</u>
- praca laboratoryjna: **90%** - wykonywanie oznaczeń laboratoryjnych
- analiza i zestawienie wyników: **80%**
- interpretacja wyników i dyskusja: **50%**
- prace nad manuskryptem (draft, wersja końcowa): **50%**
- analiza bibliograficzna: **80%**
- proces publikacji (autor korespondencyjny): **0%**

Zatem mój wkład pracy naukowej w opublikowanie manuskryptu wynosił w sumie **60%**.

2. Pichla, M., Pulaski, Ł., Kania, K. D., Stefaniuk, I., Cieniek, B., Pieńkowska, N., Bartosz, G., & Sadowska-Bartosz, I. (2020). Nitroxide Radical-Containing Redox Nanoparticles Protect Neuroblastoma SH-SY5Y Cells against 6-Hydroxydopamine Toxicity. Oxidative medicine and cellular longevity, 2020, 9260748.

- koncepcja badań: **10%** - wyznaczenie celów
- metodyka: **80%** - udział w adaptacji metod do oznaczeń
- praca terenowa: nie dotyczy
- praca laboratoryjna:**80%** - wykonywanie oznaczeń
- analiza i zestawienie wyników:**80%**
- interpretacja wyników i dyskusja:**20%**
- prace nad manuskryptem (draft, wersja końcowa): **50%**
- analiza bibliograficzna:**10%**
- proces publikacji (autor korespondencyjny):**0%**

Zatem mój wkład pracy naukowej w opublikowanie manuskryptu wynosił w sumie **50%**.

Jako współautor akceptuję przedstawiony przez Panią mgr inż. Monikę Pichla udział w przygotowaniu powyżej publikacji naukowej, która stanowić będzie część Jej dysertacji doktorskiej:

1. Łukasz Pułaski (udział 3%) ....

2. Katarzyna Dominika Kania (udział 10%) ....

3. Ireneusz Stefaniuk (udział 3%) ....

4. Bogumił Cieniek (udział 2%) ....

5. Natalia Pieńkowska (udział 4%) ....

6. Grzegorz Bartosz (udział 3%) .... *G. Bartosz* ....

7. Izabela Sadowska-Bartosz (udział 25%) .... *I Sadowska - Bartosz* ....

3. Pichla, M.; Bartosz, G.; Stefaniuk, I.; Sadowska-Bartosz, I. pH-Responsive Redox Nanoparticles Protect SH-SY5Y Cells at Lowered pH in a Cellular Model of Parkinson Disease. Molecules 2021, 26, 543.

- koncepcja badań: **10%** - wyznaczenie celów
- metodyka: **80%** - udział w adaptacji metod do oznaczeń
- praca terenowa: nie dotyczy
- praca laboratoryjna: **90%** - wykonywanie oznaczeń laboratoryjnych
- analiza i zestawienie wyników: **80%**
- interpretacja wyników i dyskusja: **50%**
- prace nad manuskryptem (draft, wersja końcowa): **50%**
- analiza bibliograficzna: **80%**
- proces publikacji (autor korespondencyjny): **0%**

Zatem mój wkład pracy naukowej w opublikowanie manuskryptu wynosił w sumie **60%**.

Jako współautor akceptuję przedstawiony przez Panią mgr inż. Monikę Pichla udział w przygotowaniu powyżej publikacji naukowej, która stanowić będzie część Jej dysertacji doktorskiej:

1. Grzegorz Bartosz (udział 5%) .... *G. Bartosz* ....

2. Ireneusz Stefaniuk (udział 5%) ....

3. Izabela Sadowska-Bartosz (udział 30%) .... *I. Sadowska - Bartosz* ....

4. Pichla, M., Bartosz, G., Pieńkowska, N., & Sadowska-Bartosz, I. (2020). Possible artefacts of antioxidant assays performed in the presence of nitroxides and nitroxide-containing nanoparticles. Analytical biochemistry, 597, 113698.

- koncepcja badań: **10%** - udział w określeniu problemu badawczego
- metodyka: **40%** - udział w adaptacji metod do oznaczeń
- praca terenowa: <u>nie dotyczy</u>
- praca laboratoryjna: **90%** - wykonywanie oznaczeń laboratoryjnych
- analiza i zestawienie wyników: **65%**
- interpretacja wyników i dyskusja: **40%**
- prace nad manuskryptem (draft, wersja końcowa): **40%**
- analiza bibliograficzna: **10%**
- proces publikacji (autor korespondencyjny): **0%**

Zatem mój wkład pracy naukowej w opublikowanie manuskryptu wynosił w sumie **50%**.

Jako współautor akceptuję przedstawiony przez Panią mgr inż. Monikę Pichla udział w przygotowaniu powyżej publikacji naukowej, która stanowić będzie część Jej dysertacji doktorskiej:

1. Grzegorz Bartosz (udział 10% .... *G. Bartosz* ....

2. Natalia Pieńkowska (udział 10%) ....

3. Izabela Sadowska-Bartosz (udział 30%) .... *I. Sadowska - Bartosz* ....

Jako współautor akceptuję przedstawiony przez Panią mgr inż. Monikę Pichla udział w przygotowaniu powyżej publikacji naukowej, która stanowić będzie część Jej dysertacji doktorskiej:

1. Grzegorz Bartosz (udział 5%) ....

2. Ireneusz Stefaniuk (udział 5%) ....*Ireneusz Stefaniuk*..............................

3. Izabela Sadowska-Bartosz (udział 30%) ....

4. Pichla, M., Bartosz, G., Pieńkowska, N., & Sadowska-Bartosz, I. (2020). Possible artefacts of antioxidant assays performed in the presence of nitroxides and nitroxide-containing nanoparticles. Analytical biochemistry, 597, 113698.

- koncepcja badań: **10%** - udział w określeniu problemu badawczego
- metodyka: **40%** - udział w adaptacji metod do oznaczeń
- praca terenowa: nie dotyczy
- praca laboratoryjna: **90%** - wykonywanie oznaczeń laboratoryjnych
- analiza i zestawienie wyników: **65%**
- interpretacja wyników i dyskusja: **40%**
- prace nad manuskryptem (draft, wersja końcowa): **40%**
- analiza bibliograficzna: **10%**
- proces publikacji (autor korespondencyjny): **0%**

Zatem mój wkład pracy naukowej w opublikowanie manuskryptu wynosił w sumie **50%**.

Jako współautor akceptuję przedstawiony przez Panią mgr inż. Monikę Pichla udział w przygotowaniu powyżej publikacji naukowej, która stanowić będzie część Jej dysertacji doktorskiej:

1. Grzegorz Bartosz (udział 10% ....

2. Natalia Pieńkowska (udział 10%) ....

3. Izabela Sadowska-Bartosz (udział 30%) ....

Jako współautor akceptuję przedstawiony przez Panią mgr inż. Monikę Pichla udział w przygotowaniu powyżej publikacji naukowej, która stanowić będzie część Jej dysertacji doktorskiej:

1. Grzegorz Bartosz (udział 5%) .... *G. Bartosz* ....

2. Ireneusz Stefaniuk (udział 5%) ....

3. Izabela Sadowska-Bartosz (udział 30%) .... *J. Sadowska - Bartosz* ....

4. Pichla, M., Bartosz, G., Pieńkowska, N., & Sadowska-Bartosz, I. (2020). Possible artefacts of antioxidant assays performed in the presence of nitroxides and nitroxide-containing nanoparticles. Analytical biochemistry, 597, 113698.

- koncepcja badań: **10%** - udział w określeniu problemu badawczego
- metodyka: **40%** - udział w adaptacji metod do oznaczeń
- praca terenowa: <u>nie dotyczy</u>
- praca laboratoryjna: **90%** - wykonywanie oznaczeń laboratoryjnych
- analiza i zestawienie wyników: **65%**
- interpretacja wyników i dyskusja: **40%**
- prace nad manuskryptem (draft, wersja końcowa): **40%**
- analiza bibliograficzna: **10%**
- proces publikacji (autor korespondencyjny): **0%**

Zatem mój wkład pracy naukowej w opublikowanie manuskryptu wynosił w sumie **50%**.

Jako współautor akceptuję przedstawiony przez Panią mgr inż. Monikę Pichla udział w przygotowaniu powyżej publikacji naukowej, która stanowić będzie część Jej dysertacji doktorskiej:

1. Grzegorz Bartosz (udział 10% .... *G. Bartosz* ....

2. Natalia Pieńkowska (udział 10%) ....

3. Izabela Sadowska-Bartosz (udział 30%) .... *J. Sadowska - Bartosz* ....

Jako współautor akceptuję przedstawiony przez Panią mgr inż. Monikę Pichla udział w przygotowaniu powyżej publikacji naukowej, która stanowić będzie część Jej dysertacji doktorskiej:

1. Grzegorz Bartosz (udział 5%) ....

2. Ireneusz Stefaniuk (udział 5%) ....

3. Izabela Sadowska-Bartosz (udział 30%) ....

4. Pichla, M., Bartosz, G., Pieńkowska, N., & Sadowska-Bartosz, I. (2020). Possible artefacts of antioxidant assays performed in the presence of nitroxides and nitroxide-containing nanoparticles. Analytical biochemistry, 597, 113698.

- koncepcja badań: **10%** - udział w określeniu problemu badawczego
- metodyka: **40%** - udział w adaptacji metod do oznaczeń
- praca terenowa: nie dotyczy
- praca laboratoryjna: **90%** - wykonywanie oznaczeń laboratoryjnych
- analiza i zestawienie wyników: **65%**
- interpretacja wyników i dyskusja: **40%**
- prace nad manuskryptem (draft, wersja końcowa): **40%**
- analiza bibliograficzna: **10%**
- proces publikacji (autor korespondencyjny): **0%**

Zatem mój wkład pracy naukowej w opublikowanie manuskryptu wynosił w sumie **50%**.

Jako współautor akceptuję przedstawiony przez Panią mgr inż. Monikę Pichla udział w przygotowaniu powyżej publikacji naukowej, która stanowić będzie część Jej dysertacji doktorskiej:

1. Grzegorz Bartosz (udział 10% ....

2. Natalia Pieńkowska (udział 10%) .... *Natalia Pieńkowska* ....

3. Izabela Sadowska-Bartosz (udział 30%) ....

PRACE WCHODZĄCE W SKŁAD ROZPRAWY DOKTORSKIEJ

1. Pichla M., Bartosz G., Sadowska-Barotsz I., *The anti-aggregative and anti-amyloidogenic properties of nanoparticles: a promising tool for the treatment and diagnostics of neurodegenerative diseases*. Oxidative Medicine and Cellular Longevity, 2020, 3534570.

IF$_{2020}$: 5.076; MNiSW: 100

Review Article

The Antiaggregative and Antiamyloidogenic Properties of Nanoparticles: A Promising Tool for the Treatment and Diagnostics of Neurodegenerative Diseases

Monika Pichla,[1] **Grzegorz Bartosz** [iD]**,**[2] **and Izabela Sadowska-Bartosz** [iD]**[1]**

[1]*Department of Analytical Biochemistry, Institute of Food Technology and Nutrition, College of Natural Sciences, Rzeszow University, Zelwerowicza Street 4, 35-601 Rzeszów, Poland*
[2]*Department of Bioenergetics, Food Analysis and Microbiology, College of Natural Sciences, Rzeszow University, Zelwerowicza Street 4, 35-601 Rzeszów, Poland*

Correspondence should be addressed to Izabela Sadowska-Bartosz; isadowska@poczta.fm

Due to the progressive aging of the society, the prevalence and socioeconomic burden of neurodegenerative diseases are predicted to rise. The most common neurodegenerative disorders nowadays, such as Parkinson's disease, Alzheimer's disease, and amyotrophic lateral sclerosis, can be classified as proteinopathies. They can be either synucleinopathies, amyloidopathies, tauopathies, or TDP-43-related proteinopathies; thus, nanoparticles with a potential ability to inhibit pathological protein aggregation and/or degrade already existing aggregates can be a promising approach in the treatment of neurodegenerative diseases. As it turns out, nanoparticles can be a double-edged sword; they can either promote or inhibit protein aggregation, depending on coating, shape, size, surface charge, and concentration. In this review, we aim to emphasize the need of a breakthrough in the treatment of neurodegenerative disorders and draw attention to nanomaterials, as they can also serve as a diagnostic tool for protein aggregates or can be used in a high-throughput screening for novel antiaggregative compounds.

1. Introduction

Undoubtedly, the progress in medical and biological studies has led to increased quality of life and extension of life span. Furthermore, the overall fertility has dropped and these two factors contribute to the aging of the society. Due to this phenomenon, the increase in prevalence of neurodegenerative diseases is predicted to be more visible in the future than it currently is. According to the World Health Organization, it is projected that the number of people aged ≥ 65 will grow from about 524 million in 2010 to around 1.5 billion in 2050 [1]. Neurodegenerative diseases impose burden not only on people affected by this disorder but also on their caregivers. There are three major neurodegenerative diseases whose pervasiveness and incidence significantly rise with age.

First of them and the most common one is Alzheimer's disease (AD), which affects approximately 30% of people aged 85 or older. After the age of 85, the incidence of AD rises gradually from 6 to 8% per year, in contrast to the 0.5% rise per year when peoples' age ranges between 65 and 75 [2]. The second most common is Parkinson's disease (PD), which affects 10-15 per 100 000 people annually [3]. Its prevalence has been more than two times higher in 2016 (6.1 million cases) comparing to 2010 (2.5 million cases) and may reach 2% among people aged ≥ 65. Consequently, it is estimated that in 2050, there will be more than 12 million cases of PD worldwide [4]. Subsequently, amyotrophic lateral sclerosis's (ALS) annual incidence is approximately 1-2.6 new cases per 100 000 persons. This disease is characterized by rapid progression with average survival 3-4 years from onset, whereas the average age of onset nowadays is 59-60 years [5].

Indeed, there is a variety of symptoms of the aforementioned neurodegenerative diseases, but the exact pathophysiology of these conditions is still elusive. Nevertheless, it should be emphasized that they have some common pathogenic features. Among them, genetic [6] and environmental

TABLE 1: Characteristics of the most common neurodegenerative diseases.

Disease	Hallmarks	Genetic factors	Ref.
Alzheimer's disease	(i) Senile plaques comprising deposits of β-amyloid (ii) Intracellular neurofibrillary tangles (iii) Tau protein aggregation (iv) Neuronal loss	(i) Presence of specific allelic variants of *APOE* gene ($\varepsilon2$, $\varepsilon3$, and $\varepsilon4$) (ii) Apo$\varepsilon4$ allele specifically in sporadic form of AD (iii) Mutations of gene coding for amyloid precursor protein (*APP*), presenilin 1, and presenilin 2 (n or PSEN2) in the familial form of AD	[9]
Parkinson's disease	(i) Presence of Lewy bodies—neuronal inclusions of fibrillated aggregates comprising α-synuclein and ubiquitin (ii) Degeneration and loss of dopaminergic neurons especially in *substantia nigra pars compacta* (iii) Dopamine deficiency	(i) Gene mutations: *SNCA*, *Parkin*, *PINK1*, *LRRK2*, *DJ-1*, *VPS35*, *PLA2G6*, *DCTN1*, *FBX07*, and *ATP13A2*	[9]
Amyotrophic lateral sclerosis	(i) Presence of ubiquitinated inclusions comprising TDP-43, FUS, OPTN, ATXN2, C9ORF72, and UBQLN2 (ii) Slow and progressive degeneration and loss of motor neurons (iii) Neuroinflammation	(i) Gene mutations: *SOD1*, *C9ORF72*, *FUS*, and *TARDBP*	[9–12]

[7] factors can be listed. Yet, the most classical feature of all these diseases is protein misfolding in specific brain regions; thus, these disorders can be classified as proteinopathies (Table 1). The hallmark of proteinopathies is either intra- or extracellular accumulation of aggregates in the central nervous system that are abundant in β-sheets. In these diseases, altered forms of proteins, which play a physiological role, accumulate in the brain. They turn out to have pathological functions after modifications of their 3D structure, which in consequence leads to self-aggregation, aggregate growth, and eventually precipitation [8].

Unfortunately, the current and only available treatment of neurodegenerative diseases is strictly symptomatic. Treatment of PD has not significantly changed over decades: L-DOPA treatment is a gold standard for 60 years so far. Apart from levodopa-carbidopa preparations, other dopamine agonists, monoamine oxidase-B inhibitors, cholinesterase inhibitors, and selective serotonin and norepinephrine reuptake inhibitors are also used as a drug regimen [13, 14]. The treatment of AD is not much more sophisticated and is based on cholinesterase inhibitors and NDMA receptor agonist, namely, memantine. It addresses not only the behavioural and cognitive symptoms but also covers for functional ones [15]. A review of treatments for AD in clinical trials can be found in a recent article [16], demonstrating that there is no effective antiaggregative treatment so far. Similarly, the information about PD drugs in clinical trials can be found in another review [17]. When it comes to ALS, there is only one FDA approved drug—riluzole, which has a glutamine agonist activity and extends the survival of patients by only 2-3 months [18, 19].

Due to the abovementioned facts, in this review, we aim to highlight the burden of neurodegenerative diseases and discuss novel approaches to their treatment using nanomaterials (Figure 1). Furthermore, we would like to point out the versatility and impact of the nanoparticles used to combat proteinopathies, on pathological protein aggregation.

2. Protein Aggregation in Neurodegeneration

A body of evidence suggests that the accumulation and transmission of α-synuclein (α-syn) aggregates in the midbrain are highly associated with the pathogenesis of PD [20]. α-Synuclein is a presynaptic protein, which probably plays a regulatory function in modulation of synaptic plasticity, control of presynaptic vesicle pool size, release of neurotransmitters, and vesicle recycling. Its structure can be divided into three regions: an amphiphilic N-terminus, an acidic C-terminus, and a hydrophobic central domain, which is known as the nonamyloid β component (NAC). The NAC region is crucial for α-syn aggregation and formation of β-sheet fibrils, which are the main elements of Lewy bodies [21]. Studies showed that electrostatic forces play a crucial role in α-syn fibrillation; thus, this process can be obstructed by charged nanoparticles [22].

Yet, interestingly, the exact molecular mechanism, time of occurrence, and influence of protein misfolding on the onset and/or progression of these particular diseases are still beyond reach. According to Janezic et al. who introduced a new mouse model for PD studies, neurophysiological changes forerun and are not driven by α-syn aggregate formation [23]. Nevertheless, the search for antiaggregative agents is still highly desirable.

Amyloid β peptide has a leading role in the onset and progression of AD. In this disease, amyloid plaques containing aggregated amyloid-β protein (Aβ) are surrounded by morphologically altered neurons, cause synapse and memory loss, and induce neurotoxicity [24].

As a matter of fact, Aβ is physiologically present and derives from the amyloid precursor protein (APP), which is implicated in regulation of synapse formation. Unfortunately, under particular circumstances, it starts to aggregate and initiates the disease progression [25]. Amyloid-β protein monomers tend to aggregate into several forms, namely, soluble oligomers, protofibrils, and insoluble amyloid fibrils which can further aggregate into amyloid plaques. This
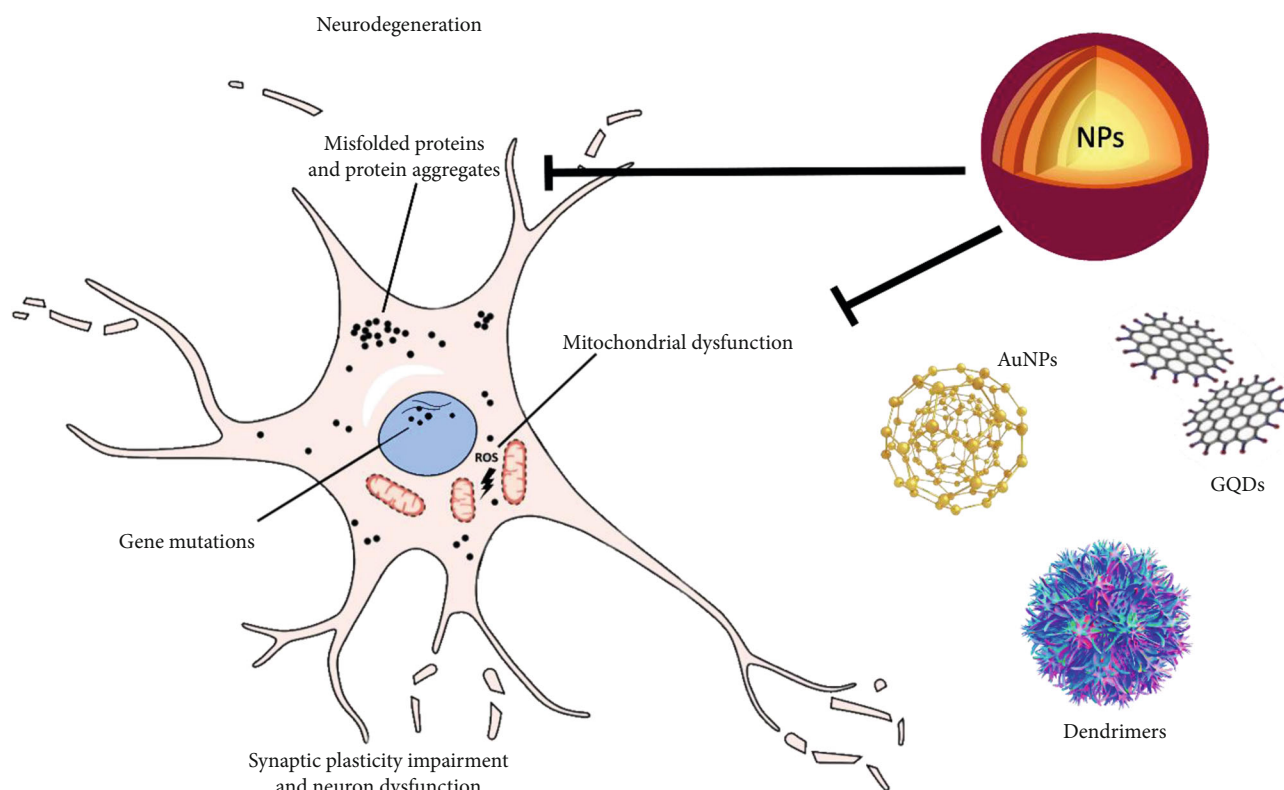
FIGURE 1: Impact of NPs on neurodegeneration hallmarks.

process is accompanied by oxidative stress, leading to the formation of oxidized proteins and lipid peroxidation. Products of lipid peroxidation, especially 4-hydroxynonenal, can in turn disrupt function of glucose and glutamate transporters and of ion-dependent ATPases [26]. Therefore, Aβ advocates synaptic membrane depolarization, uncontrolled Ca^{2+} influx, and mitochondrial damage, which cause undesirable changes in cellular activity [27].

Additionally, tau protein is being hyperphosphorylated because of changes in protein kinase activity, which are a result of Aβ aggregation. The hyperphosphorylated form of tau protein becomes a core of neurofibrillary tangle (NFT) formation, whereas physiologically tau protein fosters the assemblance of tubulin into microtubules and helps to maintain their stability. The link between the existence of NFTs and neuronal dysfunction is straightforward. Notwithstanding, the relation of Aβ and NTFs is intertwined, because the inhibition of tau generation can impact production of Aβ and its derivatives [28].

3. Nanoparticles as Therapeutics of the Future

A nanoparticle (NP) is defined as a particle of matter that is between 1 and 100 nanometres in at least one dimension. Nanoparticles arose as attractive tools for both therapeutic and diagnostic applications, especially in imaging, diagnostics, and drug delivery. They can be synthesized from a broad range of materials, such as polymers, metals, or carbon-based molecules. NPs are also highly functional because of the ease with which their shape, size, and sur-

face properties can be modified. Furthermore, NP properties can be also altered by attachment of other substances to the surface or their entrapment within the NP cavities, if these exist (Figure 2) [29].

3.1. Graphene Quantum Dots. Graphene quantum dots (GQDs) are less than 100 nm in size and are made of single- or few-layer graphene (Figure 3). They have been widely used in nanobiomedicine by virtue of their low cytotoxicity and high biocompatibility [30]. The group of Kim et al. demonstrated that GQDs were able to pass through the BBB. In the brain, they reduced α-syn fibrillization and triggered fibril disaggregation in a time-dependent manner by direct interaction with mature fibrils. The binding between GQDs and α-syn is driven by negatively charged carboxyl groups of GDQs and the positively charged α-syn region. Furthermore, these GQDs did not manifest any long-term toxicity *in vivo* and *in vitro* and also were able to prevent neuronal death, diminish Lewy body and Lewy neurite formation, and alleviate mitochondrial damage and dysfunction, and last but not least, they have the ability to prevent neuron to neuron transmission of pathological α-syn. Moreover, experiments performed on a mouse model showed that GQD protected against α-syn preformed fibril-induced loss of dopaminergic neurons and alleviated motor deficits [31].

With regard to AD, GQDs were also used to inhibit Aβ aggregation. The β-amyloid peptide consists of 39-42 amino acids, where several regions can be defined. The His13-Lys16 (HHQK) region plays a significant role in oligomerization and fibril formation. This region is a crucial component of

Ligands
(i) Amino acids
(ii) Antibodies
(iii) Antioxidants
(iv) Peptides

Coating

(i) Bare
(ii) BSA
(iii) Chitosan
(iv) Citrate
(v) PEG
(vi) PGLA
(vii) Others...

Charge

(i) Negative
(ii) Positive
(iii) Zwitterionic

NPs

Application

(i) Inhibition of protein
    aggregation
(ii) Drug screening
(iii) Diagnostics
(iv) Analyzing mechanisms
     of protein aggregation

Size
(i) 1 nm
(ii) 10 nm
(iii) 100 nm

Core

(i) Carbon–based
(ii) Cerium
(iii) Gold
(iv) Iron
(v) Silica–based
(vi) Selenium
(vii) Others...

FIGURE 2: Possible modifications of NPs for prevention and diagnostics of neurodegeneration.

Properties of GQDS:
(i) Low toxicity
(ii) High biocompatibility
(iii) Pass through BBB
(iv) Reduce α-syn fibrillization
(v) Prevent neuronal death
(vi) Diminish Lewy body formation
(vii) Alleviate mitochondrial damage
     and dysfunction
(viii) Prevent neuron to neuron transmisssion
      of α-syn
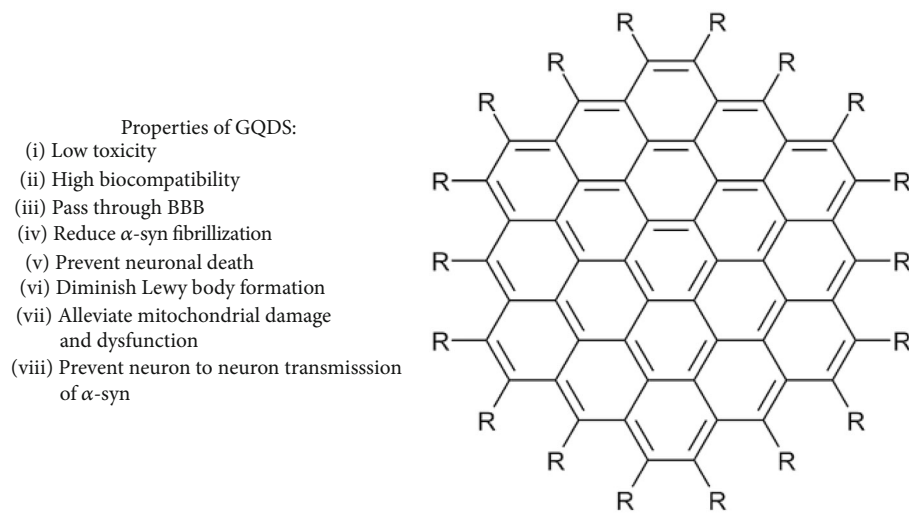
FIGURE 3: The structure and properties of GQDs.

glycosaminoglycan (GAG) binding site, which facilitates a conformational change of Aβ from soluble and unordered α-helix to stable β-sheet [32]. A construct composed of GQDs and tramiprosate, a mimic of GAGs, which specifically binds to HQQK motif and inhibits Aβ peptide aggregation, showed an inhibition of Aβ aggregation driven by breaking β-sheets. Furthermore, GQDs combined with tramiprosate evidently protected PC12 cells from Aβ-induced cytotoxicity, meanwhile exhibiting a synergistic effect [33].

3.2. Dendrimers.
Dendrimers are highly branched, tree-like polymers with unique properties thanks to their terminal functional surface groups (Figure 4). The size, shape, and surface charge change with an increase in generation. Dendrimers are highly functional because of simplicity of modifying their biological and/or physicochemical properties [34, 35]. There is evidence that generations 3, 4, and 5 of PAMAM dendrimers are able to interfere with Aβ aggregation by blocking growth of new fibrils and breaking the existing ones in a concentration- and generation-dependent
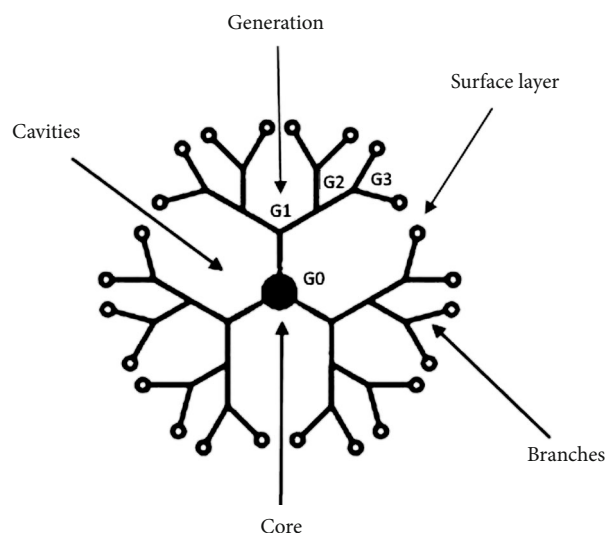
FIGURE 4: The structure of dendrimers.

manner: the higher the dendrimer concentration and generation, the lower number of new fibrils [36]. A similar impact of dendrimers on α-syn aggregates has been observed. The dendrimers inhibit formation of β-sheet structures and disrupt remaining β-sheets or the agglomerates, in concentration and generation axis [37]. Furthermore, only full-generation PAMAM dendrimers, which have the cationic amino groups on their surface, were able to interact with the basic amino acid N-terminal region of α-syn responsible for the β-sheet formation and protein aggregation, contrary to half-generation PAMAM dendrimers [38]. Third and fifth generations of polylysine dendrimers obstructed amyloid aggregation in solution, whereas generation 3 dendrimers also protected SH-SY5Y cells against amyloid-induced toxicity [39].

3.3. Metal Nanoparticles. Cerium oxide nanoparticles (CeO_2 NPs) or nanoceria are multifaceted polymers. They are characterized by good bioavailability and ability to mimic superoxide dismutase or catalase activity. They are quite potent ROS and nitric oxide scavengers. The antioxidant properties of CeO_2 NPs are linked to the Ce^{3+}/Ce^{4+} redox shift. Additionally, research shows that nanoceria are able to protect neurons against $A\beta$-induced mitochondrial fragmentation and also reduce DRP-1 hyperphosphorylation on Ser616, which is related with AD and neurodegeneration. Inhibiting this posttranslational modification turns out to be a potential mechanism of mitochondrial preservation [40]. Beyond that, another group of researchers studied the influence of CeO_2 NPs in a yeast model of PD. Nanoceria significantly increased the viability of yeast cells expressing α-syn. In addition, these NPs decreased α-syn-induced ROS production and alleviated mitochondrial dysfunction and fragmentation. The most probable mechanism of inhibiting the formation of α-syn aggregates occurs by a direct interaction of these nanoceria with α-syn monomers or oligomers; hence, their miscellaneous properties are also exhibited by the ability to adsorb α-syn on the nanoparticle surface [41].

Gold nanoparticles (AuNPs) have been extensively used in biomedicine because of their great biocompatibility, chemical inertness, and effortless size control. AuNPs are also able to abrogate aggregation of pathological proteins. Nevertheless, they may be toxic; toxicity of gold NPs significantly depends on their size, charge, and coating. Large AuNPs (36 nm and 18 nm) increase $A\beta$ fibrillation, whereas small ones are able to delay (6 nm) or utterly inhibit (1.9 nm) this process [42]. Particularly, smaller, anionic NPs exhibit better ability to halt protein aggregation. The researchers have studied four different coatings (citrate, poly(acrylic acid) (PAA), poly(allylamine) hydrochloride (PAH), or polyelectrolyte surfaces) and three different sizes of AuNPs (8 nm, 18 nm, and 40 nm). The results altogether demonstrated that PAA-coated, 18 nm AuNPs exhibited superiority in the inhibition of $A\beta$ aggregation and were the least toxic towards human neuroblastoma SH-SY5Y cells [43]. In order to improve the ability of AuNPs to cross the BBB, Prades et al. created an AuNP conjugated with two peptides, where one of the peptide sequences was designed to interact with the transferrin receptor. The authors suggest that this platform can increase the efficiency of drug delivery into the brain [44]. Noteworthily, natural compounds are also able to obstruct amyloid fibrillation and break existing amyloid fibrils, one of which is curcumin [45]. Because of its hydrophobicity and thus insolubility in water, curcumin has to be conjugated with other compounds [46]. Water-soluble curcumin-functionalized gold nanoparticles turned out to efficiently inhibit amyloid fibrillation, but also to break and dissolve $A\beta$ fibrils. Furthermore, these curcumin-AuNPs protect neuro2a cells from $A\beta_{1-40}$ fibril-induced cytotoxicity, giving nearly doubled improvement in viability. It is suspected that the great inhibitory efficiency is a result of nanoparticle binding to the fibrils via curcumin moiety and disrupting the elongation phase of fibrillation [47].

3.4. Antioxidant-Loaded NPs. Apart from the abovementioned example, other phytochemicals have also arisen as useful in prohibiting pathological protein aggregation regarding neurodegenerative diseases (Figure 5). Among them, baicalein [48], chlorogenic acid [49], gallic acid [50], and many other natural compounds [51] are able to inhibit the formation of α-syn aggregates and/or even disaggregate existing ones. Selenium nanoparticles (SeNPs) turned out to be an effective carrier of antioxidants. Their peculiar biomedical applications and wide range of therapeutical properties are ascribed mainly to the ability to modulate redox state. Moreover, SeNPs show low toxicity and great biodegradability in vivo [52]. Yang et al. investigated anti-$A\beta$-aggregative and antioxidative properties of SeNPs conjugated with chlorogenic acid (CGASeNPs). These authors hypothesized that binding CGA with nanoparticles will improve its bioavailability and stability. They proved that antiaggregative properties of CGASeNPs are contributed by their ability to bind $A\beta_{40}$ on their surface. Furthermore, CGASeNPs effectively scavenged ROS and protected PC12 cells against $A\beta$-induced toxicity [53]. Likewise, the same group designed SeNPs modified with resveratrol and tested their properties against ion metal-

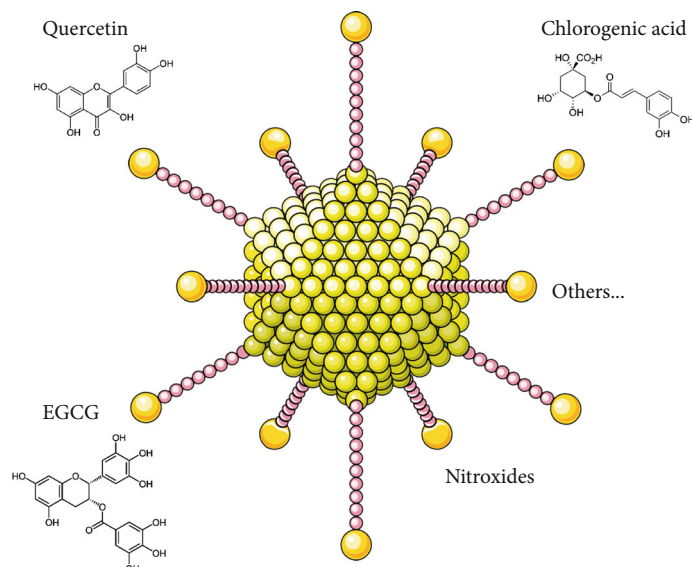FIGURE 5: Possible ligands of antioxidant-loaded nanoparticles.

induced $A\beta42$ aggregation. They obtained similar effects as described above, i.e., that resveratrol and SeNPs exhibit synergistic effect regarding the inhibition of pathological protein aggregation [54]. A nanocomposite engineered from quercetin, SeNPs, and polysorbate 80 can serve as another example of SeNPs combined with antioxidants. *In vitro* analyses showed that the nanocomposite exhibited greater solubility in water comparing to quercetin *per se*, which has poor aqueous solubility. On top of that, such nanocomposite had an exceptional antioxidative activity, inhibited $A\beta_{1-42}$ monomer aggregation, and protected PC12 cells from hydrogen peroxide-induced cell death [55]. Zhang et al. studied both EGCG-SeNPs and NPs conjugated with EGCG and Tet-1 peptide. Tet-1-EGCG-SeNPs showed better efficacy comparing to NPs without the peptide. Both types of NPs not only protected PC-12 cells against amyloid-induced cytotoxicity and inhibited $A\beta$ fibrillation but were also able to dissociate existing fibrils into nontoxic monomeric state. Nevertheless, peptide-containing NPs had overall better performance due to increased neuronal targeting efficiency *in vitro* [56]. NPs loaded with other antioxidants, namely, ferulic acid (as a powerful anti-inflammatory agent) and tannic acid (acting as an inhibitor of α-syn fibrillation), exhibited potent inhibitory effect on α-syn aggregation, diminished proinflammatory responses, and reduced oxidative stress caused by α-syn [57]. Additionally, curcumin-loaded NPs inhibited amyloid-like aggregation of superoxide dismutase (SOD) 1, which occurs in about 20% of familial ALS cases [58].

Nanoparticles loaded with synthetic antioxidants can also serve as antiaggregative agents. Nitroxides exhibited better efficacy in prevention of nitration reactions and were more reactive than natural antioxidant, vitamin E [59]. It has been established that nitroxide-containing redox NPs are able to alleviate typical aspects of neurodegenerative diseases, namely, protect cells against oxidative stress, improve mitochondrial function, and inhibit $A\beta$ aggregation [60, 61].

4. Other Therapeutic Approaches

Unquestionably, transition metals are among the main culprits of pathological protein accumulation. Moreover, they widely contribute to an altered redox state; thus, chelators might bring alleviation of the toxic activity of these metals. Liu et al. created a chelating nanoparticle, in a nutshell—a NP conjugated with 2-methyl-N-(2′-aminoethyl)-3-hydroxyl-4-pyridinone. This construct significantly inhibited $A\beta$ aggregation, protected human cortical neuronal cells from $A\beta$-induced cytotoxicity, and had no impact on cell proliferation [62].

Given the fact that the nanoparticle efficacy in inhibiting protein aggregation greatly depends on the surface charge, the use of amino acids as coating agents is not surprising; they may enhance biocompatibility of nanoparticles. It is mainly due to the fact that amino acids are zwitterionic. Antosova et al. proved that amino acid-coated superparamagnetic nanoparticles can be quite a powerful tool for treatment of amyloidopathies. The group showed that tryptophan-coated NPs exhibited the best antiaggregative properties [63]. Furthermore, others demonstrated that histidine-coated nanoparticles can completely suppress amyloid fibril formation [64]. Moreover, lysine-coated Fe_3O_4 NPs were less toxic than bare iron oxide NPs, strongly bound to monomeric α-syn, and inhibited the early phases of its aggregation [65].

NPs can be also used as safer carriers for gene therapy, instead of viral vectors. Niu et al. created multifunctional magnetic nanoparticles which are a complex platform that combines elements of cell targeting, controlled drug release, and gene therapy. The authors developed a NP that interferes with α-syn synthesis by shRNA, hence

alleviating its toxic effect, so cell death is inhibited both *in vitro* and *in vivo* [66].

5. The Dark Side of the Nanoparticles with a Useful Outcome

Despite undoubted success of some nanoparticles as promising antineurodegenerative compounds, it is important to mention that there is also data on their possible contribution to the disease progression. A plethora of evidence suggests that the nanostructures can influence protein fibrillation depending on various conditions, including the coating, size, surface charge, and concentration. Such discrepancy has been seen for example in silica-based nanoparticles, where positively charged silica nanoparticles inhibited α-syn fibrillation and negatively charged one had an opposite effect [67]. Also, it was also established that SiO_2NPs upregulate α-syn expression, inhibit protein levels of the ubiquitin-proteasome system, and induce autophagy by interference in the PI3K-Akt-mTOR signalling pathway [68].

Contrary to that, negatively charged gold nanoparticles act as chaperones and prevent Aβ fibrillation [69]. Yet, regarding α-syn, the opposite effect was seen: gold nanoparticles are also a double-edged sword. Citrate-capped (negatively charged) AuNPs speeded up the formation of α-syn aggregates in nanomolar concentrations, and time of the nucleation phase was dependent on the surface availability. The smaller the NPs (10-14 nm), the more aggregate growth acceleration, whereas particular sizes (22 nm) were able to inhibit the fibrils' growth; thus, in summary, the AuNP aggregative properties hinge on their size and concentration [70].

Nowadays, numerous NPs have been used in a variety of fields, namely, electronics, pharmaceuticals, cosmetics, and fabrics; hence, their toxicity has started to be more widely observed and studies on the health risks are a bit behind the prompt development of nanotechnology, regardless of a body of evidence of toxic effects of NPs, both *in vitro* and *in vivo* [71]. For example, Shah et al. prove that nanoscale-alumina can accumulate in the brains of exposed animals and thus induce oxidative stress and neurodegeneration. It promoted the production of toxic Aβ through the amyloidogenic pathway, caused overexpression of APP, and increased the β-secretase BACE1 activity that boosted the formation of Aβ aggregates. Their findings suggest that exposure to nanoalumina might increase the probability of the neurodegenerative disease onset [72].

It is worth mentioning that TiO_2NPs are commonly used in numerous daily use products like cosmetics or antiseptic agents. These NPs turned up to induce α-syn fibrillation *via* shortening its nucleation process and may contribute to PD onset [73]. Additionally, there is a positive correlation between α-syn expression levels and TiO_2NP concentration [74]. Moreover, exposure of wild-type mice to inhalation of nickel-containing NP air for 3 h increased both Aβ40 and Aβ42 amyloid peptide levels in the brain by 72-129% [75].

Moreover, Yarjanli et al. gave excellent examples of the role of iron in neurodegeneration. They speculated whether iron ions released from the NPs are capable to activate positive feedback loop among iron accumulation. First and foremost, there is evidence that released iron ions can support Fenton's reaction and produce ROS from hydrogen peroxide and superoxide. Further than that, iron NPs can decrease GSH content, which may lead to increased oxidative stress and mitochondrial degradation. Due to these factors, it is not a surprise that these NPs can boost protein aggregation. Nevertheless, the authors emphasize that the toxicity of iron NPs is dependent on their size, shape, surface charge, coating, functional groups, and concentration and their utility must be considered in regard to these aforementioned aspects [76].

In any case, the knowledge about the diverse nature of nanoparticles was used to look for their other applications in the field of neurodegenerative disorders. For the case in point, nanoparticle-induced protein fibrillation can be employed as a fast screening method for novel potential antiaggregative compounds [77] and also as a methodology for rapid detection of protein aggregation that can be used to analyze the fibrillation process as well [78]. Likewise, NPs can serve as advanced, real-time screening platform which will help to identify various mechanisms of Aβ aggregation [79].

Here, SOD1-functionalized AuNPs served as a colorimetric detection platform for SOD1 aggregate evaluation. The test is simple and sensitive comparing to other methods as it is based on absorbance; thus, such a sensor system can serve as a diagnostic tool of SOD1 aggregates which are a hallmark of a fraction of familial ALS [80].

A step further, some nanoparticles might be designed not only to inhibit aggregation of pathological proteins but also to serve as a diagnostic tool. The results presented by Skaat et al. indicate that the conjugation of a BAM10 antibody to the near-infrared fluorescent Fe_3O_4 nanoparticles not only significantly hinders Aβ40 fibrillation but also acts as their marker; thus, the aggregates can be detected by MRI or fluorescence imaging [81]. Another example of "traceable" and successful antineurodegenerative NPs is the superparamagnetic iron oxide nanoparticles conjugated with two cell targeting molecules—a peptide with strong affinity to transferrin receptor used in order to enable NP crossing the BBB and mazindol, a dopamine inhibitor which stimulates dopamine transporter internalization to facilitate specific internalization to dopaminergic neurons. EGCG attached to this NP prevents α-syn aggregation [82].

6. Conclusions

This review gives an insight into the burden and predictions of the prevalence of the most common neurodegenerative diseases and the lack of effective treatment. Contemporary regimen is solely symptomatic; thus, we wanted to point out the emerging significance of nanoparticles as a promising approach in the treatment and diagnostics of these disorders. Despite the complexity of mechanisms underlying neurodegenerative diseases, some pathological aspects tend to overlap; thus, nanoparticles can act on many levels. Further, both *in vitro* and *in vivo* studies are extremely important to the discovery of the most efficient treatment of these diseases.

Abbreviations

Aβ: Amyloid-β protein
AD: Alzheimer's disease
ALS: Amyotrophic lateral sclerosis
APP: Amyloid precursor protein
AuNPs: Gold nanoparticles
BBB: Blood-brain barrier
CGASeNPs: SeNPs conjugated with chlorogenic acid
L-DOPA: L-3,4-Dihydroxyphenylalanine
EGCG: Epigallocatechin gallate
GAGs: Glycosaminoglycans
GQDs: Graphene quantum dots
GSH: Glutathione
NAC: Nonamyloid β component
NFTs: Neurofibrillary tangles
NMDA: N-Methyl-D-aspartate
NPs: Nanoparticles
PAMAM: Poly(amidoamine)
PD: Parkinson's disease
ROS: Reactive oxygen species
SeNPs: Selenium nanoparticles
SOD: Superoxide dismutase
α-syn: Alpha-synuclein.

Conflicts of Interest

The authors declare that there is no conflict of interest regarding the publication of this paper.

Authors' Contributions

M. P. wrote the main part of the manuscript. G. B. participated in the revision of the manuscript. I. S.-B. was responsible for the concept of the review and preparation of the manuscript. She was also responsible for providing the funding for the study. All authors have read and approved the final manuscript.

Acknowledgments

References

[1] World Health Organization, "Global health and ageing," 2011, May 2020, https://www.who.int/ageing/publications/global_health/en/.

[2] H. Checkoway, J. I. Lundin, and S. N. Kelada, "Neurodegenerative diseases," *IARC Scientific Publications*, vol. 2011, no. 163, pp. 407–419, 2011.

[3] O. Tysnes and A. Storstein, "Epidemiology of Parkinson's disease," *Journal of Neural Transmission*, vol. 124, no. 8, pp. 901–905, 2017.

[4] W. A. Rocca, "The burden of Parkinson's disease: a worldwide perspective," *The Lancet Neurology*, vol. 17, no. 11, pp. 928-929, 2018.

[5] E. O. Talbott, A. M. Malek, and D. Lacomis, "The epidemiology of amyotrophic lateral sclerosis," *Handbook of Clinical Neurology*, vol. 138, pp. 225–238, 2016.

[6] L. Pihlstrøm, S. Wiethoff, and H. Houlden, "Genetics of neurodegenerative diseases: an overview," *Handbook of Clinical Neurology*, vol. 145, pp. 309–323, 2017.

[7] R. C. Brown, A. H. Lockwood, and B. R. Sonawane, "Neurodegenerative diseases: an overview of environmental risk factors," *Environmental Health Perspectives*, vol. 113, no. 9, pp. 1250–1256, 2005.

[8] T. A. Bayer, "Proteinopathies, a core concept for understanding and ultimately treating degenerative disorders?," *European Neuropsychopharmacology*, vol. 25, no. 5, pp. 713–724, 2015.

[9] M. G. Erkkinen, M. O. Kim, and M. D. Geschwind, "Clinical neurology and epidemiology of the major neurodegenerative diseases," *Cold Spring Harbor Perspectives in Biology*, vol. 10, no. 4, article a033118, 2018.

[10] S. Millecamps, S. Boillée, I. Le Ber et al., "Phenotype difference between ALS patients with expanded repeats in C9ORF72 and patients with mutations in other ALS-related genes," *Journal of Medical Genetics*, vol. 49, no. 4, pp. 258–263, 2012.

[11] S. Saberi, J. E. Stauffer, D. J. Schulte, and J. Ravits, "Neuropathology of amyotrophic lateral sclerosis and its variants," *Neurologic Clinics*, vol. 33, no. 4, pp. 855–876, 2015.

[12] A. M. Blokhuis, E. J. Groen, M. Koppers, L. H. van den Berg, and R. J. Pasterkamp, "Protein aggregation in amyotrophic lateral sclerosis," *Acta Neuropathologica*, vol. 125, no. 6, pp. 777–794, 2013.

[13] M. J. Armstrong and M. S. Okun, "Diagnosis and treatment of Parkinson disease: a review," *Journal of the American Medical Association*, vol. 323, no. 6, pp. 548–560, 2020.

[14] P. Rizek, N. Kumar, and M. S. Jog, "An update on the diagnosis and treatment of Parkinson disease," *Canadian Medical Association Journal*, vol. 188, no. 16, pp. 1157–1165, 2016.

[15] G. T. Grossberg, G. Tong, A. D. Burke, and P. N. Tariot, "Present algorithms and future treatments for Alzheimer's disease," *Journal of Alzheimer's Disease*, vol. 67, no. 4, pp. 1157–1171, 2019.

[16] J. Cummings, G. Lee, A. Ritter, M. Sabbagh, and K. Zhong, "Alzheimer's disease drug development pipeline: 2019," *Alzheimer's & Dementia*, vol. 5, no. 1, pp. 272–293, 2019.

[17] P. Brundin, K. D. Dave, and J. H. Kordower, "Therapeutic approaches to target alpha-synuclein pathology," *Experimental Neurology*, vol. 298, Part B, pp. 225–235, 2017.

[18] H. Lu, W. D. Le, Y. Y. Xie, and X. P. Wang, "Current therapy of drugs in amyotrophic lateral sclerosis," *Current Neuropharmacology*, vol. 14, no. 4, pp. 314–321, 2016.

[19] M. Hinchcliffe and A. Smith, "Riluzole: real-world evidence supports significant extension of median survival times in patients with amyotrophic lateral sclerosis," *Degenerative Neurological and Neuromuscular Disease*, vol. 7, pp. 61–70, 2017.

[20] P. Desplats, H.-J. Lee, E.-J. Bae et al., "Inclusion formation and neuronal cell death through neuron-to-neuron transmission of -synuclein," *Proceedings of the National Academy of Sciences of the United States of America*, vol. 106, no. 31, pp. 13010–13015, 2009.

[21] F. N. Emamzadeh, "Alpha-synuclein structure, functions, and interactions," *Journal of Research in Medical Sciences*, vol. 21, no. 1, p. 29, 2016.

[22] H. Mohammad-Beigi, A. Hosseini, M. Adeli et al., "Mechanistic understanding of the interactions between nano-objects with different surface properties and α-synuclein," *ACS Nano*, vol. 13, no. 3, pp. 3243–3256, 2019.

[23] S. Janezic, S. Threlfell, P. D. Dodson et al., "Deficits in dopaminergic transmission precede neuron loss and dysfunction in a new Parkinson model," *Proceedings of the National Academy of Sciences of the United States of America*, vol. 110, no. 42, pp. E4016–E4025, 2013.

[24] G. M. Shankar, B. L. Bloodgood, M. Townsend, D. M. Walsh, D. J. Selkoe, and B. L. Sabatini, "Natural oligomers of the Alzheimer amyloid- protein induce reversible synapse loss by modulating an NMDA-type glutamate receptor-dependent signaling pathway," *Journal of Neuroscience*, vol. 27, no. 11, pp. 2866–2875, 2007.

[25] R. J. O'Brien and P. C. Wong, "Amyloid precursor protein processing and Alzheimer's disease," *Annual Review of Neuroscience*, vol. 34, no. 1, pp. 185–204, 2011.

[26] C. Cheignon, M. Tomas, D. Bonnefont-Rousselot, P. Faller, C. Hureau, and F. Collin, "Oxidative stress and the amyloid beta peptide in Alzheimer's disease," *Redox Biology*, vol. 14, pp. 450–464, 2018.

[27] M. P. Mattson, "Pathways towards and away from Alzheimer's disease," *Nature*, vol. 430, no. 7000, pp. 631–639, 2004.

[28] S. Sadigh-Eteghad, B. Sabermarouf, A. Majdi, M. Talebi, M. Farhoudi, and J. Mahmoudi, "Amyloid-beta: a crucial factor in Alzheimer's disease," *Medical Principles and Practice*, vol. 24, no. 1, pp. 1–10, 2015.

[29] W. H. De Jong and P. J. Borm, "Drug delivery and nanoparticles:applications and hazards," *International Journal of Nanomedicine*, vol. 3, no. 2, pp. 133–149, 2008.

[30] P. Tian, L. Tang, K. S. Teng, and S. P. Lau, "Graphene quantum dots from chemistry to applications," *Materials Today Chemistry*, vol. 10, pp. 221–258, 2018.

[31] D. Kim, J. M. Yoo, H. Hwang et al., "Graphene quantum dots prevent α-synucleinopathy in Parkinson's disease," *Nature Nanotechnology*, vol. 13, no. 9, pp. 812–818, 2018.

[32] Q. Nie, X. G. Du, and M. Y. Geng, "Small molecule inhibitors of amyloid β peptide aggregation as a potential therapeutic strategy for Alzheimer's disease," *Acta Pharmacologica Sinica*, vol. 32, no. 5, pp. 545–551, 2011.

[33] Y. Liu, L. P. Xu, Q. Wang, B. Yang, and X. Zhang, "Synergistic inhibitory effect of GQDs-tramiprosate covalent binding on amyloid aggregation," *ACS Chemical Neuroscience*, vol. 9, no. 4, pp. 817–823, 2017.

[34] S. Svenson and D. A. Tomalia, "Dendrimers in biomedical applications—reflections on the field," *Advanced Drug Delivery Reviews*, vol. 57, no. 15, pp. 2106–2129, 2005.

[35] A. S. Chauhan, "Dendrimers for drug delivery," *Molecules*, vol. 23, no. 4, p. 938, 2018.

[36] B. Klajnert, M. Cortijo-Arellano, J. Cladera, and M. Bryszewska, "Influence of dendrimer's structure on its activity against amyloid fibril formation," *Biochemical and Biophysical Research Communications*, vol. 345, no. 1, pp. 21–28, 2006.

[37] A. Rekas, V. Lo, G. E. Gadd, R. Cappai, and S. I. Yun, "PAMAM dendrimers as potential agents against fibrillation ofα-synuclein, a Parkinson's disease-related protein," *Macromolecular Bioscience*, vol. 9, no. 3, pp. 230–238, 2009.

[38] K. Milowska, M. Malachowska, and T. Gabryelak, "PAMAM G4 dendrimers affect the aggregation of α-synuclein," *International Journal of Biological Macromolecules*, vol. 48, no. 5, pp. 742–746, 2011.

[39] I. M. Neelov, A. Janaszewska, B. Klajnert et al., "Molecular properties of lysine dendrimers and their interactions with Aβ-peptides and neuronal cells," *Current Medicinal Chemistry*, vol. 20, no. 1, pp. 134–143, 2013.

[40] J. M. Dowding, W. Song, K. Bossy et al., "Cerium oxide nanoparticles protect against Aβ-induced mitochondrial fragmentation and neuronal cell death," *Cell Death & Differentiation*, vol. 21, no. 10, pp. 1622–1632, 2014.

[41] R. Ruotolo, G. De Giorgio, I. Minato, M. G. Bianchi, O. Bussolati, and N. Marmiroli, "Cerium oxide nanoparticles rescue α-synuclein-induced toxicity in a yeast model of Parkinson's disease," *Nanomaterials*, vol. 10, no. 2, p. 235, 2020.

[42] G. Gao, M. Zhang, D. Gong, R. Chen, X. Hu, and T. Sun, "The size-effect of gold nanoparticles and nanoclusters in the inhibition of amyloid-β fibrillation," *Nanoscale*, vol. 9, no. 12, pp. 4107–4113, 2017.

[43] K. A. Moore, K. M. Pate, D. D. Soto-Ortega et al., "Influence of gold nanoparticle surface chemistry and diameter upon Alzheimer's disease amyloid-β protein aggregation," *Journal of Biological Engineering*, vol. 11, no. 1, p. 5, 2017.

[44] R. Prades, S. Guerrero, E. Araya et al., "Delivery of gold nanoparticles to the brain by conjugation with a peptide that recognizes the transferrin receptor," *Biomaterials*, vol. 33, no. 29, pp. 7194–7205, 2012.

[45] F. Yang, G. P. Lim, A. N. Begum et al., "Curcumin inhibits formation of amyloid β oligomers and fibrils, binds plaques, and reduces Amyloidin vivo," *Journal of Biological Chemistry*, vol. 280, no. 7, pp. 5892–5901, 2005.

[46] S. Dolai, W. Shi, C. Corbo et al., "'Clicked' sugar-curcumin conjugate: modulator of amyloid-β and tau peptide aggregation at ultralow concentrations," *ACS Chemical Neuroscience*, vol. 2, no. 12, pp. 694–699, 2011.

[47] S. Palmal, A. R. Maity, B. K. Singh, S. Basu, N. R. Jana, and N. R. Jana, "Inhibition of amyloid fibril growth and dissolution of amyloid fibrils by curcumin-gold nanoparticles," *Chemistry*, vol. 20, no. 20, pp. 6184–6191, 2014.

[48] X. Li, G. Zhang, Q. Nie et al., "Baicalein blocks α-synuclein secretion from SN4741 cells and facilitates α-synuclein polymerization to big complex," *Neuroscience Letters*, vol. 655, pp. 109–114, 2017.

[49] M. Teraoka, K. Nakaso, C. Kusumoto et al., "Cytoprotective effect of chlorogenic acid against α-synuclein-related toxicity in catecholaminergic PC12 cells," *Journal of Clinical Biochemistry and Nutrition*, vol. 51, no. 2, pp. 122–127, 2012.

[50] Y. Liu, J. A. Carver, A. N. Calabrese, and T. L. Pukala, "Gallic acid interacts with α-synuclein to prevent the structural collapse necessary for its aggregation," *Biochimica et Biophysica Acta*, vol. 1844, no. 9, pp. 1481–1485, 2014.

[51] H. Javed, M. F. Nagoor Meeran, S. Azimullah, A. Adem, B. Sadek, and S. K. Ojha, "Plant extracts and phytochemicals targeting α-synuclein aggregation in Parkinson's disease models," *Frontiers in Pharmacology*, vol. 9, p. 1555, 2019.

[52] B. Hosnedlova, M. Kepinska, S. Skalickova et al., "Nano-selenium and its nanomedicine applications: a critical review," *International Journal of Nanomedicine*, vol. 13, pp. 2107–2128, 2018.

[53] L. Yang, N. Wang, and G. Zheng, "Enhanced effect of combining chlorogenic acid on selenium nanoparticles in inhibiting amyloid β aggregation and reactive oxygen species formation in vitro," *Nanoscale Research Letters*, vol. 13, no. 1, p. 303, 2018.

[54] L. Yang, W. Wang, J. Chen, N. Wang, and G. Zheng, "A comparative study of resveratrol and resveratrol-functional selenium nanoparticles: inhibiting amyloid β aggregation and reactive oxygen species formation properties," *Journal of Biomedical Materials Research Part A*, vol. 106, no. 12, pp. 3034–3041, 2018.

[55] Y. Qi, P. Yi, T. He et al., "Quercetin-loaded selenium nanoparticles inhibit amyloid-β aggregation and exhibit antioxidant activity," *Colloids and Surfaces A: Physicochemical and Engineering Aspects*, vol. 602, article 125058, 2020.

[56] J. Zhang, X. Zhou, Q. Yu et al., "Epigallocatechin-3-gallate (EGCG)-stabilized selenium nanoparticles coated with Tet-1 peptide to reduce amyloid-β aggregation and cytotoxicity," *ACS Applied Materials & Interfaces*, vol. 6, no. 11, pp. 8475–8487, 2014.

[57] N. Zhao, X. Yang, H. R. Calvelli et al., "Antioxidant nanoparticles for concerted inhibition of α-synuclein fibrillization, and attenuation of microglial intracellular aggregation and activation," *Frontiers in Bioengineering and Biotechnology*, vol. 8, p. 112, 2020.

[58] N. K. Bhatia, A. Srivastava, N. Katyal et al., "Curcumin binds to the pre-fibrillar aggregates of Cu/Zn superoxide dismutase (SOD1) and alters its amyloidogenic pathway resulting in reduced cytotoxicity," *Biochimica et Biophysica Acta*, vol. 1854, no. 5, pp. 426–436, 2015.

[59] I. Sadowska-Bartosz and G. Bartosz, "Redox nanoparticles: synthesis, properties and perspectives of use for treatment of neurodegenerative diseases," *Journal of Nanobiotechnology*, vol. 16, no. 1, p. 87, 2018.

[60] P. Boonruamkaew, P. Chonpathompikunlert, L. B. Vong et al., "Chronic treatment with a smart antioxidative nanoparticle for inhibition of amyloid plaque propagation in Tg2576 mouse model of Alzheimer's disease," *Scientific Reports*, vol. 7, no. 1, p. 3785, 2017.

[61] M. Pichla, Ł. Pulaski, K. D. Kania et al., "Nitroxide radical-containing redox nanoparticles protect neuroblastoma SH-SY5Y cells against 6-hydroxydopamine toxicity," *Oxidative Medicine and Cellular Longevity*, vol. 2020, Article ID 9260748, 19 pages, 2020.

[62] G. Liu, P. Men, W. Kudo, G. Perry, and M. A. Smith, "Nanoparticle–chelator conjugates as inhibitors of amyloid-β aggregation and neurotoxicity: a novel therapeutic approach for Alzheimer disease," *Neuroscience Letters*, vol. 455, no. 3, pp. 187–190, 2009.

[63] A. Antosova, Z. Bednarikova, M. Koneracka et al., "Amino acid functionalized superparamagnetic nanoparticles inhibit lysozyme amyloid fibrillization," *Chemistry*, vol. 25, no. 31, pp. 7501–7514, 2019.

[64] S. Palmal, N. R. Jana, and N. R. Jana, "Inhibition of amyloid fibril growth by nanoparticle coated with histidine-based polymer," *Journal of Physical Chemistry C*, vol. 118, no. 37, pp. 21630–21638, 2014.

[65] N. Joshi, S. Basak, S. Kundu, G. De, A. Mukhopadhyay, and K. Chattopadhyay, "Attenuation of the early events of α-synuclein aggregation: a fluorescence correlation spectroscopy and laser scanning microscopy study in the presence of surface-coated Fe$_3$O$_4$ nanoparticles," *Langmuir*, vol. 31, no. 4, pp. 1469–1478, 2015.

[66] S. Niu, L.-K. Zhang, L. Zhang et al., "Inhibition by multifunctional magnetic nanoparticles loaded with alpha-synuclein RNAi plasmid in a Parkinson's disease model," *Theranostics*, vol. 7, no. 2, pp. 344–356, 2017.

[67] N. Taebnia, D. Morshedi, M. Doostkam et al., "The effect of mesoporous silica nanoparticle surface chemistry and concentration on the α-synuclein fibrillation," *RSC Advances*, vol. 5, no. 75, pp. 60966–60974, 2015.

[68] H. Xie and J. Wu, "Silica nanoparticles induce alpha-synuclein induction and aggregation in PC12-cells," *Chemico-Biological Interactions*, vol. 258, pp. 197–204, 2016.

[69] Y. H. Liao, Y. J. Chang, Y. Yoshiike, Y. C. Chang, and Y. R. Chen, "Negatively charged gold nanoparticles inhibit Alzheimer's amyloid-β fibrillization, induce fibril dissociation, and mitigate neurotoxicity," *Small*, vol. 8, no. 23, pp. 3631–3639, 2012.

[70] Y. D. Alvarez, J. A. Fauerbach, J. V. Pellegrotti, T. M. Jovin, E. A. Jares-Erijman, and F. D. Stefani, "Influence of gold nanoparticles on the kinetics of α-synuclein aggregation," *Nano Letters*, vol. 13, no. 12, pp. 6156–6163, 2013.

[71] T. T. Win-Shwe and H. Fujimaki, "Nanoparticles and neurotoxicity," *International Journal of Molecular Sciences*, vol. 12, no. 9, pp. 6267–6280, 2011.

[72] S. A. Shah, G. H. Yoon, A. Ahmad, F. Ullah, F. Ul Amin, and M. O. Kim, "Nanoscale-alumina induces oxidative stress and accelerates amyloid beta (Aβ) production in ICR female mice," *Nanoscale*, vol. 7, no. 37, pp. 15225–15237, 2015.

[73] S. Mohammadi and M. Nikkhah, "TiO$_2$ nanoparticles as potential promoting agents of fibrillation of α-synuclein, a Parkinson's disease-related protein," *Iranian Journal of Biotechnology*, vol. 15, no. 2, pp. 87–94, 2017.

[74] J. Wu and H. Xie, "Effects of titanium dioxide nanoparticles on α-synuclein aggregation and the ubiquitin-proteasome system in dopaminergic neurons," *Artificial Cells, Nanomedicine, and Biotechnology*, vol. 44, no. 2, pp. 690–694, 2014.

[75] S. H. Kim, E. M. Knight, E. L. Saunders et al., "Rapid doubling of Alzheimer's amyloid-β40 and 42 levels in brains of mice exposed to a nickel nanoparticle model of air pollution," *F1000Research*, vol. 1, p. 70, 2012.

[76] Z. Yarjanli, K. Ghaedi, A. Esmaeili, S. Rahgozar, and A. Zarrabi, "Iron oxide nanoparticles may damage to the neural tissue through iron accumulation, oxidative stress, and protein aggregation," *BMC Neuroscience*, vol. 18, no. 1, p. 51, 2017.

[77] S. H. Han, Y. J. Chang, E. S. Jung, J. W. Kim, D. L. Na, and I. Mook-Jung, "Effective screen for amyloid β aggregation inhibitor using amyloid β-conjugated gold nanoparticles," *International Journal of Nanomedicine*, vol. 6, pp. 1–12, 2010.

[78] I. Choi and L. P. Lee, "Rapid detection of Aβ aggregation and inhibition by dual functions of gold nanoplasmic particles: catalytic activator and optical reporter," *ACS Nano*, vol. 7, no. 7, pp. 6268–6277, 2013.

[79] K. Tokuraku, M. Marquardt, and T. Ikezu, "Real-time imaging and quantification of amyloid-beta peptide aggregates by novel quantum-dot nanoprobes," *PLoS One*, vol. 4, no. 12, p. e8492, 2009.

[80] S. Hong, I. Choi, S. Lee, Y. I. Yang, T. Kang, and J. Yi, "Sensitive and colorimetric detection of the structural evolution of

superoxide dismutase with gold nanoparticles," *Analytical Chemistry*, vol. 81, no. 4, pp. 1378–1382, 2009.

[81] H. Skaat, E. Corem-Slakmon, I. Grinberg et al., "Antibody-conjugated, dual-modal, near-infrared fluorescent iron oxide nanoparticles for antiamyloidgenic activity and specific detection of *amyloid-β* fibrils," *International Journal of Nanomedicine*, vol. 8, pp. 4063–4076, 2013.

[82] Y. Li, Z. Chen, Z. Lu et al., ""Cell-addictive" dual-target traceable nanodrug for Parkinson's disease treatment via flotillins pathway," *Theranostics*, vol. 8, no. 19, pp. 5469–5481, 2018.

2. Pichla M., Pułaski, Ł., Kania K. D., Stefaniuk I., Cieniek B., Pieńkowska N., Bartosz G., & Sadowska-Bartosz I. *Nitroxide Radical-Containing Redox Nanoparticles Protect Neuroblastoma SH-SY5Y Cells against 6-Hydroxydopamine Toxicity*. Oxidative Medicine and Cellular Longevity, 2020, 9260748.

IF2020: 5.076; MNiSW: 100

Research Article

Nitroxide Radical-Containing Redox Nanoparticles Protect Neuroblastoma SH-SY5Y Cells against 6-Hydroxydopamine Toxicity

Monika Pichla [ID],[1] **Łukasz Pulaski,**[2,3] **Katarzyna Dominika Kania,**[3] **Ireneusz Stefaniuk,**[4] **Bogumił Cieniek,**[5] **Natalia Pieńkowska,**[1] **Grzegorz Bartosz** [ID],[2] **and Izabela Sadowska-Bartosz** [ID][1]

[1]*Department of Analytical Biochemistry, Institute of Food Technology and Nutrition, College of Natural Sciences, Rzeszow University, Zelwerowicza Street 4, 35-601 Rzeszow, Poland*
[2]*Department of Molecular Biophysics, Faculty of Biology and Environmental Protection, University of Lodz, Pomorska Street 141/143, 90-236 Lodz, Poland*
[3]*Laboratory of Transcriptional Regulation, Institute of Medical Biology, Polish Academy of Sciences, Lodowa Street 106, 93-232 Lodz, Poland*
[4]*Teaching and Research Center of Microelectronics and Nanotechnology, College of Natural Sciences, University of Rzeszow, Pigonia 1, 35-959 Rzeszow, Poland*
[5]*Department of Experimental Physics, Teaching and Research Center of Microelectronics and Nanotechnology, College of Natural Sciences, University of Rzeszow, Pigonia 1, 35-959 Rzeszow, Poland*

Correspondence should be addressed to Izabela Sadowska-Bartosz; isadowska@poczta.fm

Parkinson's disease (PD) patients can benefit from antioxidant supplementation, and new efficient antioxidants are needed. The aim of this study was to evaluate the protective effect of selected nitroxide-containing redox nanoparticles (NRNPs) in a cellular model of PD. Antioxidant properties of NRNPs were studied in cell-free systems by protection of dihydrorhodamine 123 against oxidation by 3-morpholino-sydnonimine and protection of fluorescein against bleaching by 2,2-azobis(2-amidinopropane) hydrochloride and sodium hypochlorite. Model blood-brain barrier penetration was studied using hCMEC/D3 cells. Human neuroblastoma SH-SY5Y cells, exposed to 6-hydroxydopamine (6-OHDA), were used as an *in vitro* model of PD. Cells were preexposed to NRNPs or free nitroxides (TEMPO or 4-amino-TEMPO) for 2 h and treated with 6-OHDA for 1 h and 24 h. The reactive oxygen species (ROS) level was estimated with dihydroethidine 123 and Fluorimetric Mitochondrial Superoxide Activity Assay Kit. Glutathione level (GSH) was measured with *ortho*-phtalaldehyde, ATP by luminometry, changes in mitochondrial membrane potential with JC-1, and mitochondrial mass with 10-Nonyl-Acridine Orange. NRNP1, TEMPO, and 4-amino-TEMPO (25-150 μM) protected SH-SY5Y cells from 6-OHDA-induced viability loss; the protection was much higher for NRNP1 than for free nitroxides. NRNP1 were better antioxidants *in vitro* and permeated better the model BBB than free nitroxides. Exposure to 6-OHDA decreased the GSH level after 1 h and increased it considerably after 24 h (apparently a compensatory overresponse); NRNPs and free nitroxides prevented this increase. NRNP1 and free nitroxides prevented the decrease in ATP level after 1 h and increased it after 24 h. 6-OHDA increased the intracellular ROS level and mitochondrial superoxide level. Studied antioxidants mostly decreased ROS and superoxide levels. 6-OHDA decreased the mitochondrial potential and mitochondrial mass; both effects were prevented by NRNP1 and nitroxides. These results suggest that the mitochondria are the main site of 6-OHDA-induced cellular damage and demonstrate a protective effect of NRNP1 in a cellular model of PD.

1. Introduction

Age-related diseases such as Parkinson's disease (PD) constitute a significant socioeconomic burden for modern populations. As human mean lifespan increases, increasing occurrence of PD has features of a pandemic. From 1990 to 2015, the number of people with this disease doubled worldwide to at least over 6 million. Driven mostly by increasing longevity, this number is foreseen to double again to over 12 million by 2040 [1]. Parkinson's disease is slowly progressive, and disease-modifying drugs are still not available. Parkinson's disease is a long-term degenerative disorder generally proceeding with motor and nonmotor symptoms [2, 3], which usually worsen with advancing age, leading to care dependency. Disease manifestation is indicated by the presence of Lewy bodies (abnormal protein aggregates predominantly containing α-synuclein, ubiquitin, Parkinson juvenile disease protein 2 (Parkin), PTEN-induced kinase-1 (PINK1), and other less abundant proteins) and death of dopaminergic neurons in the *substantia nigra* projecting to the striatum as well as microgliosis [4, 5]. Environmental as well as genetic factors (or unknown factors in idiopathic or sporadic cases) have been implicated in the mechanism underlying the pathogenesis of PD [6]. Nearly 10% of PD cases may be caused by mutations in over 12 different genes implicated in the regulation of proteasomal degradation pathways (Parkin, ubiquitin carboxy-terminal hydrolase L1), mitochondrial homeostasis (PINK1, mitochondrial serine protease Omi/Htra, integral mitochondrial protein DJ-1, and leucine-rich repeat kinase 2), lysosome function (ATPase cation transporting 13A2 (ATPase cation transporting 13A2)), antioxidant response pathways (oncogene DJ-1 also known as a Parkinson disease protein 7) and mitophagy (PINK1 and Parkin) [7, 8]. Nevertheless, currently, the molecular mechanisms underlying all PD features remain unknown, hampering the development of a successful treatment.

An *in vitro* model usually used in PD research is the neuroblastoma SH-SY5Y cell line. This line is a subline of the SK-N-SH cell line, which was established in a culture in 1970 from a bone marrow aspirate of a metastatic neuroblastoma of a four-year-old female and has undergone three rounds of clonal selection [9, 10]. The initial characterization of the SH-SY5Y cell line showed modest activity of dopamine-β-hydroxylase and negligible levels of choline acetyltransferase, acetylcholinesterase, butyrylcholinesterase and tyrosine hydroxylase activities, and basal noradrenaline release [11]. In order to create SH-SY5Y-derived cell models that mimic PD, we choose the pharmacological strategy (6-hydroxydopamine (6-OHDA) treatment). 6-Hydroxydopamine is a structural analogue of catecholamines, dopamine, and noradrenaline and exerts toxic effects on catecholaminergic neurons [12]. Although the 6-OHDA model does not cover all PD symptoms, it does reproduce the main cellular processes involved in PD. Up to now, four main mechanisms have been proposed to explain the cytotoxic action of 6-OHDA: (1) extra- or intracellular autooxidation of 6-OHDA proceeding with the formation of superoxide, hydrogen peroxide (H_2O_2), and hydroxyl radicals [2, 13]; (2) enzymatic formation of H_2O_2 due mainly to the action of

monoamine oxidase [3, 14]; (3) direct inhibition of mitochondrial respiratory chain complex I [4, 15]; and (4) dysregulation of autophagy [5, 16]. These mechanisms may act independently or in combination to generate reactive oxygen species (ROS) [17]. The resulting oxidative stress (OS) may be intensified by an augmentation of cytoplasmic free calcium ions (as a result of either glutamate excitotoxicity or increase in mitochondrial membrane permeability), finally inducing cell death [18]. Upon import by dopamine active transporters in dopamine neurons [19], 6-OHDA was reported to undergo rapid autooxidation (~15 min) producing hydrogen peroxide, hydroxyl radicals, and peroxynitrite and inducing a transient increase in the mitochondrial superoxide level [20, 21]. Furthermore, 6-OHDA elicits dynamin-related protein-1- (Drp1-) dependent mitochondrial fission and loss of mitochondrial content by upregulating Beclin-1-independent mitophagy and alters microtubule dynamics [22]. 6-Hydroxydopamine was reported to cause global repression of prosurvival transcription programs including decreased cyclic AMP-regulated protein kinase signaling, to promote the mislocalization of prosurvival transcription factors from the nucleus to the cytosol [23] and to block nuclear import of prosurvival transcription factors in SH-SY5Y cells [24–26].

Antioxidants have been proposed to ameliorate the development of neurodegenerative diseases including PD [27]. Nevertheless, the effects of antioxidant intervention, including increased consumption of dietary antioxidants, were reported to be generally modest [28, 29]. These findings suggest that new antioxidant compounds, of increased efficacy, should be searched for. Particularly, synthetic antioxidants seem more promising in this respect as they allow combining different functions within one molecule and overcoming limitations of evolutionary selected biosynthetic pathways. Apart from the antioxidant function, these compounds may have other beneficial actions; e.g., they can interfere with protein aggregate formation or inhibit undesired enzymatic activities. Free nitroxyl radicals (nitroxides), such as 4-hydroxy-2,2,6,6-tetramethylpiperidine-1-oxyl (TEMPOL), are promising in this respect [30]. They are many-faceted antioxidants, which have enzyme-like, catalytic superoxide dismutase activity; inhibit the Fenton reaction by the ability to oxidize transition metal ions; and terminate radical chain reactions by radical recombination. They can accept electrons from the mitochondrial electron transport chain. Moreover, they react also with protein tyrosyl and tryptophanyl radicals [31]. We have demonstrated that nitroxides are efficient, i.e., in preventing glycation and reactions of peroxynitrite [32, 33]. A drawback of nitroxides is their short life time *in vivo* and toxic effects, including induction of apoptotic cell death at high concentrations [34, 35] and lowering of blood pressure *in vivo* [36]. Lately, drug delivery systems using nanomedicines have been proposed; they are expected to have various clinical applications [37]. For example, since nanoparticles with long-term blood circulation specifically accumulate in tumour tissues after intravenous administration [38], controlled drug release from nanoparticles at tumour sites increases the therapeutic effects of the anticancer drug and suppresses its severe side effects [39]. It can be expected that the application of a
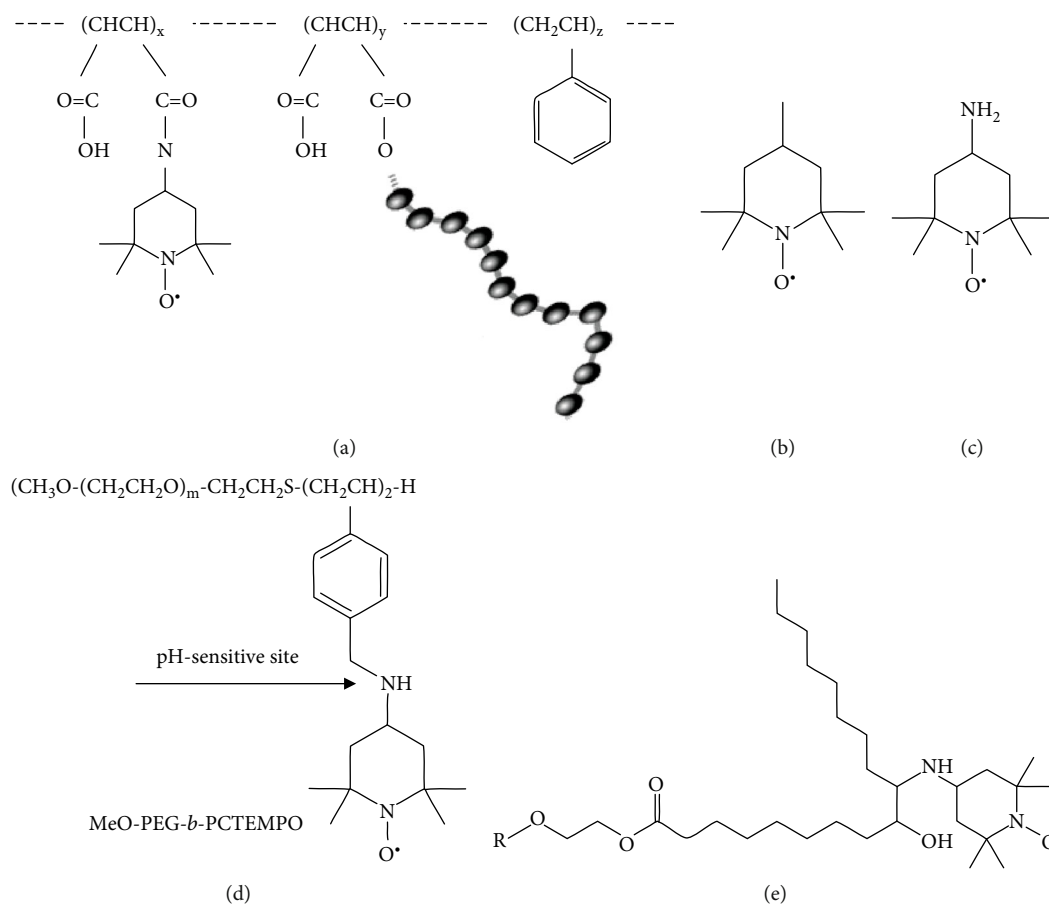
FIGURE 1: Structures of studied antioxidant compounds: nitroxide radical-containing redox nanoparticles 1 (copolymer based on poly(styrene-co-malein anhydride; NRNP1) (a), free nitroxide radicals: 2,2,6,6-tetramethylpiperidine-1-oxyl (TEMPO) (b), 4-amino-2,2,6,6-tetramethylpiperidine-1-oxyl (4-amino-TEMPO) (c), pH-sensitive radical-containing nanoparticles (NRNP2) (d), and nitroxide radicals-containing redox nanoparticles 3 (a copolymer of sorbitan-fatty acid esters with 4-amino-TEMPO; NRNP3) (e).

nanotechnological solution consisting of nanoparticles containing covalently bound nitroxides (nitroxide radical-containing redox nanoparticles (NRNPs)) to neurons will be much more efficient than treatment with natural antioxidants. This redox polymer contains nitroxide radicals as ROS scavengers in the hydrophobic segments bound via covalent linkages and forms a polymeric micelle of about 40 nm diameter under physiological conditions, which confines the nitroxide radicals in its core [40]. The main aim of our studies was the evaluation of NRNP1 (copolymer based on poly(styrene-co-malein anhydride) (Figure 1(a))) [41] toxicity and its ability to penetrate the blood-brain barrier (BBB) as well as its efficacy in ameliorating 6-OHDA toxicity in the cellular SH-SY5Y model of PD, in comparison with free nitroxides (2,2,6,6-tetramethylpiperidine-1-oxyl (TEMPO; Figure 1(b)) or 4-amino-2,2,6,6-tetramethylpiperidine-1-oxyl (4-amino-TEMPO; Figure 1(c))). In initial experiments, a pH-sensitive radical-containing nanoparticle (designed and developed using a self-assembling amphiphilic block copolymer (PEG-b-PCTEMPO)) composed of a hydrophilic poly (ethylene glycol) (PEG) segment and a hydrophobic poly (chloromethylstyrene) (PCMS) segment in which the chloromethyl groups were converted to 2,2,6,6-tetramethylpiperidinyloxys (TEMPOs) via the amination of PEG-b-PCMS block

copolymer with 4-amino-TEMPO (NRNP2; Figure 1(d)), and a copolymer of sorbitan-fatty acid esters with 4-amino-TEMPO (NRNP3; Figure 1(e)) were also used.

2. Materials and Methods

2.1. Materials and Equipment Used in Studies of Cell-Free Systems. Xylenol orange (cat. no. chem*237045902*5 g) was obtained from Polish Chemical Reagents (POCH, Gliwice, Poland); fluorescein (cat. no. chem*114277705*10 g), perchloric acid ($HClO_4$; cat. no. chem*115649402*1 l), and sodium hypochlorite (NaOCl, 15% active chlorine basis, cat. no. 528066510) were purchased from Chempur (Piekary Śląskie, Poland); phosphate-buffered saline (PBS: 145 mM NaCl, 1.9 mM NaH_2PO_4, and 8.1 mM Na_2HPO_4, cat. no. PBS405) was obtained from Lab Empire (Rzeszów, Poland), and DMEM/F12 (cat. no. 11039-021) was purchased from Thermo Fisher Scientific (Waltham, MA, USA). 5-Amino-3-(4-morpholinyl)-1,2,3-oxadiazolium chloride (SIN-1 chloride, $OONO^-$ donor, cat. no. 0756/50) was obtained from Tocris Bioscience (Bristol, United Kingdom). SIN-1 chloride solutions (1 mM) were prepared in PBS and aliquots were frozen and kept at −80°C until use. HPLC analysis proved that under these conditions, SIN-1 chloride was stable for

several months. 2,2-Azobis(2-amidinopropane) dihydrochloride (AAPH, cat. no. 440914) was purchased from Polysciences (Warrington, PA, USA). A stock solution of AAPH was freshly prepared in PBS before each experiment, kept on ice, and used daily. Dihydrorhodamine 123 (DHR123) (cat. no. D23806) was purchased from Thermo Fisher Scientific (Waltham, MA, USA). A stock solution of NaOCl was diluted in 0.1 M NaOH, and its concentration was determined spectrophotometrically at 290 nm using the molar absorption coefficient of $\varepsilon_{290\,nm} = 350\,M^{-1}\,cm^{-1}$ [42]. Under such conditions NaOCl exists exclusively as OCl$^-$. Before use, the stock solution of NaOCl was diluted in PBS. At pH 7.4, both forms, HOCl and OCl$^-$, are present in the solution at comparable concentrations. All other reagents, if not mentioned otherwise, were purchased from Sigma-Aldrich Corp. (St. Louis, MO, USA) and were of analytical grade. 6-Hydroxydopamine hydrobromide (6-OHDA) (cat. no. H116) was provided by Sigma-Aldrich (St. Louis, MO, USA). Distilled water was purified using a Milli-Q system (Millipore, Bedford, MA, USA). Fluorometric and absorptiometric measurements were done in a Tecan Infinite 200 PRO multimode reader or a Spark multimode microplate reader (Tecan Group Ltd., Männedorf, Switzerland). All measurements were performed in triplicate and repeated at least three times on different preparations.

2.2. Materials and Equipment Used to Study the Neuroblastoma Cell Line.

The certified human neuroblastoma cell line SH-SY5Y (ATCC CRL-2266) was purchased from American Type Culture Collection (ATCC, Rockville, MD, USA). Dulbecco's Modified Eagle Medium Nutrient Mixture F-12 (DMEM/F12) without Phenol Red (cat. no. 11039-021), Dulbecco's phosphate-buffered saline 1x with Ca^{2+} and Mg^{2+} ions, Geltrex™ LDEV-Free Reduced Growth Factor Basement Membrane Matrix (cat. no. A1413202), and MitoTracker Deep Red FM (cat. no. M22426) were obtained from Thermo Fisher Scientific (Waltham, MA, USA). Foetal bovine serum (FBS, cat. no. 04-001-1A), 10x Trypsin-EDTA solution (cat. no. 03-051-5B), PBS without Ca^{2+} and Mg^{2+} ions (cat. no. 02-023-1A), and Penicillin-Streptomycin Solution (cat. no. 03-031-1B) were obtained from Biological Industries (Cromwell, CT, USA). The tetrazolium dye 3-(4,5-dimethylthiazol-2-yl)-2,5-diphenyltetrazolium bromide (MTT, cat. no. M2128), 2,2,6,6-tetramethylpiperidine-1-oxyl (TEMPO, cat. no. T-7263), 4-amino-2,2,6,6-tetramethylpiperidin-1-yloxyl (4-amino-TEMPO, cat. no. 163945), 0.4% Trypan Blue solution (cat. no. T8154), isopropanol (cat. no. I9516), N-ethylmaleimide (NEM, cat. no. E3876), trichloroacetic acid (TCA, cat. no. T4885), diethylenetriaminepentaacetic acid (DTPA, cat. no. D1133), L-ascorbic acid (cat. no. A0278), ortho-phthalaldehyde (cat. no. P1378), L-glutathione reduced (GSH, cat. no. PHR1359), dihydroethidium (DHE, cat. no. D7008), 4′,6-diamidino-2-phenylindole (DAPI, 4′,6-diamidino-2-phenylindole, dihydrochloride) (cat. no. D9542), Triton X-100 (cat. no. 9002-93-1), phalloidin conjugated with Atto-488 (cat. no. 49409), and acridine orange 10-nonyl bromide (NAO, cat. no. A7847) were provided by Sigma-Aldrich (St. Louis, MO, USA). 96% ethanol (cat. no. 396420113), 37% Formaldehyde Solution, and hydrochloric acid 35-38% (cat. no. 115752837) were provided by Chempur (Poland). CellTiter-Glo® Luminescent Cell Viability Assay (cat. no. G7571) was purchased from Promega (Madison, WI, USA). JC-1 Mitochondrial Membrane Potential Assay Kit was purchased from Abnova (Taiwan, China). Cell Meter™ Fluorimetric Mitochondrial Superoxide Activity Assay Kit Optimized for Microplate Reader was provided by AAT Bioquest (Sunnyvale, CA, USA).

Cell culture 75 cm^2 flasks (cat. no. 156499), transparent 96-well culture plates (cat. no. 161093), and black (cat. no. 165305) and white (cat. no. 165306) 96-well plates with an optical bottom were obtained from Thermo Fisher Scientific (Waltham, MA, USA). Other sterile cell culture materials and 24-well plates were purchased from Nerbe (Winsen, Germany) and NEST Biotechnology (Wuxi, China).

6-Hydroxydopamine hydrobromide stabilized with 0.01% ascorbic acid was reconstituted according to the manufacturer's protocol in 2 mL of PBS, aliquoted; 10 mM stocks were frozen in -20°C; 4-amino-TEMPO (10 mM stock solution) was dissolved in PBS and both of them were filtered using 0.22 μm filter. TEMPO (50 mM stock solution) was dissolved in dimethyl sulfoxide (DMSO); the final highest concentration of DMSO in cell media was ≤0.02%.

The radical-containing nanoparticles used for the initial experiments were synthesized by the group of Prof. Nagasaki (University of Tsukuba) (NRNP1: 1.64 mM stock solution in water; the pH-sensitive radical-containing-nanoparticle, NRNP2: 1.81 mM stock solution in water) [41, 43]. Then, syntheses of the NRNPs (NRNP1, NRNP2, and NRNP3) were conducted based on the experience of the team of Dr. J. Skolimowski (Department of Analytical Biochemistry, University of Rzeszow). Electron paramagnetic resonance signals were measured to estimate the amount of nitroxyl radicals in the nanoparticles.

Distilled water was purified using a Milli-Q system (Millipore, Bedford, MA, USA). Fluorometric and absorptiometric measurements were done using a Spark multimode microplate reader (Tecan Group Ltd., Männedorf, Switzerland). Images were taken using a ZEISS LSM 710 inverted confocal microscope (Oberkochen, Germany). All measurements were performed at least in triplicate (usually ninefold) and repeated at least three times on different preparations.

2.3. Materials Used to Study the Human Immortalized Brain Endothelial Cell Line.

The in vitro studies were carried out also on the human immortalized brain endothelial cell line (hCMEC/D3) (kindly donated by Prof. Pierre Couraud from INSERM, Paris, France [44]). Rat collagen (cat. no. I #3440-100-01) by Cultrex was obtained from R&D Systems, (McKinley Pl NE, MN, USA). Human basic fibroblast growth factor (bFGF; cat. no. F0291-25UG), L-ascorbic acid (cat. no. A4544), HEPES Buffer (cat. no. 1 M–HO887), and hydrocortisone (cat. no. H-0135; 1 mg) were purchased from Sigma-Aldrich, (St. Louis, MO, USA). Chemically Defined Lipid Concentrate (cat. no. 11905-031) and Pen-Strep (cat. no. 15140122) were provided by Gibco (Thermo Fisher Scientific, Waltham, MA, USA). Trypsin 0.05%/EDTA, 0.02% in PBS, without Ca^{2+} and Mg^{2+} (cat. no. P10-023100) was purchased from PAN-Biotech GmbH (Aidenbach, Germany).

Endothelial cell growth basal medium-2 (EBM-2) (cat. no. CC3156) was obtained from Lonza (Basel, Switzerland); foetal bovine serum (FBS Superior; cat. no. S 0615) was provided by Biochrom (Merck, Germany). Thin Cert–Tissue Culture Inserts for Multiwell Plates (cat. no. 662640) were obtained from Greiner Bio-One (Kremsmünster, Austria).

2.4. NRNP Characterization

2.4.1. Scanning Electron Microscopy. The morphology of studied NRNPs was visualized using scanning electron microscope (SEM) with energy-dispersive X-ray spectroscopy (EDS) analyzer Quanta™ 3D 200i (FEI Co. Field Emission Instruments, Hillsboro, OR, USA).

2.4.2. Electron Spin Resonance (ESR) Spectroscopy. Nitroxide residues per sum of hydrophilic and hydrophobic segment masses (molecular weight) were determined using ESR. Nitroxide signal intensity was measured immediately after addition of selected concentration of NRNPs or free nitroxides using microhematocrit capillaries (nonheparinized microhematocrit tubes ~75 μL; 1.55 × 75 mm; Medlab Products, Raszyn, Poland) in a Bruker multifrequency and multiresonance FT-EPR ELEXSYS E580 apparatus (Bruker BioSpin, Billerica, MA, USA). The spectrometer operated at X-band (9.850537 GHz). The following settings were used: central field, 3353.0 G; modulation amplitude, 1 G; modulation frequency, 100 kHz; microwave power, 23.77 mW; power attenuation 8.0 dB; scan range, 100 G; conversion time, 25 ms; and sweep time, 25.6 s. The spectra were recorded in 1024 channels, with number of scans, 3. The spectra were recorded and analysed using Xepr 2.6b.74 software. Xepr is a comprehensive software package of the ELEXSYS series, accommodating the needs of every user with highly developed acquisition and processing tools. The signal was integrated twice to determine its area and thus the concentration of the radical.

2.4.3. Penetration of NRNPs into SH-SY5Y Cells. Cells from about 80% confluent T-75 flask were trypsinized, centrifuged (5 min, 900 rpm) and resuspended in 3 mL of medium containing 100 μM NRNP1; divided into three parts; and incubated for 1, 2, and 4 hours, respectively. After an appropriate period of time, cells were centrifuged, and the pellet was washed with PBS and then centrifuged once again (supernatant was collected for further examination). The pellet was suspended in 200 μL PBS. Signal intensity of the nitroxide was measured using microhematocrit capillaries.

2.5. Analysis of Cell-Free Systems

2.5.1. Antiradical Activity: ABTS* Scavenging. The antioxidant properties of 6-OHDA were estimated using the 2,2′-azinobis(3-ethylbenzthiazoline-6-sulfonic acid) radical (ABTS*) according to a procedure previously proposed by us [45]. Appropriate amounts of 6-OHDA solution and of solutions of selected amino acids were added to a solution of ABTS* and diluted so that 200 μL of the solution had an absorbance of 1.0 in a microplate well, at 734 nm. The decrease in ABTS* absorbance was measured after 1 min ("fast" scavenging) and between 10 and 30 min ("slow" scavenging) of incubation at room temperature (21 ± 1°C). From the plots of the dependence of absorbance decrease (ΔA) on the compound concentration, the value of ΔA/mM was calculated for the compounds tested based on a Trolox calibration curve. The compounds studied were dissolved in PBS.

2.5.2. Assay of Hydrogen Peroxide Generation. Evaluation of H_2O_2 generation by 100 μM (final concentration) 6-OHDA solution in DMEM/F12 complete medium without phenol red was performed by incubation of the samples for 3 h at 37 ± 1°C with shaking. The peroxide content was estimated before and after incubation by the ferric-xylenol orange method [46]. After that, 180 μL/well of samples and 20 μL/well of the xylenol orange reagent were mixed together (2.5 mM xylenol orange/2.5 mM Mohr's salt (Fe$(NH_4)_2(SO_4)_2$) in 1.1 M perchloric acid). The absorbance was measured at 560 nm after a 30-minute incubation at room temperature.

2.5.3. Protection against Oxidation of Dihydrorhodamine 123 (DHR123). Dihydrorhodamine 123 (190 μL of 1 μM solution in 0.1 M phosphate buffer, pH 7.4) was added to each well of a 96-well plate containing the compounds studied in a range of concentrations (0.005–10 μM). The final volume of a sample was 200 μL. SIN-1 (1 μL of 1 mM solution) was added to each well, and kinetic measurement of fluorescence increase was carried using the excitation/emission wavelengths of 460/528 nm at 37°C for 2 h. From the area under curve values of fluorescence, IC$_{50}$ values were determined.

2.5.4. Protection of Fluorescein against Bleaching Induced by NaOCl or AAPH. Inhibition of fluorescein bleaching was determined with a method proposed by us [45]. Briefly, an aliquot of hypochlorite was added to a microplate well containing 100 μL of 0.2 μM fluorescein dissolved in PBS and the solution was mixed immediately. The amount of hypochlorite required to decrease fluorescence down to ca 5–10% of the initial value was determined (it corresponded to 1.75 nmol of hypochlorite). These conditions were used for subsequent measurements, in which nitroxides and NRNPs dissolved in PBS in a range of concentrations (0.125–10 μM) were added to the fluorescein solution before addition of hypochlorite, keeping the volume of the sample constant (100 μL). Fluorescence was measured after 15 min incubation at room temperature at the excitation/emission wavelengths of 485 and 538 nm, respectively.

AAPH stock solution was added to wells containing 0.2 μM fluorescein dissolved in PBS to obtain the final concentration of 10 mM and the solution was mixed immediately. These conditions were used for subsequent measurements, in which compounds dissolved in PBS in a range of concentrations (0.25–10 μM) were present in the fluorescein solution before the addition of AAPH, keeping the volume of the sample constant (100 μL). Fluorescence was measured after 1 hour incubation at 37°C. Percent of protection was

calculated according to the formula:

$$\% \text{ Protection} = (F_n\text{-}F_o)/(F_c\text{-}F_o) \times 100\% \tag{1}$$

where F_n is fluorescence of a sample containing fluorescein, hypochlorite/AAPH, and a compound studied; F_o is fluorescence of fluorescein treated with hypochlorite/AAPH only; and F_c is fluorescence of the nontreated fluorescein.

From the concentration dependence of protection on the antioxidant concentration, the concentrations of compounds providing 50% protection (IC_{50}) against the fluorescein bleaching were calculated.

2.6. Assessment of Penetration across a Model of the Blood-Brain Barrier (BBB) by NRNP1 and Free Nitroxides in an In Vitro Model

2.6.1. hCMEC/D3 Cell Culture.
The human immortalized brain endothelial line cells (hCMEC/D3) [44] were seeded onto culture flasks previously coated with collagen I (150 μg/mL, at 37°C for a least one hour) and maintained in endothelial cell basal medium 2 (EBM-2) containing 5% FBS. 1% penicillin-streptomycin, hydrocortisone (1.4 μM), ascorbic acid (5 μg/mL), 1% chemically defined lipid concentrate, and HEPES (10 mM), bFGF (1 ng/mL) under standard conditions: 37°C, 100% humidity, and the atmosphere being 5% CO_2 and 95% air. Experiments were performed on cells from the passages between 26 and 35. The cells were periodically tested for Mycoplasma.

2.6.2. Transport across a Model of the Blood-Brain Barrier.
The transport of NRNP1 as well as free nitroxides across BBB was analysed using transwell inserts (ThinCert™, Greiner Bio-One). The hCMEC/D3 cells were plated onto sterile 24-well cell culture inserts (pore diameter 0.4 μm), coated with collagen I, and grown to confluence for approximately five days. For the experiment, a medium with a final concentration (5 μM) of compounds studied was prepared directly before adding. The culture medium was replaced in either top or bottom compartment by a medium with appropriate compounds, and after 1, 20, 40, or 60 min, inserts were removed from lower reservoirs and solutions were transferred from lower reservoirs and from inserts to a fresh 96-well plate. Collected samples were measured three times in a Bruker multifrequency and multiresonance FT-EPR ELEXSYS E580 apparatus. Before the experiment, the transendothelial electrical resistance (TEER) was measured in duplicate inserts (five times in every single insert) using the epithelial volt-ohm meter Millicell® ERS-2 (Millipore) with MERSSTX01 electrode. All TEER values were determined after subtracting the background (TEER for cells free insert coated with collagen I) and by correction for surface area. The values were $>40\,\Omega\,\text{cm}^{-2}$. Wells showing too low TEER values were eliminated from the measurements [47].

2.6.3. Electron Spin Resonance (ESR) Spectroscopy.
ESR signal intensity of free nitroxides of NRNPs (~15 μL) was measured using microhematocrit capillaries (nonheparinized microhematocrit tubes; 1.55×75 mm; Medlab Products, Raszyn, Poland) in a Bruker multifrequency and multiresonance FT-

EPR ELEXSYS E580 apparatus (Bruker BioSpin, Billerica, MA, USA). The spectrometer was operated at X-band (around 9.4 GHz). The following settings were used: central field, around 3354.0 G; modulation amplitude, 0.3 G; modulation frequency, 100 kHz; microwave power, 94.64 mW; power attenuation 2.0 dB; scan range, 100 G; conversion time, 25 ms; and sweep time, 25.6 s. The spectra were recorded with 1024 points per scan, with the accumulated number of scans, 3. The spectra were recorded and analysed using Xepr 2.6b.74 software. The signal was integrated twice to determine its area and thus the concentration of the radical.

2.7. SH-SY5Y Cell Culture.
SH-SY5Y cell line was cultured in DMEM/F12 without phenol red, supplemented with 10% v/v heat-inactivated foetal bovine serum (hi-FBS) and 1% v/v penicillin and streptomycin solution. Cells were maintained at 37°C in 5% carbon dioxide and 95% humidity. The medium was changed twice a week, and the cells were passaged at about 80% confluence. For all studies, cells up to 14 passages were used. The morphology was examined under an inverted microscope with phase contrast Zeiss Primo Vert (Oberkochen, Germany); cell viability was estimated by Trypan Blue exclusion test and cells were counted using Thoma hemocytometer (Marienfeld Superior, Lauda-Königshofen, Germany).

Optimal cell number was experimentally determined. Cells were seeded into covered plates at various densities 2, 3, 3.5, 4, and 5×10^4 cells/well of a 96-well plate in 100 μL of cell culture medium and incubated for 24 hours. Then, a MTT assay was performed as described below. Another cytotoxicity assay, using Neutral Red has proved to be unsuitable due to significant cell loss during multiple washing steps.

2.7.1. Cell Viability Assay.
Human neuroblastoma cells were seeded in 96-well clear plate previously covered with 1% Geltrex™ LDEV-Free Reduced Growth Factor Basement Membrane Matrix (according to the manufacturer's protocol) at an amount of 3.5×10^4 cells/well in 100 μL culture medium (optimal cell number determined as described above). After 24 hour incubation, the medium was gently removed and replaced with cell culture medium supplemented with adequate compounds (6-OHDA, redox nanoparticles (NRNP1, NRNP2, and NRNP3), 4-amino-TEMPO, or TEMPO) at various concentrations in order to evaluate their self-cytotoxicity. After 24-hour exposure, the medium was removed and replaced with 100 μL of 0.5 mg/mL MTT solution in 1x PBS with ions and incubated for 4 hours in a CO_2 incubator. Then, 100 μL/well of isopropanol : HCl (250: 1 v/v) solution was added into cells in order to dissolve formazan crystals and shaken for about 20-30 minutes. The dissolution was controlled under inverted microscope. Absorbance was measured at 570 nm.

2.7.2. Treatment of SH-SY5Y Cells with NRNPs and Free Nitroxides.
In order to analyse antineurodegenerative properties of the compounds studied (NRNP1 and free nitroxides), cells were seeded as described above (SH-SY5Y Cell Culture and Cell Viability Assay). After overnight incubation to allow cell adhesion, the medium was replaced with 50 μL/well of the

studied compounds in the medium at chosen concentrations (4-amino-TEMPO and NRNP1: 75, 100, and $150\,\mu M$ or TEMPO: 100, $150\,\mu M$). Subsequent to 2-hour preincubation with the antioxidants, $50\,\mu L$/well of $120\,\mu M$ 6-OHDA was added (final concentration: $60\,\mu M$, slightly lower than IC_{50}) and then incubated, respectively, for 1 or 24 hours.

2.7.3. Measurement of Reduced Glutathione Content. The content of reduced glutathione (GSH) was assayed with *orthophthalaldehyde* (OPA) [48]. SH-SY5Y cells were seeded in a clear 96-well plate at an amount of 4×10^4 cells/well in $100\,\mu L$ culture medium and treated with selected antioxidants as described in Section 2.7.2. GSH was measured after 1 and 24 h incubation with $60\,\mu M$ 6-OHDA. Following incubation with 6-OHDA, the medium was gently removed and cells were washed with PBS ($150\,\mu L$/well). Phosphate-buffered saline was gently removed by aspiration. Subsequently, $60\,\mu L$/well of freshly prepared cold lysis buffer (RQB buffer: 20 mM HCl, 5% TCA, 5 mM DTPA, and 10 mM L-ascorbic acid) was added; then, the plates were shaken at 900 rpm for 5 minutes and centrifuged at 4000 rpm (5 minutes, room temperature).

Cell lysates were transferred into two separate black 96-well plates with a black bottom in a volume of $25\,\mu L$/well afterwards ('+ NEM' and '- NEM'). Into the first plate '+ NEM', $4\,\mu L$/well of newly prepared 7.5 mM NEM in ice-cold RQB buffer were added. Then, $40\,\mu L$/well of 1 M phosphate buffer (pH 7.0) was pipetted into both plates, which were shaken for 5 minutes at 900 rpm. Then, $160\,\mu L$/well of ice-cold 0.1 M phosphate buffer (pH 6.8) and $25\,\mu L$/well of newly prepared 0.5% OPA in methanol were added into '+NEM' and '-NEM' plates. Then, the plates were shaken at 900 rpm for 30 minutes. Fluorescence was measured with a TECAN Spark® multimode plate reader at 355/430 nm. GSH concentration was established by subtracting the fluorescence of the plate without NEM from the fluorescence of the NEM-containing plate and GSH content was calculated, respectively, with reference to protein content in each well.

2.7.4. Protein Assay. Protein content was determined according to Lowry et al. [49].

2.7.5. Assessment of Intracellular ATP Level. Intracellular ATP level was determined using CellTiter-Glo® Luminescent Cell Viability Assay (Promega, Madison, WI, USA), which is based on the enzymatic and luminescent transformation of luciferin to oxyluciferin in the presence of ATP. Cells were seeded into white 96-well plate with an optical bottom, cultured and treated with adequate compounds as described in Sections 2.7.1 and 2.7.2. Cells were assayed after 1 and 24 h incubation in separate plates (assessing both short- and long-term effects of 6-OHDA), by adding $100\,\mu L$ of CellTiter-Glo® Reagent to the cell culture medium present in each well, shaken and incubated according to the manufacturer's protocol. Luminescence was recorded using a TECAN Spark® multimode plate reader (Tecan Group Ltd., Switzerland).

2.7.6. Measurement of Reactive Oxygen Species (ROS) Using Fluorescent Probe (DHE). Cells were seeded, cultured, and posttreatment handled as previously described (Section 2.7.2) onto black 96-well plates with a clear bottom. This test was performed after 1 h or 24 h incubation with 6-OHDA of cells preincubated with antioxidants. $100\,\mu L$/well of freshly prepared DHE working solution in PBS was added; the final concentration of DHE is equal to $10\,\mu M$. The fluorescence was measured immediately at 37°C, at 405/570 nm for 2 hours, and at 1 min intervals.

2.7.7. Fluorimetric Estimation of Mitochondrial Superoxide Radical Level ($O_2^{\cdot-}$). Mitochondrial superoxide level was measured using Cell Meter™ Fluorimetric Mitochondrial Superoxide Activity Assay Kit Optimized for Microplate Reader (AAT Bioquest, Sunnyvale, CA, USA). Cells were seeded, cultured, and posttreatment handled as previously described (Section 2.7.2) onto black 96-well plates with a clear bottom. A test was performed after 1 and 24 h incubation with 6-OHDA. After an appropriate period of time, assay was performed according to the manufacturer's protocol: the medium was gently removed and $100\,\mu L$/well of reagent was added. The plate was incubated for 45 minutes in a CO_2 incubator. After that, fluorescence was measured at 540/590 nm for 4 hours at 2 min intervals.

2.7.8. Mitochondrial Membrane Potential Evaluation ($\Delta\psi_m$). Mitochondrial membrane potential was assayed using JC-1 (5,5′,6,6′-tetrachloro-1,1′,3,3′-tetraethylbenzimidazolylcarbocyanine iodide) with a Mitochondrial Membrane Potential Assay Kit (Abnova, Taiwan, China). JC-1 is a dye that can selectively enter the mitochondria and reversibly shift colour from green to red as the membrane potential rises. In healthy cells with high $\Delta\psi_m$, JC-1 forms complexes well known as J-aggregates with profound red fluorescence. On the other hand, in injured cells with low $\Delta\psi_m$, JC-1 remains in the monomeric state and exhibits green fluorescence exclusively.

Cells were seeded into black microplates with an optical bottom and treated as described in Section 2.7.2. After an appropriate period of time of exposure to $60\,\mu M$ 6-OHDA (1 h or 24 h), the medium was softly removed and replaced with 100x diluted JC-1 reagent in complete culture medium and incubated at 37°C for 30 min. Then, a microplate was centrifuged at 4000 rpm at room temperature for 5 min. The reagent was gently removed, and cells were washed with $150\,\mu L$/well Cell-Based Assay Buffer and centrifuged once again at the same conditions. Then, the buffer was removed and $100\,\mu L$/well of the new buffer was added. Fluorescence was measured at 540/570 nm (red fluorescence) and 485/535 nm (green fluorescence). The results were expressed as a ratio of red to green relative fluorescence units. Mitochondrial depolarization was indicated by a decrease in the polymer/monomer fluorescence intensity ratio.

2.7.9. Mitochondrial Mass Assessment. Cells were seeded at an amount of 2×10^5 cells/well onto a 24-well plate and cultured as previously described (Section 2.7.2). After 24-hour exposure to 6-OHDA, cells were trypsinized, counted, transferred to Eppendorf tubes, and centrifuged for 6 minutes at 2000 rpm (the same centrifugation conditions were maintained during this assay), then washed with 1 mL of PBS and centrifuged again. Next, 1 mL of $10\,\mu M$ NAO (solution in PBS) was added into the samples, and cells were incubated
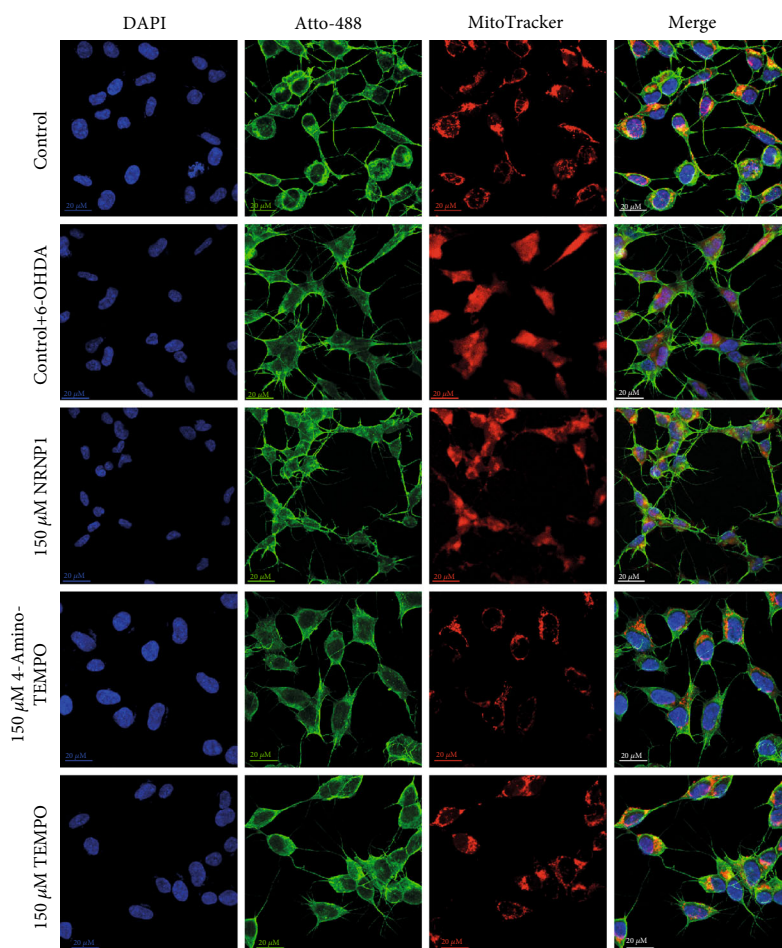
(a)
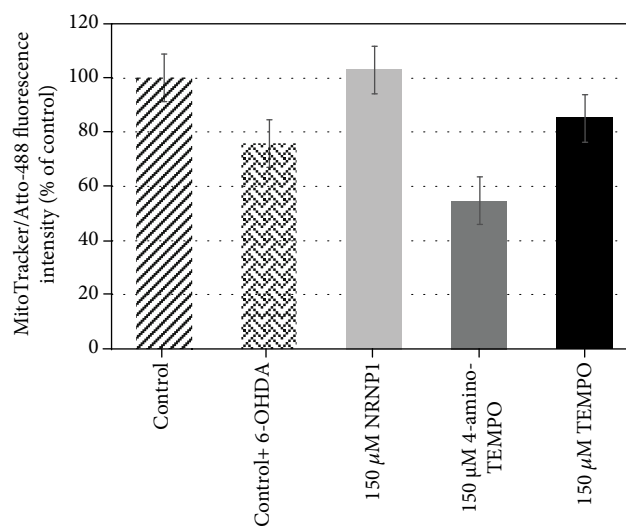
(b)

FIGURE 2: Morphological changes in the cellular structure. Confocal images of SH-SY5Y 63× preexposed to NRNP1 or free nitroxides (TEMPO or 4-amino-TEMPO) for 2 h and treated with 6-OHDA for 24 h. Nuclei were stained with DAPI (blue), phalloidin conjugated with Atto-488 (green), and mitochondria with MitoTracker Deep Red FM (red). All scale bars (control, bottom right) are 20 μm (a). In ImageJ, the fluorescence intensity was expressed as a mean gray value separately for the red channel (from MitoTracker) and separately for the green channel (phalloidin). The ratio of MitoTracker to phalloidin fluorescence (i.e., the ratio of the signal from the mitochondria to the number of cells (actin skeleton)) was calculated. The calculated values were expressed as a percentage of untreated control (b).
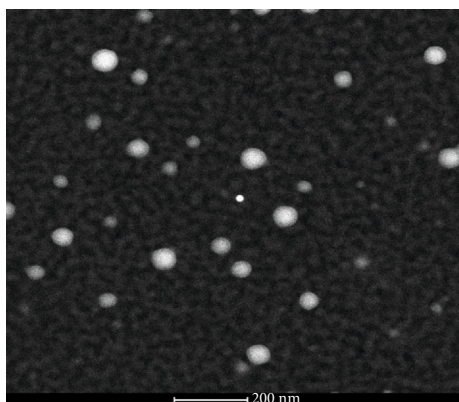
Figure 3: SEM picture of NRNP1.

for 10 min at 37°C. Afterwards, the cells were centrifuged and washed with 1 mL of PBS, and later, the pellet was resuspended in 300 μL of PBS. Each sample was transferred into a 96-well black plate (100 μL/well; 3 repetitions). Fluorescence was measured at 435/535 nm. The results were calculated with reference to the number of cells.

2.7.10. MitoTracker Labeling. SH-SY5Y cells were seeded on a 8-well chamber slide (Lab-Tek™ II Chamber Slide™ System cat. no. 154534, Thermo Scientific, Waltham, MA, USA) at an amount of 7×10^4 cells/400 μL culture medium and then treated as described in Section 2.7.2 long treatment). Following the treatment, the medium was removed and replaced with 250 nM solution of MitoTracker Deep Red FM (cat. no. M22426, Thermo Scientific, Waltham, MA, USA) in PBS and incubated for 45 min, in CO$_2$ incubator. Then, cells were washed with PBS (200 μL/well) and fixed with 200 μL/well 3.7% formaldehyde for 15 min. After that, cells were washed with PBS (200 μL/well), permeabilized with 0.1% Triton X-100 solution at an amount of 200 μL/well for 10 min, and washed with PBS (700 μL/well). Then, 150 μL/well of phalloidin working solution (prepared accordingly to the manufacturer's protocol) was added and for 60 min incubated for 60 min. After washing the cells with PBS (700 μL/well), nuclei were stained with 600 nM DAPI (200 μL/well). Images were taken using a Zeiss LSM 710 inverted confocal microscope (Oberkochen, Germany) under 63x magnification. The ratio of fluorescence intensity of the mitochondria and cytoskeleton (expressed as mean gray value) was calculated using ImageJ software and results were graphed for the images in Figure 2(a).

2.8. Statistical Analysis. Kruskal–Wallis test or Student *t*-test was performed to estimate the differences between 6-OHDA-treated control cells and antioxidant-treated cells to assess their properties in each individual assay; $P \leq 0.05$ was considered statistically significant in both cases. Also, differences between the 6-OHDA-treated and nontreated controls were assessed by an appropriate test (one of those described above). Statistical analysis of the data was performed using STATISTICA software package (version 13.3, StatSoft Inc. 2016, Tulsa, OK, USA, http://www.statsoft.com).

3. Results

3.1. Analysis of NRNPs in Cell-Free Systems

3.1.1. Scanning Electron Microscopy (SEM). In the scanning electron microscope, NRNP1 were visible as spherical structures of diameter of up to 100 nm (mean diameter of about 40 nm) (Figure 3).

3.1.2. Content of Nitroxyl Residues in the Polymers. Nitroxide residues per sum of hydrophilic and hydrophobic segment masses (segment molecular weight) were determined using ESR and 4-amino-TEMPO as a standard of ESR signal. The results indicated 27.6 radical residues per molecular weight of a segment (7500 g/mol) for NRNP1, 7.7 radical residues per segment molecular weight (8300 g/mol) for NRNP2, and 8.4 radical residues per molecular weight of a segment of NRNP3 (2246-2417 g/mol).

3.1.3. Antioxidant Properties of NRNPs. NRNPs dose dependently inhibited DHR123 oxidation induced by SIN-1 chloride (Figure 4) and fluorescein bleaching induced by NaOCl and AAPH. The nanoparticles were more effective than 4-amino-TEMPO as reflected by lower IC$_{50}$ values (Table 1). These results demonstrate good antioxidant properties of NRNPs.

3.1.4. Behaviour of 6-Hydroxydopamine in Cell-Free Systems. No production of ROS was found upon incubation of 6-OHDA in DMEM/F12 using H$_2$DCFDA and DHE (not shown). Nevertheless, small amounts of H$_2$O$_2$ were generated (much lower than in the case of ascorbate). The commercial preparation of 6-OHDA used is stabilized with ascorbate (ca 568 μM ascorbate/10 mM 6-OHDA). If the H$_2$O$_2$ produced was due to autoxidation of ascorbate, up to 6 μM H$_2$O$_2$ would be generated by autoxidation of 100 μM 6-OHDA solution; the value found indicates autoxidation of 6-OHDA in the cell culture medium leading to the production of H$_2$O$_2$. However, 6-OHDA showed also some antioxidant properties, being able to reduce ABTS*. The "fast" scavenging (occurring within 1 min) was low (about 1/6 that of standard antioxidants, ascorbate, or glutathione) and about 1/10 of such antioxidant amino acids as tyrosine and tryptophan). Moreover, 6-OHDA showed also "slow" scavenging, determined in our assay as the reactivity between 10 and 30 min of reaction, not exhibited by other compounds studied, including ascorbate, and even higher than the "fast" scavenging (Table 2); thus, it could not be due to the stabilizing ascorbate but to the antioxidant activity of 6-OHDA itself.

3.2. Protective Effect of Nitroxide Redox Nanoparticles on SH-SY5Y Cells Treated with 6-Hydroxydopamine

3.2.1. Protection of SH-SY5Y Cells against the Cytotoxicity of 6-OHDA. 6-Hydroxydopamine showed a dose-dependent cytotoxicity against SH-SY5Y cells. The IC$_{50}$ value of 6-OHDA is equal to 64 μM after 24 h treatment (Figure 5). All antioxidants studied exhibited slight intrinsic cytotoxicity at concentrations between 75 and 150 μM for 4-amino-TEMPO and NRNPs and 100 and 150 μM for TEMPO, when applied alone,

(a)

(b)
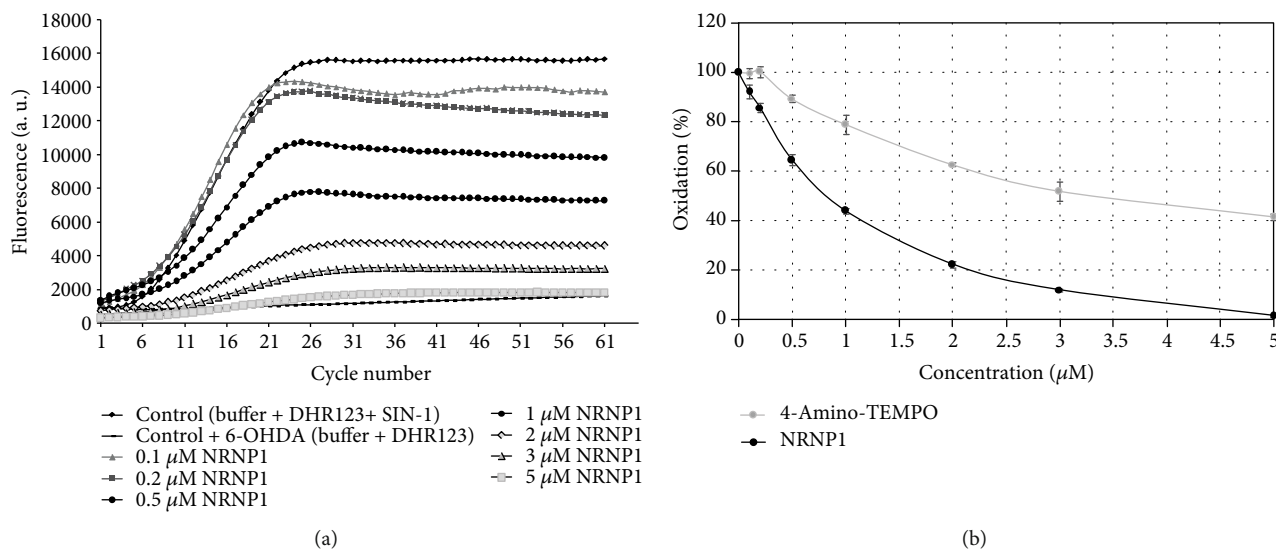
Figure 4: NRNP1 protect dihydrorhodamine 123 against oxidation by SIN-1: (a) kinetics of oxidation and (b) concentration dependence of the effect; for comparison, the effect of 4-amino-TEMPO is shown.

Table 1: Protection against dihydrorhodamine 123 oxidation by SIN-1: and against fluorescein bleaching by hypochlorite and AAPH (IC_{50} values).

Compound.	Protection against DHR 123 oxidation (IC_{50}, μM)	Protection against fluorescein bleaching by NaOCl (IC_{50}, μM)	Protection against fluorescein bleaching by AAPH (IC_{50}, μM)
NRNP1	0.98 ± 0.06	2.11 ± 0.12	0.56 ± 0.03
NRNP2	0.25 ± 0.02	1.52 ± 0.06	1.45 ± 0.08
4-Amino-TEMPO	3.35 ± 0.13	5.48 ± 0.14	7.85 ± 0.15

Table 2: Reducing activity of the 6-hydroxydopamine, antioxidant amino acids, and standard antioxidants (ABTS* assay) and generation of hydrogen peroxide in DMEM/F12 medium.

Compound.	Fast ABTS* scavenging activity (Mol TE/Mol)	Slow ABTS* scavenging activity (Mol TE/Mol)	H_2O_2 (μM)
6-Hydroxydopamine	0.172 ± 0.006	0.201 ± 0.006	7.8 ± 1.5
Tyrosine	1.845 ± 0.063	—	—
Tryptophan	1.883 ± 0.074	—	—
Ascorbic acid	1.114 ± 0.017	—	33.6 ± 0.9
Glutathione	1.027 ± 0.004	—	nd*

mean $\pm$ SD; $n \geq 3$ (independent samples). and*: not detectable amounts; TE: Trolox equivalents.

after 24 h incubation (Figure 6(a)). However, NRNP1 showed a profound neuroprotective effect against 6-OHDA-induced cytotoxicity at 75-150 μM. The improvement in viability was about 30% and 50% better compared to 4-amino-TEMPO and TEMPO, respectively (Figure 6(b)). NRNP2 and NRNP3 offered lower protection (Figures 7(b) and 7(d)); so, they were not used in further experiments.

3.2.2. Penetration of NRNP1 into SH-SY5Y Cells. After 1 h, 2 h, and 4 h incubation of 100 μL of 100 μM NRNP1 with 3 $\times 10^6$ cells, about 1.84%, 34%, and 32% of the nanoparticles, respectively, was internalized by the cells (judging from comparison of intensities of EPR signal after oxidation of the samples with 1 mM $K_3[Fe (CN)_6]$).

3.2.3. Penetration of a Model of the Blood-Brain Barrier (BBB). NRNP1, like TEMPO and 4-amino-TEMPO, penetrated the model BBB of hCMEC/D3 cells. The transport took place in both directions at comparable rates, indicating the lack of an active transporter (Figure 8).

3.2.4. ATP Level. A decrease in intracellular ATP level was observed even after 1 h incubation with 6-OHDA, but about 10% improvement was seen in samples preincubated with antioxidants. Nitroxides and NRNP1 alone did not induce significant changes. However, a long-term exposure to 6-OHDA reduced ATP level to about 65%, whereas both NRNP1 and 4-amino-TEMPO exhibited a similar effect, i.e., an about 20% protection (Figure 9).
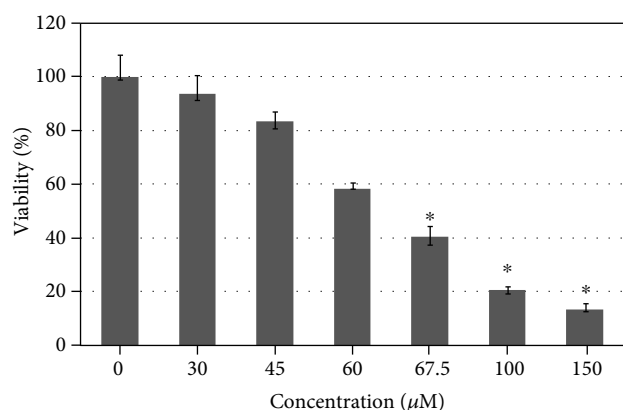
FIGURE 5: Cytotoxicity of 6-hydroxydopamine after 24 hour treatment. The whiskers are in lower (25%) and upper (75%) quartile ranges. $^*P \leq 0.05$, Kruskal–Wallis test against the nontreated control; $n = 9$.

3.2.5. Glutathione Level. The effects of 6-OHDA on GSH content in SH-SY5Y cells without and after 2 h treatment with NRNP1 and free nitroxides were examined after 1 and 24 h incubation. Short-term (1 h) incubations with 6-OHDA did not statistically significantly affect GSH content. In contrast, 24 h incubation with 6-OHDA induced a significant increase in the GSH content (Figure 10).

Preincubation with nitroxides or NRNPs followed by 6-OHDA treatment did not affect significantly the GSH level except for a small decrease at 150 μM NRNPs after short-term incubation. After 24 h treatment, amelioration of the increase in the GSH level was seen for 4-amino-TEMPO, and a complete abolition of the increase with even some decrease below the control level was noted for NRNPs. TEMPO showed no significant effect on the 6-OHDA-induced changes in the GSH level (Figure 10).

3.2.6. Level of Reactive Oxygen Species. A slight rise in ROS level measured with DHE, which shows some specificity towards O_2^{-}, was observed after 1 h incubation with 6-OHDA, and a significant increase after 24 h was also observed. All of the studied antioxidants decreased the ROS level, except NRNP1 at 75 μM concentration (Figure 11(a)). While after 24 h, the nanoparticles further increased ROS level, the level of ROS was unchanged in the presence of free radicals except for the highest concentration of TEMPO, which considerably decreases the level of ROS (Figure 11(b)). 6-OHDA exposure caused a substantial increase in the mitochondrial superoxide level, when measured with O_2^{-}-specific probe, MitoROS™. Free nitroxides counteracted this effect very efficiently even at the lowest concentration (75 μM) (Figures 11(c) and 11(d)), whereas NRNP1 attenuated this effect only after 24 h (Figure 11(d)).

3.2.7. Mitochondrial Membrane Potential. We estimated mitochondrial membrane potential ($\Delta\psi_m$) changes by JC-1 staining of SH-SY5Y cells treated with various concentrations of NRNP1 and free nitroxides. The results demonstrated that mitochondrial membrane potential was significantly reduced in 6-OHDA-treated cells (after short-

term and long-term treatment). After short-term exposure to 6-OHDA, NRNP1 did not exhibit a protective effect in this manner; there was even a further decrease in Ψ_m at 100 and 150 μM concentrations of NRNPs. Only 4-amino-TEMPO and TEMPO at 100 μM and 150 μM concentrations, respectively, showed some preventive effect. After long-term treatment, a considerable reduction in Ψ_m was observed, where selected antioxidants at nearly all concentrations slightly exhibited a protective effect, except NRNPs at 150 μM concentration (Figures 12(a) and 12(b)).

3.2.8. Mitochondrial Mass. The long-term incubation with 6-OHDA caused a significant decrease in the mitochondrial mass up to 50% compared to the nontreated control. NRNP1 (except 75 μM concentration), 4-amino-TEMPO, and TEMPO hampered this effect; yet, 150 μM concentration of NRNP1 and 100 μM of TEMPO evoked the most effective outcome. Other antioxidants attenuated changes in the mitochondrial mass at a similar level, producing an about 20% increase compared to the 6-OHDA-treated control (Figure 12(c)).

3.2.9. MitoTracker Labelling. Cultures of SH-SY5Y cells treated as described in Section 2.7.2 were stained with Mito-Tracker Deep Red FM and phalloidin, which target the intracellular mitochondrial network and cytoskeletal actin filaments, respectively. In addition, cell nuclei were simultaneously stained with DAPI (targeting DNA in the cell nucleus; ultraviolet excitation with blue emission) (Figure 2(a)). The ratio of fluorescence intensity of mitochondria and cytoskeleton (expressed as mean gray value) was calculated using ImageJ software. The analysis shows an about 20% decrease in the signal ratio between the 6-OHDA-treated and untreated controls. There is an about 20% higher signal ratio in a sample treated with 150 μM NRNP1 and an about 20% lower when treated with 150 μM 4-amino-TEMPO compared to the 6-OHDA-treated control sample (Figure 2(b)). TEMPO, however, gives a similar signal ratio with the 6-OHDA-treated control. These results well correlated with the results of mitochondrial mass estimation. The cells treated with 6-OHDA have evenly scattered mitochondria compared to the control cells. In cells treated with NRNP1, this tendency is also observed, but there are some clusters of mitochondria visible. In other samples, mitochondria are more concentrated in proximity to cellular membrane, which correlates with untreated control.

4. Discussion

It should be emphasized that current PD treatments ameliorate only the symptoms of the disease without halting its progress. Finding new medicines inhibiting the development of this disease can open new perspectives for the patients and considerably reduce healthcare expenses. Oxidative stress inevitably accompanies PD. The employment of antioxidants in this disease has been proposed to ameliorate OS and its consequences [50–54]. Nevertheless, the effects of antioxidants, among them natural components of the diet are

(a)

(b)
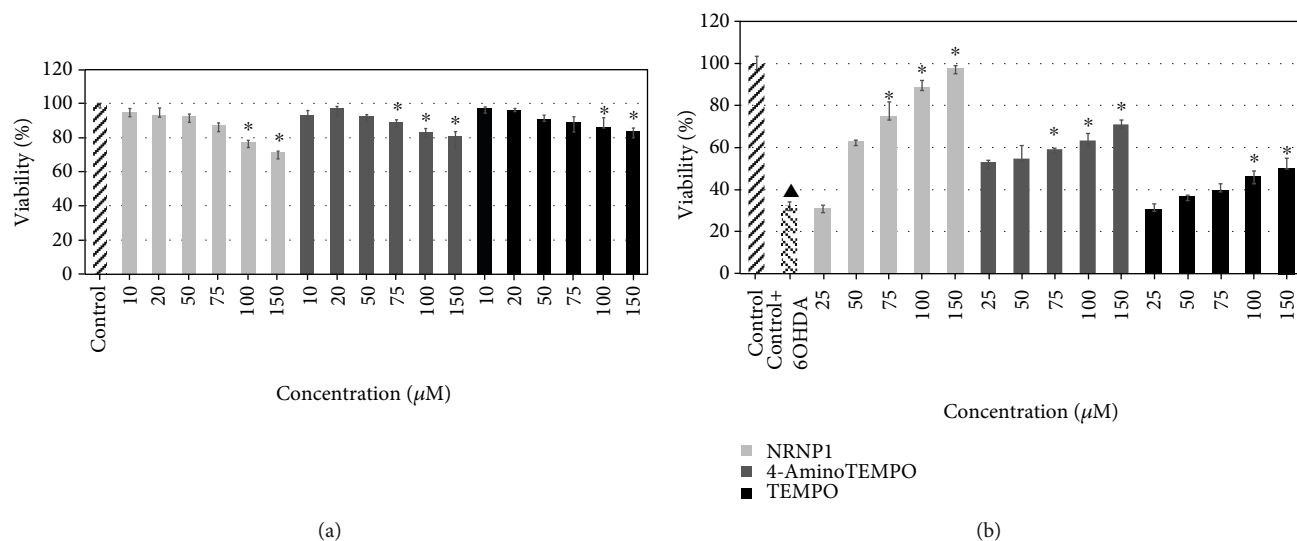
Figure 6: Self-cytotoxicity of selected antioxidants after 24 hour treatment (a) and their protective properties against the cytotoxicity of 60 μM 6-hydroxydopamine (b). The whiskers are in lower (25%) and upper (75%) quartile ranges. *$P \leq 0.05$, Kruskal–Wallis test against the 6-OHDA-treated control. ▲$P \leq 0.05$ differences between the controls; $n = 9$.

(a)

(b)

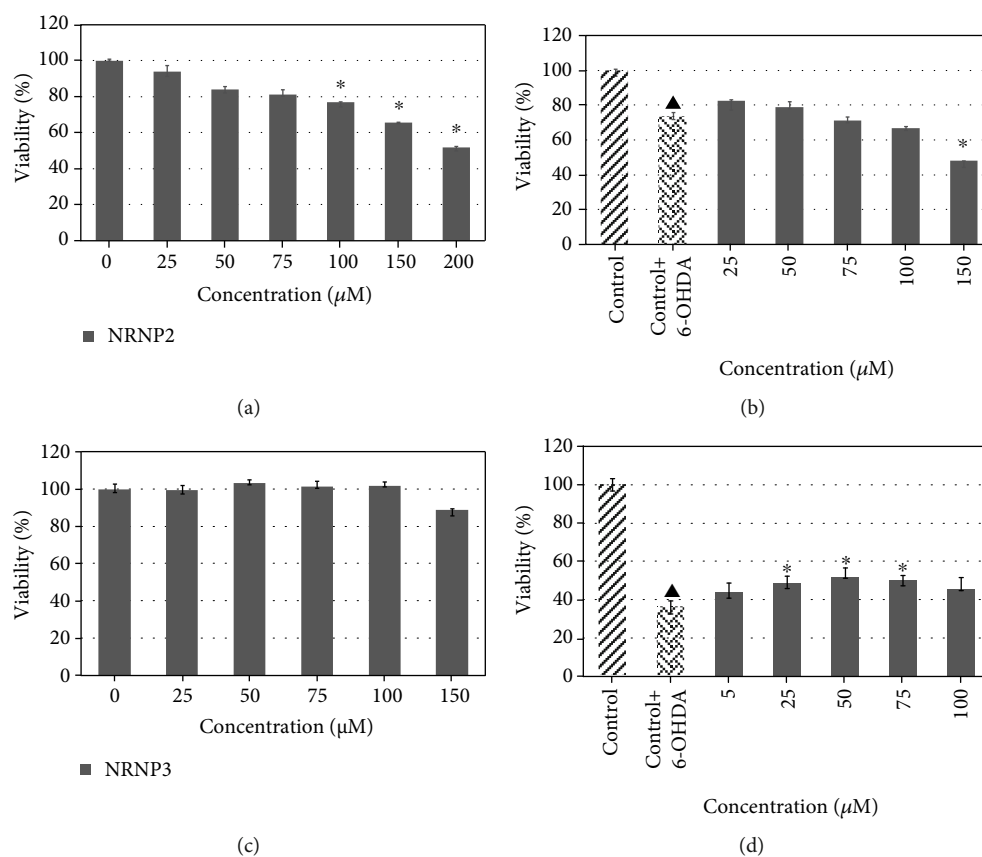

(c)

(d)

Figure 7: Self-cytotoxicity of NRNP2 after 24 hour treatment (a) and their protective properties of NRNP2 against the cytotoxicity of 60 μM 6-hydroxydopamine (b) and self-cytotoxicity of NRNP3 after 24 hour treatment (c) and protective properties of NRNP3 against the cytotoxicity of 60 μM 6-hydroxydopamine (d). The whiskers are in lower (25%) and upper (75%) quartile ranges. *$P \leq 0.05$, Kruskal–Wallis test against the nontreated control. ▲$P \leq 0.05$ differences between the controls; $n = 9$.

(a)

(b)
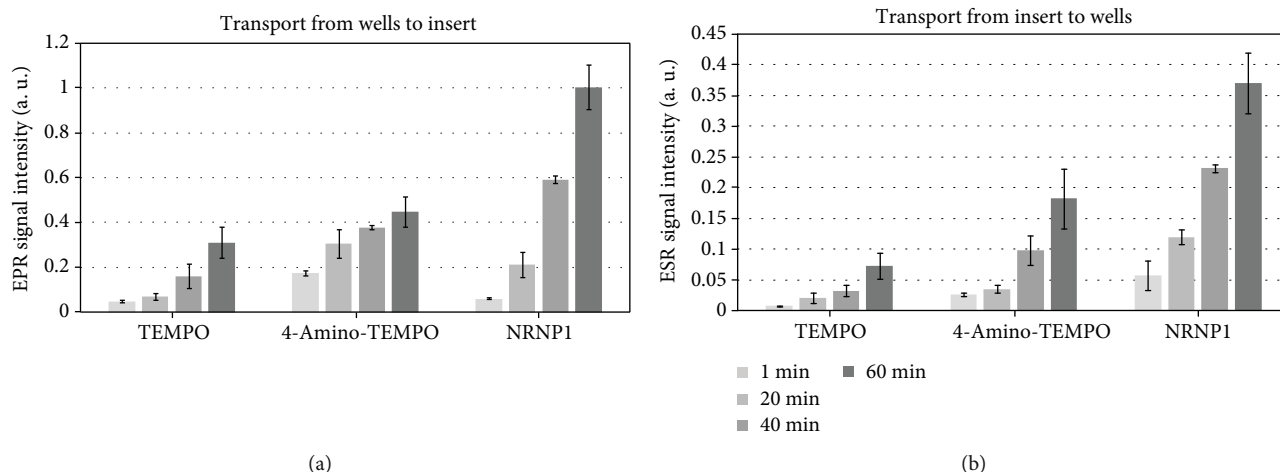
FIGURE 8: Two-directional transport of nitroxides and NRNP1 (from the basolateral to the apical compartment (a) and from the apical to the basolateral compartment (b)) across the model of the blood-brain barrier.: $n = 9$.

(a)

(b)
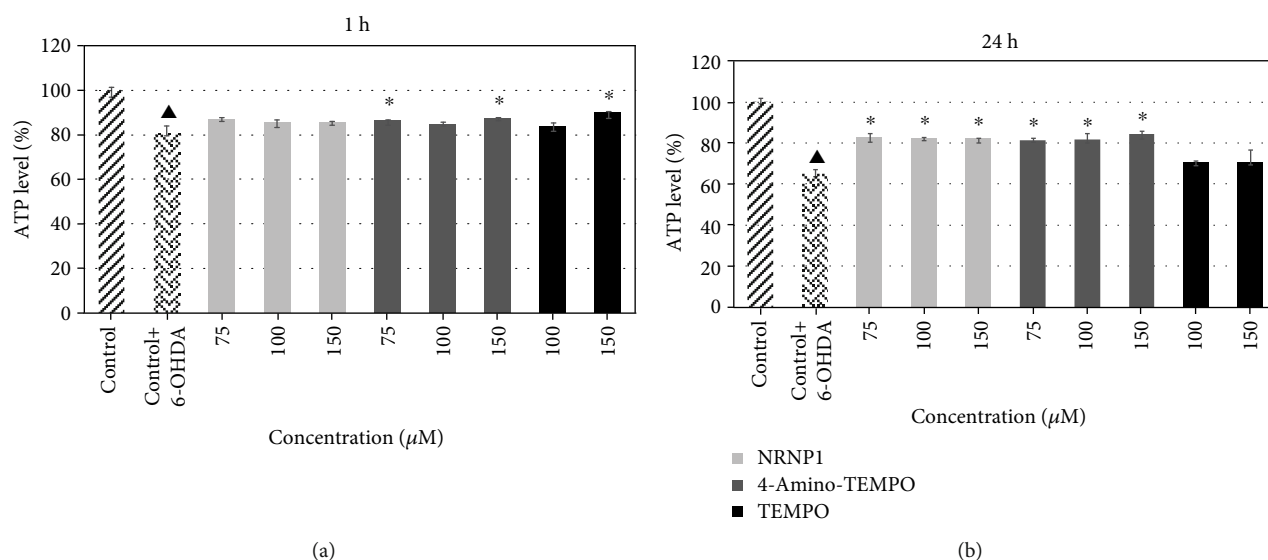
FIGURE 9: ATP levels after treatment with selected antioxidants and 6-hydroxydopamine after 1 (a) and 24 hours (b). The whiskers are in lower (25%) and upper (75%) quartile ranges. $^*P \leq 0.05$, Kruskal–Wallis test against the 6-OHDA-treated control. ▲$P \leq 0.05$ differences between controls; $n = 9$.

limited and new, more efficient antioxidants are searched for. Redox nanoparticles, polymers containing covalently linked nitroxyl radicals, showing low toxicity, and good stability *in vivo*, seem to be promising candidates for ameliorating OS in PD [55].

6-Hydroxydopamine treatment of neuronal cells is an acknowledged cellular model of PD. The damage of cells exposed to 6-OHDA has been ascribed to several mechanisms, including generation of ROS by autoxidation of 6-OHDA and mitochondrial damage, which may also lead to increased ROS production in the mitochondria [53, 56, 57]. We did not observe a significant generation of ROS by 6-OHDA in the absence of cells under tissue culture conditions. 6-OHDA produced low amounts of H_2O_2 in the medium, but at the same time, it showed also antioxidant properties, scavenging ABTS* in a fast and in a slow reactions, its fast

reactivity being similar to tyrosine and tryptophan, albeit lower (Table 2). However, 6-OHDA increased the intracellular levels of cytoplasmic and mitochondrial ROS (mainly superoxide) as estimated with DHE and MitoROS™ 520 (Figures 11(a) and 11(b)). 6-Hydroxydopamine exhibited a dose-dependent toxicity against SH-SY5Y cells (Figure 5). Nitroxide radical-containing redox nanoparticles as well as free nitroxides, TEMPO, and 4-amino-TEMPO protected against 6-OHDA toxicity, NRNP1 being the most effective on the (segment) molar basis (Figure 6(b)). The compounds studied, when administered alone, were slightly cytotoxic at the highest concentrations applied (Figure 6(a)); though, when applied together with 6-OHDA, they were protective. Apparently, the protective effect of NRNPs and nitroxides is due to their antioxidant properties. Antioxidant properties of NRNPs have been described in the literature [41, 43]. We

(a)

(b)
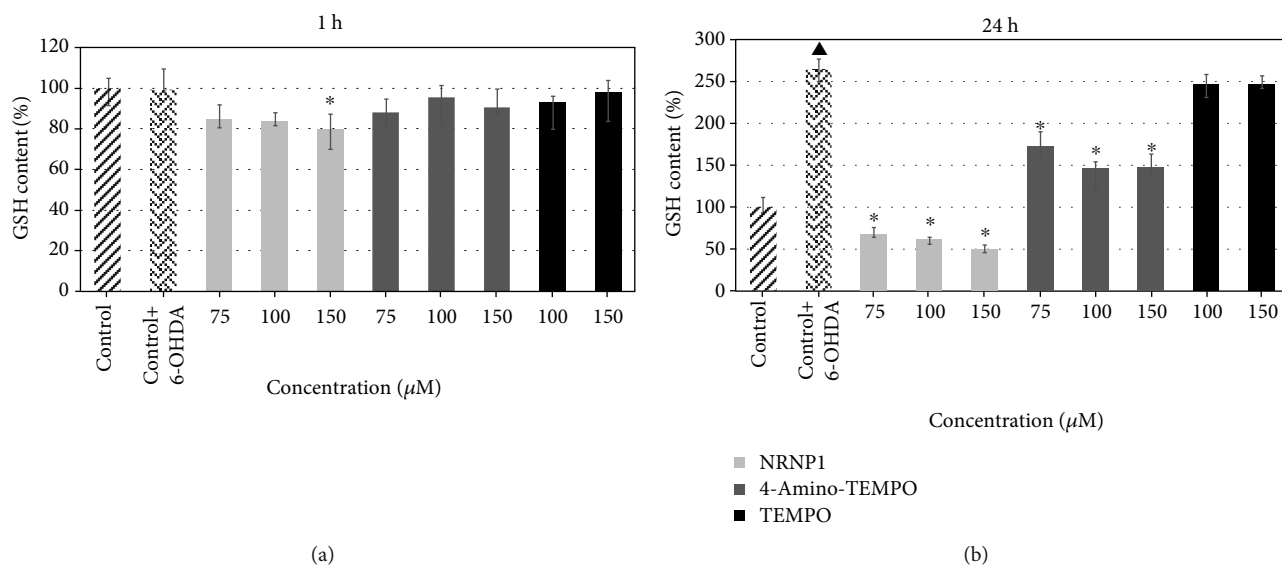
FIGURE 10: GSH content after treatment with selected antioxidants and 6-hydroxydopamine after 1 (a) and 24 hours (b). The whiskers are in lower (25%) and upper (75%) quartile ranges. $^*P \leq 0.05$, Kruskal–Wallis test against the 6-OHDA-treated control. ▲$P \leq 0.05$ differences between controls; $n = 9$.

(a)

(b)

(c)

(d)
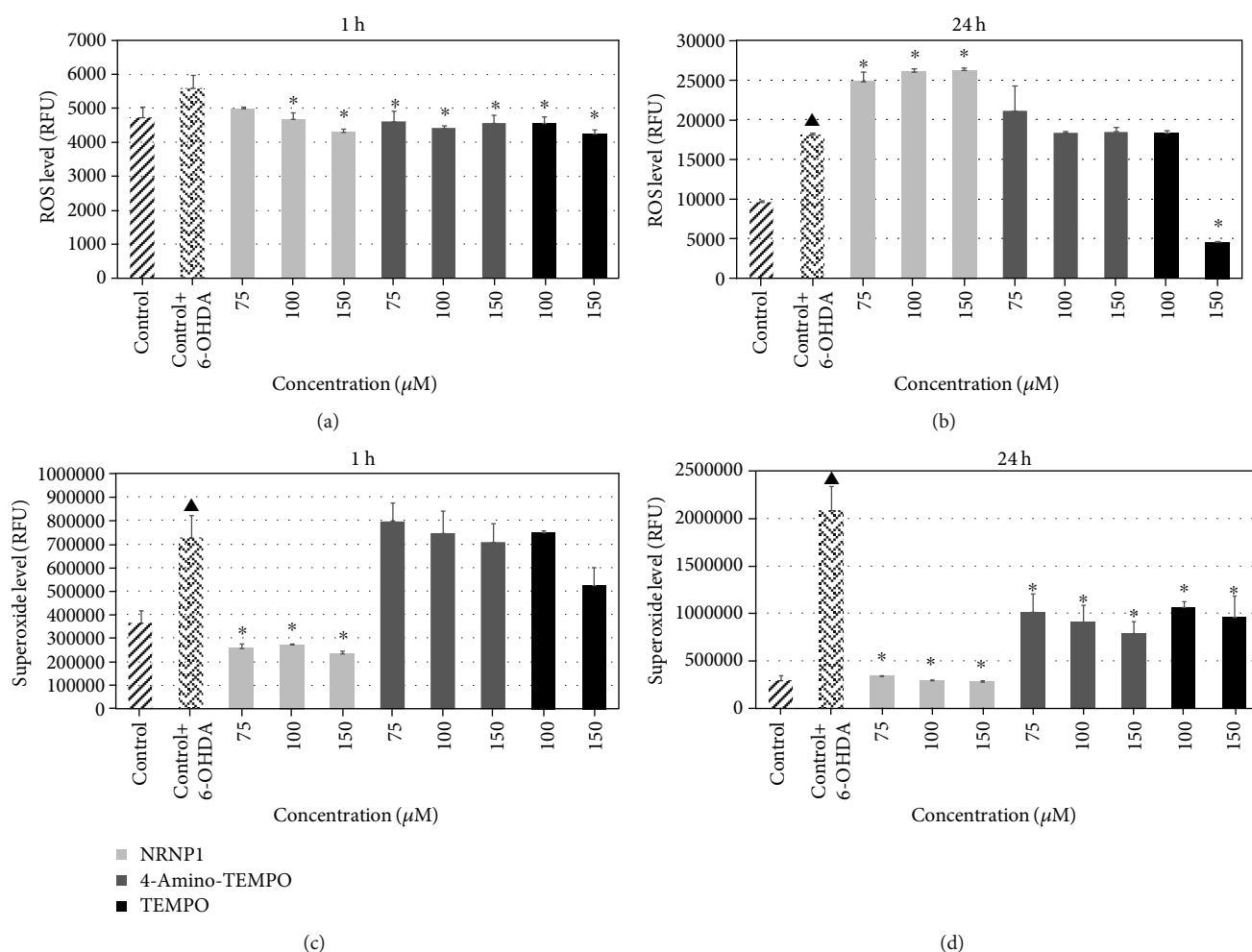
FIGURE 11: ROS level estimated with DHE after treatment with selected antioxidants and 6-hydroxydopamine for 1 (a) and 24 hours (b) and superoxide level after treatment with selected antioxidants and 6-hydroxydopamine for 1 (c) and 24 hours (d). The whiskers are in standard deviation. $^*P \leq 0.05$, Student t-test against the 6-OHDA-treated control. ▲$P \leq 0.05$ differences between the controls; $n = 3$.

(a)

(b)

(c)
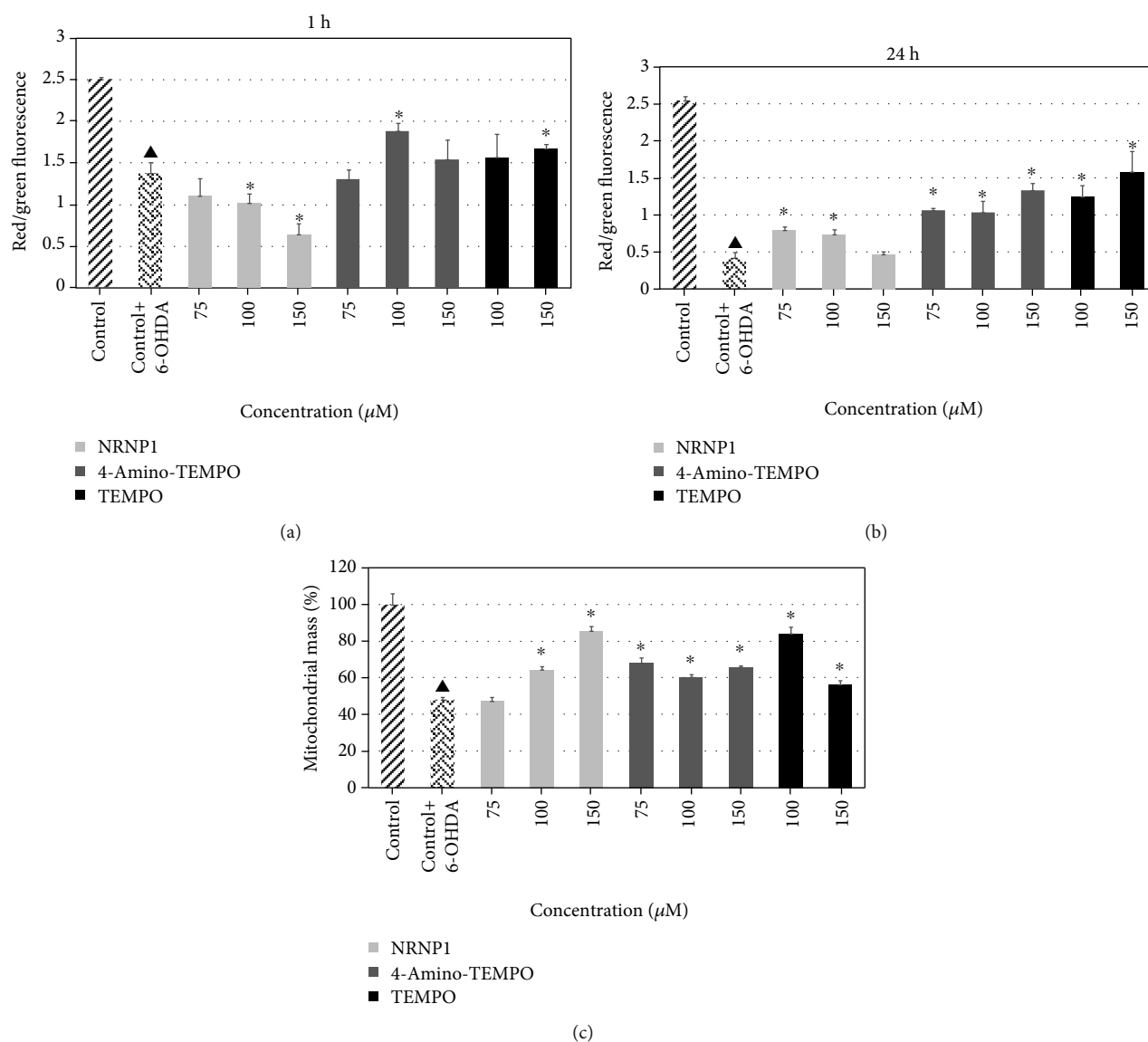
Figure 12: Changes in the mitochondrial potential after treatment with selected antioxidants and 6-hydroxydopamine for 1 (a) and 24 hours (b) and changes in the mitochondrial mass after treatment with selected antioxidants and 6-hydroxydopamine for 24 hours (c). The whiskers are in standard deviation. $^*P \leq 0.05$ Student t-test against the 6-OHDA-treated control. ▲$P \leq 0.05$ differences between the controls; $n = 3$ (a, b) and 9 (c).

demonstrated protective effects of NRNPs against oxidation by SIN-1 chloride and protection of fluorescein against bleaching by AAPH and hypochlorite (Table 1).

6-Hydroxydopamine increased the level of cytoplasmic ROS (mainly superoxide) after 1 h and 24 h incubation. An increase in the intracellular ROS level in the 6-OHDA-treated cells has been also reported by other authors [55]. While the increase after 1 h was attenuated by NRNP1 and free nitroxides (Figure 11(a)), the ROS increase after 24 h was not affected by free nitroxides except for the highest concentration of TEMPO, but augmented by NRNP1 (Figure 11(b)). The 6-OHDA-induced increase in the super-oxide level was most pronounced in the mitochondria. In this case, NRNP1 showed a strong protective effect, while free nitroxides was effective only after 24 h (Figures 11(c) and

11(d)). The apparent increase in the ROS level in the pres-ence of NRNP1 (Figure 11(b)) is surprising; we attribute it to the direct oxidation of the fluorogenic probe by NRNP1 observed by us [58].

Of critical importance for any substance considered for having a possible effect on the course of PD is its ability to penetrate the BBB. Brain endothelial cells (BECs) forming the BBB express the adenosine triphosphate-binding cassette efflux transporters, P-glycoprotein (P-gp), and the breast cancer resistance protein (BCRP), which have a similar sub-strate overlap, and act to prevent toxins and unwanted blood-borne signaling molecules from entering the brain [59]. To date, there have been no reported investigations regarding the assessment of BBB penetration by NRNPs and free nitroxides in an *in vitro* model employing human

brain capillary endothelium cells hCMEC/D3 [44, 47]. Our results show that NRNP1 are able to penetrate the BBB, judging from the penetration of the BBB model formed by hCMEC/D3 cells. Two-directional transport at comparable rates indicates penetration of the barrier not mediated by an active transporter. Basing on the EPR signal intensity, the transport of NRNP1 was faster than that of free nitroxides as per amount of free radical residues (Figure 8), indicating a possible transcellular vesicular transport component.

The level of glutathione was not significantly altered by 6-OHDA after 1 h incubation and significantly increased after 24 h. Apparently, this is a compensative effect being a response to a rapid GSH depletion by 6-OHDA (not visualized by our studies) due to the activation of GSH biosynthesis. Such an effect has been described previously for SH-SY5Y cells [60]. These authors concluded that 6-OHDA induced a concentration-dependent increase in GSH and total glutathione concentrations after 24 h. After exposure to $50\,\mu$M 6-OHDA, GSH concentrations were increased up to 12-fold after 24 h with no change in the GSH : GSSG ratio. Gene analysis suggested that the increase in GSH concentration was due to the increased expression of the GSH biosynthesis genes, coding for glutamate cysteine ligase modifier and catalytic subunits. To resume, 6-OHDA induces OS in SH-SY5Y cells resulting in an adaptive increase in cellular GSH concentrations. NRNP1 and 4-amino-TEMPO prevented this effect (Figure 10).

It should be noted that nitroxides also react with GSH [58] and thus may induce a compensative GSH biosynthesis in cells exposed to nitroxides as well as after 24 h; in the case of NRNP1, this effect was not observed, most probably due to different reactivity of NRNP1 with GSH, with respect to free nitroxides (Figure 10). Previous studies pointed to a much lower reactivity of NRPN1 with respect to free nitroxides for another reducing agent, ascorbate [41].

6-Hydroxydopamine induced a decrease in the cellular ATP content, apparently due to mitochondrial dysfunction. This decrease was counteracted by NRNP1 and free nitroxides (Figure 9). Indeed, 6-OHDA induced mitochondrial depolarization as detected by the JC-1 probe, which was attenuated by NRNP1 and nitroxides after 24 h incubation. A decrease in the mitochondrial mass was also observed in the 6-OHDA-treated cells; this decrease was prevented by NRNP1 and nitroxides (Figure 12). Similar direction of changes was seen when the intensity of mitochondrial staining with MitoTracker Red was compared (Figure 2). This phenomenon might be correlated with the fact that several studies have shown that 6-OHDA affects mitochondrial fusion and fission causing an imbalance in mitochondrial dynamics, and it is proven that it may contribute to the pathogenesis of neurodegenerative diseases [61–63]. Previous studies demonstrated that 6-OHDA (albeit at a high concentration of $150\,\mu$M) caused a loss of cell viability and mitochondrial depolarization [55, 64].

It can be suggested on the basis of the presented results that the main effect of 6-OHDA on SH-SY5Y cells consists of the mitochondrial damage. 6-Hydroxydopamine, as a positively charged compound, can be expected to accumulate in the mitochondria and increase ROS production primarily in the mitochondria. The resulting mitochondrial damage can lead to the depolarization of the inner mitochondrial membrane, a decrease in the mitochondrial mass, and diminution of ATP production, resulting in many site cellular damage. Mitochondrial damage by 6-OHDA was attributed to two mechanisms: ROS production and inhibition of the mitochondrial respiratory chain complexes I and IV [65]. As both ROS and reactive nitrogen species (RNS) were implicated in the 6-OHDA damage to nigrostriatal dopaminergic neurons seen in PD [66], it should be emphasized that nitroxyl radicals (and NRNPs) react with both ROS and RNS, being able of catalytic decomposition of peroxynitrite [32]. Another factor involved in the 6-OHDA cytotoxicity is iron, especially Fe^{2+} contained in the intracellular labile iron pool; iron chelators reducing this pool protect SH-SY5Y cells against 6-OHDA toxicity [67]. Nitroxides and NRPNs are able to oxidize Fe^{2+} ions, eliminating their activity in free radical reactions, and this effect may also contribute to their protective action. Thus, nitroxide radical-containing redox nanoparticles are effective compounds for the protection of neuronal cells against the 6-OHDA-induced damage, and as they are more stable *in vivo* and less prone to reduction than free nitroxides [40, 54], they could be promising as agents inhibiting the neuronal damage in PD.

5. Conclusion

Our results suggest that the mitochondria are the main site of 6-OHDA-induced cellular damage and demonstrate a protective effect of NRNP1 in a cellular model of PD. Understanding the protective effects of NRNP1 against PD progress requires further careful *in vivo* investigation.

Abbreviations

4-amino-TEMPO:	4-Amino-2,2,6,6-tetramethylpiperidine-1-oxyl
6-OHDA:	6-Hydroxydopamine
AAPH:	2,2-Azobis (2-amidinopropane) dihydrochloride
ABTS*:	2,2′-Azinobis (3-ethylbenzthiazoline-6-sulfonic acid) radical
BBB:	Blood-brain barrier
DHE:	Dihydroethidium
DHR123:	Dihydrorhodamine 123
DMEM/F12:	Dulbecco's Modified Eagle Medium Nutrient Mixture F-12
DMSO:	Dimethyl sulfoxide
Drp1:	Dynamin-related protein-1
DTPA:	Diethylenetriaminepentaacetic acid
EBM-2:	Endothelial cell growth basal medium-2
ESR:	Electron spin resonance
FBS:	Foetal bovine serum
GSH:	L-Glutathione reduced
JC-1:	5,5′,6,6′-Tetrachloro-1,1′,3,3′-tetraethylbenzimidazolylcarbocyanine iodide
Mohr's salt:	Fe $(NH_4)_2(SO_4)_2$

MTT:	3-(4,5-Dimethylthiazol-2-yl)-2,5-diphenyltetrazolium bromide
NAO:	Acridine orange 10-nonyl bromide
NEM:	N-Ethylmaleimide
NRNPs:	Nitroxide-containing redox nanoparticles
OPA:	ortho-Phthalaldehyde
OS:	Oxidative stress
Parkin:	Parkinson juvenile disease protein 2
PBS:	Phosphate-buffered saline
PD:	Parkinson's disease
PEG-b-PCTEMPO:	A self-assembling amphiphilic block copolymer composed of a hydrophilic poly (ethylene glycol) (PEG) segment and a hydrophobic poly (chloromethylstyrene) (PCMS)
PINK1:	PTEN-induced kinase-1
RNS:	Reactive nitrogen species
ROS:	Reactive oxygen species
SEM:	Scanning electron microscopy
SIN-1:	5-Amino-3-(4-morpholinyl)-1,2,3-oxadiazolium chloride
TCA:	Trichloroacetic acid
TE:	Trolox equivalents
TEMPO:	2,2,6,6-Tetramethylpiperidine-1-oxyl
TEMPOL:	4-Hydroxy-2,2,6,6-tetramethylpiperidine-1-oxyl
$\Delta\psi_m$:	Mitochondrial membrane potential
IC_{50}:	Half maximal inhibitory concentration.

Data Availability

Data available on request. Please contact I. Sadowska-Bartosz, e-mail: isadowska@poczta.fm.

Conflicts of Interest

The authors declare that they have no conflicts of interest.

Authors' Contributions

I. S.-B. was responsible for the concept of the study, design of experiments and supervision of experimental work, performed part of experiments, and had a leading role in the analysis of the results and preparation of the manuscript. She was also responsible for providing the funding for the study. M. P. performed the main part of experiments in the cellular system (SH-SY5Y cells) and their statistical evaluation as well as contributed reagents/materials/analysis tools. Ł. P and K. D. K performed experiments on hCMEC/D3 cells as well as contributed reagents/materials/analysis tools. I. S. and B. C. carried out EPR measurements and interpreted the data. N. P. took part in the execution of experiments on the SH-SY5Y cell line. G. B. participated in the revision of the manuscript. All authors have read and approved the final manuscript.

References

[1] E. R. Dorsey, R. Constantinescu, J. P. Thompson et al., "Projected number of people with Parkinson disease in the most populous nations, 2005 through 2030," *Neurology*, vol. 68, no. 5, pp. 384–386, 2007.

[2] K. R. Chaudhuri and A. H. Schapira, "Non-motor symptoms of Parkinson's disease: dopaminergic pathophysiology and treatment," *Lancet Neurology*, vol. 8, no. 5, pp. 464–474, 2009.

[3] R. Xia and Z.-H. Mao, "Progression of motor symptoms in Parkinson's disease," *Neuroscience Bulletin*, vol. 28, no. 1, pp. 39–48, 2012.

[4] D. T. Dexter and P. Jenner, "Parkinson disease: from pathology to molecular disease mechanisms," *Free Radical Biology and Medicine*, vol. 62, pp. 132–144, 2013.

[5] R. K. Dagda, T. Das Banerjee, and E. Janda, "How Parkinsonian toxins dysregulate the autophagy machinery," *International Journal of Molecular Sciences*, vol. 14, no. 11, pp. 22163–22189, 2013.

[6] T. Sherer, R. Betarbet, and J. Greenamyre, "Environment, mitochondria, and Parkinson's disease," *The Neuroscientist*, vol. 8, no. 3, pp. 192–197, 2002.

[7] M. R. Cookson, "The biochemistry of Parkinson's disease," *Annual Review of Biochemistry*, vol. 74, pp. 29–52, 2005.

[8] R. K. Dagda and C. T. Chu, "Mitochondrial quality control: insights on how Parkinson's disease related genes PINK1, parkin, and Omi/HtrA2 interact to maintain mitochondrial homeostasis," *Journal of Bioenergetics and Biomembranes*, vol. 41, no. 6, pp. 473–479, 2009.

[9] J. L. Biedler, S. Roffler-Tarlov, M. Schachner, and L. S. Freedman, "Multiple neurotransmitter synthesis by human neuroblastoma cell lines and clones," *Cancer Research*, vol. 38, no. 11, pp. 3751–3757, 1978.

[10] J. Kovalevich and D. Langford, "Considerations for the use of SH-SY5Y neuroblastoma cells in neurobiology," *Methods in Molecular Biology*, vol. 1078, pp. 9–21, 2013.

[11] H. Xicoy, B. Wieringa, and G. J. M. Martens, "The SH-SY5Y cell line in Parkinson's disease research: a systematic review," *Molecular Neurodegeneration*, vol. 12, no. 1, p. 10, 2017.

[12] N. Simola, M. Morelli, and A. R. Carta, "The 6-hydroxydopamine model of Parkinson's disease," *Neurotoxicity Research*, vol. 11, no. 3-4, pp. 151–167, 2007.

[13] D. Blum, S. Torch, N. Lambeng et al., "Molecular pathways involved in the neurotoxicity of 6-OHDA, dopamine and MPTP: contribution to the apoptotic theory in Parkinson's disease," *Progress in Neurobiology*, vol. 65, no. 2, pp. 135–172, 2001.

[14] K. Chiba, A. Trevor, and N. Castagnoli Jr., "Metabolism of the neurotoxic tertiary amine, MPTP, by brain monoamine oxidase," *Biochemical and Biophysical Research Communications*, vol. 120, no. 2, pp. 574–578, 1984.

[15] P. Jenner, A. H. Schapira, and C. D. Marsden, "New insights into the cause of Parkinson's disease," *Neurology*, vol. 42, no. 12, pp. 2241–2250, 1992.

[16] B. Wang, N. Abraham, G. Gao, and Q. Yang, "Dysregulation of autophagy and mitochondrial function in Parkinson's disease," *Translational Neurodegeneration*, vol. 5, no. 1, 2016.

[17] J. F. Harrison, S. B. Hollensworth, D. R. Spitz, W. C. Copeland, G. L. Wilson, and S. P. LeDoux, "Oxidative stress-induced apoptosis in neurons correlates with mitochondrial DNA base excision repair pathway imbalance," *Nucleic Acids Research*, vol. 33, no. 14, pp. 4660–4671, 2005.

[18] S. Singh, S. Kumar, and M. Dikshit, "Involvement of the mitochondrial apoptotic pathway and nitric oxide synthase in dopaminergic neuronal death induced by 6-hydroxydopamine and lipopolysaccharide," *Redox Report*, vol. 15, no. 3, pp. 115–122, 2010.

[19] A. Storch, A. Kaftan, K. Burkhardt, and J. Schwarz, "6-Hydroxydopamine toxicity towards human SH-SY5Y dopaminergic neuroblastoma cells: independent of mitochondrial energy metabolism," *Journal of Neural Transmission*, vol. 107, no. 3, pp. 281–293, 2000.

[20] G. N. L. Jameson and W. Linert, "6-Hydroxydopamine, dopamine, and ferritin: a cycle of reactions sustaining Parkinson's disease?," *Oxidative Stress and Disease*, vol. 5, pp. 247–272, 2000.

[21] J. Lotharius, L. L. Dugan, and K. L. O'Malley, "Distinct mechanisms underlie neurotoxin-mediated cell death in cultured dopaminergic neurons," *Journal of Neuroscience*, vol. 19, no. 4, pp. 1284–1293, 1999.

[22] M. Gomez-Lazaro, N. A. Bonekamp, M. F. Galindo, J. Jordán, and M. Schrader, "6-Hydroxydopamine (6-OHDA) induces Drp1-dependent mitochondrial fragmentation in SH-SY5Y cells," *Free Radical Biology and Medicine*, vol. 44, no. 11, pp. 1960–1969, 2008.

[23] E. M. Chalovich, J. H. Zhu, J. Caltagarone, R. Bowser, and C. T. Chu, "Functional repression of cAMP response element in 6-hydroxydopamine-treated neuronal cells," *Journal of Biological Chemistry*, vol. 281, no. 26, pp. 17870–17881, 2006.

[24] V. P. Patel, D. B. Defranco, and C. T. Chu, "Altered transcription factor trafficking in oxidatively-stressed neuronal cells," *Biochimica et Biophysica Acta*, vol. 1822, no. 11, pp. 1773–1782, 2012.

[25] D. Blum, S. Torch, M. F. Nissou, A. L. Benabid, and J. M. Verna, "Extracellular toxicity of 6-hydroxydopamine on PC12 cells," *Neuroscience Letters*, vol. 283, no. 3, pp. 193–196, 2000.

[26] J. C. Bensadoun, O. Mirochnitchenko, M. Inouye, P. Aebischer, and A. D. Zurn, "Attenuation of 6-OHDA-induced neurotoxicity in glutathione peroxidase transgenic mice," *European Journal of Neuroscience*, vol. 10, no. 10, pp. 3231–3236, 1998.

[27] S. Deb, A. Dutta, B. C. Phukan et al., "Neuroprotective attributes of L-theanine, a bioactive amino acid of tea, and its potential role in Parkinson's disease therapeutics," *Neurochemistry International*, vol. 129, p. 104478, 2019.

[28] Y. S. Ho, D. C. Poon, T. F. Chan, and R. C. Chang, "From small to big molecules: how do we prevent and delay the progression of age-related neurodegeneration?," *Current Pharmaceutical Design*, vol. 18, no. 1, pp. 15–26, 2012.

[29] M. E. Ferreira, A. S. de Vasconcelos, T. da Costa Vilhena et al., "Oxidative stress in Alzheimer's disease: should we keep trying antioxidant therapies?," *Cellular and Molecular Neurobiology*, vol. 35, no. 5, pp. 595–614, 2015.

[30] Q. Liang, A. D. Smith, S. Pan et al., "Neuroprotective effects of TEMPOL in central and peripheral nervous system models of Parkinson's disease," *Biochemical Pharmacology*, vol. 70, no. 9, pp. 1371–1381, 2005.

[31] B. P. Soule, F. Hyodo, K. Matsumoto et al., "The chemistry and biology of nitroxide compounds," *Free Radical Biology and Medicine*, vol. 42, no. 11, pp. 1632–1650, 2007.

[32] I. Sadowska-Bartosz, A. Gajewska, J. Skolimowski, R. Szewczyk, and G. Bartosz, "Nitroxides protect against peroxynitrite-induced nitration and oxidation," *Free Radical Biology and Medicine*, vol. 89, pp. 1165–1175, 2015.

[33] I. Sadowska-Bartosz, S. Galiniak, J. Skolimowski, I. Stefaniuk, and G. Bartosz, "Nitroxides prevent protein *glycoxidationin vitro*," *Free Radical Research*, vol. 49, no. 2, pp. 113–121, 2014.

[34] S. Suy, J. B. Mitchell, D. Ehleiter, A. Haimovitz-Friedman, and U. Kasid, "Nitroxides tempol and tempo induce divergent signal transduction pathways in MDA-MB 231 breast cancer cells," *Journal of Biological Chemistry*, vol. 273, no. 28, pp. 17871–17878, 1998.

[35] Q. L. Zhao, Y. Fujiwara, and T. Kondo, "Mechanism of cell death induction by nitroxide and hyperthermia," *Free Radical Biology and Medicine*, vol. 40, no. 7, pp. 1131–1143, 2006.

[36] U. Simonsen, F. H. Christensen, and N. H. Buus, "The effect of tempol on endothelium-dependent vasodilatation and blood pressure," *Pharmacology & Therapeutics*, vol. 122, no. 2, pp. 109–124, 2009.

[37] B. Y. S. Kim, J. T. Rutka, and W. C. W. Chan, "Nanomedicine," *New England Journal of Medicine*, vol. 363, no. 25, pp. 2434–2443, 2010.

[38] Y. Matsumura and H. Maeda, "A new concept for macromolecular therapeutics in cancer chemotherapy: mechanism of tumoritropic accumulation of proteins and the antitumor agent smancs," *Cancer Research*, vol. 46, 12 part 1, pp. 6387–6392, 1986.

[39] Y. Bae, S. Fukushima, A. Harada, and K. Kataoka, "Design of environment-sensitive supramolecular assemblies for intracellular drug delivery: polymeric micelles that are responsive to intracellular pH change," *Angewandte Chemie International Edition*, vol. 42, no. 38, pp. 4640–4643, 2003.

[40] P. Chonpathompikunlert, T. Yoshitomi, L. B. Vong, N. Imaizumi, Y. Ozaki, and Y. Nagasaki, "Recovery of cognitive dysfunction via orally administered redox-polymer nanotherapeutics in SAMP8 mice," *PLoS One*, vol. 10, no. 5, article e0126013, 2015.

[41] T. Yoshitomi, D. Miyamoto, and Y. Nagasaki, "Design of core–shell-type nanoparticles carrying stable radicals in the core," *Biomacromolecules*, vol. 10, no. 3, pp. 596–601, 2009.

[42] J. C. Morris, "The acid ionization Constant of HOCl from 5 to 35°," *Journal of Physical Chemistry*, vol. 70, no. 12, pp. 3798–3805, 1966.

[43] T. Yoshitomi, R. Suzuki, T. Mamiya, H. Matsui, A. Hirayama, and Y. Nagasaki, "pH-sensitive radical-containing-nanoparticle (RNP) for the L-band-EPR imaging of low pH circumstances," *Bioconjugate Chemistry*, vol. 20, no. 9, pp. 1792–1798, 2009.

[44] B. B. Weksler, E. A. Subileau, N. Perrière et al., "Blood-brain barrier-specific properties of a human adult brain endothelial cell line," *FASEB Journal*, vol. 19, no. 13, pp. 1872–1874, 2005.

[45] M. Grzesik, K. Naparło, G. Bartosz, and I. Sadowska-Bartosz, "Antioxidant properties of catechins: comparison with other antioxidants," *Food Chemistry*, vol. 241, pp. 480–492, 2018.

[46] C. A. Gay and J. M. Gebicki, "Measurement of protein and lipid hydroperoxides in biological systems by the ferric-xylenol orange method," *Analytical Biochemistry*, vol. 315, no. 1, pp. 29–35, 2003.

[47] L. M. Tai, P. S. Reddy, M. A. Lopez-Ramirez et al., "Polarized P-glycoprotein expression by the immortalised human brain endothelial cell line, hCMEC/D3, restricts apical-to-basolateral permeability to rhodamine 123," *Brain Research*, vol. 1292, pp. 14–24, 2009.

[48] A. P. Senft, T. P. Dalton, and H. G. Shertzer, "Determining glutathione and glutathione disulfide using the fluorescence probe o-phthalaldehyde," *Analytical Biochemistry*, vol. 280, no. 1, pp. 80–86, 2000.

[49] O. H. Lowry, N. J. Rosebrough, A. L. Farr, and R. J. Randall, "Protein measurement with the Folin phenol reagent," *Journal of Biological Chemistry*, vol. 193, no. 1, pp. 265–275, 1951.

[50] I. Carrera and R. Cacabelos, "Current drugs and potential future neuroprotective compounds for Parkinson's disease," *Current Neuropharmacology*, vol. 17, no. 3, pp. 295–306, 2019.

[51] F. Pohl and P. K. T. Lin, "The potential use of plant natural products and plant extracts with antioxidant properties for the prevention/treatment of neurodegenerative diseases: in vitro, in vivo and clinical trials," *Molecules*, vol. 23, no. 12, article molecules23123283, p. 3283, 2018.

[52] X. Zhao, M. Zhang, C. Li, X. Jiang, Y. Su, and Y. Zhang, "Benefits of Vitamins in the Treatment of Parkinson's Disease," *Oxidative Medicine and Cellular Longevity*, vol. 2019, 14 pages, 2019.

[53] S.-F. Wang, L.-F. Liu, M.-Y. Wu et al., "Baicalein prevents 6-OHDA/ascorbic acid-induced calcium-dependent dopaminergic neuronal cell death," *Scientific Reports*, vol. 7, no. 1, p. 8398, 2017.

[54] I. Sadowska-Bartosz and G. Bartosz, "Redox nanoparticles: synthesis, properties and perspectives of use for treatment of neurodegenerative diseases," *Journal of Nanobiotechnology*, vol. 16, no. 1, p. 87, 2018.

[55] L. Elyasi, S. H. Eftekhar-Vaghefi, and S. Esmaeili-Mahani, "Morphine protects SH-SY5Y human neuroblastoma cells against 6-hydroxydopamine-induced cell damage: involvement of anti-oxidant, calcium blocking, and anti-apoptotic properties," *Rejuvenation Research*, vol. 17, no. 3, pp. 255–263, 2014.

[56] L. Wei, L. Ding, M. S. Mo et al., "Wnt3a protects SH-SY5Y cells against 6-hydroxydopamine toxicity by restoration of mitochondria function," *Translational Neurodegeneration*, vol. 4, no. 1, 2015.

[57] J. Iglesias-González, S. Sánchez-Iglesias, E. Méndez-Álvarez et al., "Differential toxicity of 6-hydroxydopamine in SH-SY5Y human neuroblastoma cells and rat brain mitochondria: protective role of catalase and superoxide dismutase," *Neurochemical Research*, vol. 37, no. 10, pp. 2150–2160, 2012.

[58] M. Pichla, G. Bartosz, N. Pieńkowska, and I. Sadowska-Bartosz, "Possible artefacts of antioxidant assays performed in the presence of nitroxides and nitroxide-containing nanoparticles," *Analytical Biochemistry*, vol. 597, p. 113698, 2020.

[59] W. Loscher and H. Potschka, "Role of drug efflux transporters in the brain for drug disposition and treatment of brain diseases," *Progress in Neurobiology*, vol. 76, no. 1, pp. 22–76, 2005.

[60] M. A. Tirmenstein, C. X. Hu, M. S. Scicchitano et al., "Effects of 6-hydroxydopamine on mitochondrial function and glutathione status in SH-SY5Y human neuroblastoma cells," *Toxicology In Vitro*, vol. 19, no. 4, pp. 471–479, 2005.

[61] M. F. Galindo, M. E. Solesio, S. Atienzar-Aroca, M. J. Zamora, and J. Jordán Bueso, "Mitochondrial dynamics and mitophagy in the 6-hydroxydopamine preclinical model of Parkinson's disease," *Parkinson's Disease*, vol. 2012, Article ID 131058, 8 pages, 2012.

[62] Y. Xi, D. Feng, K. Tao et al., "MitoQ protects dopaminergic neurons in a 6-OHDA induced PD model by enhancing Mfn2-dependent mitochondrial fusion via activation of PGC-1α," *Biochimica et Biophysica Acta Molecular Basis of Disease*, vol. 1864, no. 9, pp. 2859–2870, 2018.

[63] M. E. Solesio, S. Saez-Atienzar, J. Jordán, and M. F. Galindo, "Characterization of mitophagy in the 6-Hydoxydopamine Parkinson's disease model," *Toxicological Sciences*, vol. 129, no. 2, pp. 411–420, 2012.

[64] H. Pasban-Aliabadi, S. Esmaeili-Mahani, and M. Abbasnejad, "Orexin-a protects human neuroblastoma SH-SY5Y cells against 6-Hydroxydopamine-induced neurotoxicity: involvement of PKC and PI3K signaling pathways," *Rejuvenation Research*, vol. 20, no. 2, pp. 125–133, 2017.

[65] Y. Glinka, M. Gassen, and M. B. H. Youdim, "Mechanism of 6-hydroxydopamine neurotoxicity," *Advances in Research on Neurodegeneration*, vol. 50, supplement, pp. 55–66, 1997.

[66] S. Przedborski and H. Ischiropoulos, "Reactive oxygen and nitrogen species: weapons of neuronal destruction in models of Parkinson's disease," *Antioxidants & Redox Signaling*, vol. 7, no. 5-6, pp. 685–693, 2005.

[67] D. G. Workman, A. Tsatsanis, F. W. Lewis et al., "Protection from neurodegeneration in the 6-hydroxydopamine (6-OHDA) model of Parkinson's with novel 1-hydroxypyridin-2-one metal chelators," *Metallomics*, vol. 7, no. 5, pp. 867–876, 2015.

3. **Pichla, M.**; Bartosz, G.; Stefaniuk, I.; Sadowska-Bartosz, I. *pH-Responsive Redox Nanoparticles Protect SH-SY5Y Cells at Lowered pH in a Cellular Model of Parkinson Disease*. Molecules 2021, 26, 543.

IF$_{2020}$: 3.267; MNiSW: 100

Article

pH-Responsive Redox Nanoparticles Protect SH-SY5Y Cells at Lowered pH in a Cellular Model of Parkinson's Disease

Monika Pichla [1], Grzegorz Bartosz [2], Ireneusz Stefaniuk [3] and Izabela Sadowska-Bartosz [1,*]

[1] Laboratory of Analytical Biochemistry, Institute of Food Technology and Nutrition, College of Natural Sciences, Rzeszow University, 4 Zelwerowicza Street, 35-601 Rzeszow, Poland; monika.pichla@outlook.com

[2] Department of Bioenergetics, Food Analysis and Microbiology, Institute of Food Technology and Nutrition, College of Natural Sciences, Rzeszow University, 4 Zelwerowicza Street, 35-601 Rzeszow, Poland; gbartosz@ur.edu.pl

[3] Teaching and Research Center of Microelectronics and Nanotechnology, College of Natural Sciences, University of Rzeszow, 35-959 Rzeszow, Poland; istef@univ.rzeszow.pl

[*] Correspondence: isadowska@poczta.fm or sadowska@ur.edu.pl; Tel.: +48-17-7855408; Fax: +48-17-8721425

Abstract: The damage to SH-SY5Y cells by 6-hydroxydopamine (6-OHDA) is an established cellular model of Parkinson's disease (PD). Redox nanoparticles are a promising tool for therapy, including neurodegenerative diseases. As pH of the brain tissue at sites affected by PD is lowered down to 6.5, we studied the effect of pH-responsive redox nanoparticles (poly(ethylene glycol)-*b*-poly[4-(2,2,6,6-tetramethylpiperidine-1-oxyl)aminomethylstyrene]), which change their structure in a pH-dependent manner and become active below pH 7 (NRNPs ^{PH}), on the viability of SH-SY5Y cells treated with 6-OHDA at pH 6.5 and 7.4. Pretreatment of the cells with NRNPs ^{PH} (15–75 μM) prior to the 6-OHDA treatment increased their survival in a concentration-dependent manner at pH 6.5, but not at pH 7.4. Among several parameters studied (ATP and GSH content, the level of reactive oxygen species, mitochondrial potential, mitochondrial mass), only the mitochondrial mass was dose-dependently protected by NRNPs ^{PH} at pH 6.5, but not at pH 7.4. These results indicate that the action of NRNPs ^{PH} on mitochondria underlies their protective effect in this cellular model of PD. These results may have potential importance for future applications of NRNPs ^{PH} in preclinical and perhaps clinical studies.

Keywords: pH-responsive redox nanoparticles; human neuroblastoma SH-SY5Y cells; Parkinson's disease; 6-hydroxydopamine

1. Introduction

It is astonishing that, despite the extraordinary progress of medicine, the treatment of neurodegenerative diseases has not progressed for over half a century, and still is purely symptomatic [1]. Where does the blame lie? Therapeutics do not have an easy road when it comes to reaching a target site. There are numerous biological obstacles that hinder the effective delivery of drugs, e.g., non-specificity, inadequate accumulation, opsonization, and sequestration via mononuclear phagocyte system, drug efflux pumps, evading lysosomal and endosomal compartments and general cellular internalization [2]. Thankfully, nanomedicine can offer help in overcoming these blockades and delivering cargo to particular intracellular regions. Redox-active nanoparticles of various structure scavenging reactive oxygen species (ROS) have been proposed to combat oxidative stress [3,4]. A promising approach to face these obstructions is a use of nanoparticles designed to undergo modifications in material properties as a result of exposure to different internal or external stimuli such as: pH, redox state [5–7], enzymatic activity [8], temperature, magnetic or electric field, ultrasounds or light [9].

The pH-sensitive have started to gain research interest, because they can be exploited at three levels, namely organ, tissue, and cellular level, in order to increase and improve

drug uptake by the gastrointestinal tract, take advantage of tumor microenvironment to advance drug specificity and lastly, profit from the "proton sponge" effect to internalize drugs, respectively [10]. Nanoparticles can be engineered to change their size, shape of surface chemistry in response to the stimuli, to disassemble or release the load. This can be achieved by various strategies. One of them is the exploitation of charge shifting compounds, next, the use of acid labile linkages or crosslinkers [11]. The importance and possibilities of the use of nanoparticles against neurodegeneration have been reviewed elsewhere [12,13].

Neurodegenerative diseases are complex and the exact etiopathogenesis is still unknown [14], which does not help to create fully reliable disease models. Nevertheless, mitochondrial dysfunction is an inseparable part of neurodegenerative diseases. It causes a drop in pH by the leakage of protons into the cytosol [15], hence a decreased pH of brain tissue might be exploited to target the treatment, similarly as the tumor microenvironment. Data provided by Genoud et al. indicate that average pH of human brain tissue affected by Parkinson's disease (PD) is as low as ~6.5 [16].

The pH-sensitive antioxidant-loaded nanoparticles (poly(ethylene gly-col)-*b*-poly[4-(2,2,6,6-tetramethylpiperidine-1-oxyl)aminomethylstyrene] nanoparticles) possessing nitroxide radicals as a side chain of a polymer segment, called further NRNPs $^{\text{pH}}$, were designed and developed for selective action at lower pH. These nanoparticles in aqueous solution have a form of self-assembling polymeric micelles, which disintegrate in the acidic environment, by virtue of the protonation of amino groups present in their core [17,18]. NRNPs $^{\text{pH}}$ were employed to effectively scavenge overproduced ROS in inflamed tissues and cancerous regions, to improve anticancer efficacy of doxorubicin in the colitis-associated mice colon cancer, and to decrease cardiac levels of ROS in doxorubicin-treated mice [19]. They showed also a protective effect in renal ischemia-reperfusion in experimental animals [18]. The transgenic Tg2576 Alzheimer's disease (AD) mice treated with NRNPs $^{\text{pH}}$ had significantly attenuated cognitive deficits of both spatial and non-spatial memories, reduced oxidative stress, and decreased lipid peroxides as well as DNA oxidation [20]. The effect of NRNPs $^{\text{pH}}$ in PD has not been studied so far. Therefore, we decided to check their action in the cellular model of this disease.

2. Results

2.1. Penetration of pH-Sensitive NRNPs into SH-SY5Y Cells

Measurements of EPR signal of NRNPs $^{\text{pH}}$ in cells and in supernatants showed that the uptake of nanoparticles was maximal at pH 6.0 (Figure 1).
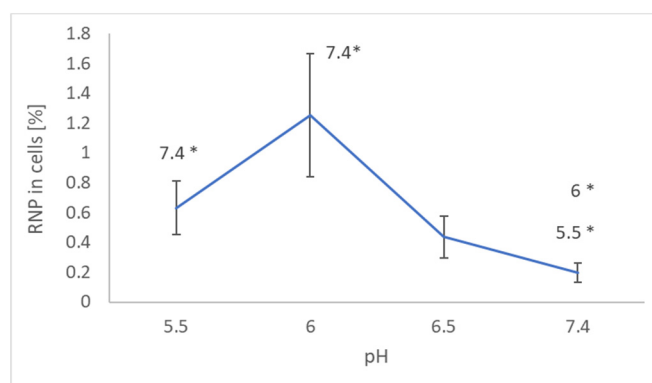
Figure 1. Effect of pH on the uptake of NRNPs $^{\text{pH}}$ by SH-SY5Y cells. * $p < 0.05$ with respect to the pH indicated, Student *t*-test; $n = 3$.

Viability of the cells did not show significant differences between pH 7.4 and 6.5 but was decreased at pH 6.0 (Figure 2). For this reason, and, taking into account that the pH in the affected regions of the brain may be lowered to about 6.5, the pH of 6.5 was compared with pH 7.4 in subsequent experiments.
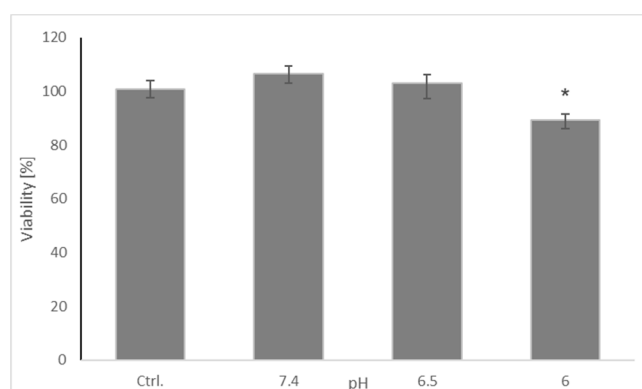
Figure 2. Effect of pH on the viability of SH-SY5Y cells. Cell viability was estimated with Presto Blue. The whiskers are lower (25%) and upper (75%) quartile ranges. * $p \leq 0.05$, Kruskal–Wallis test vs. control (Ctrl); *n* = 9.

Monitoring time course of the uptake revealed no discernible time dependence of the uptake for incubation times longer than 3 h, indicating rapid uptake by the cells. Therefore, the time of 2 h was chosen for cell pretreatment with the NRNPs ^{PH} in further experiments.

2.2. Cell Viability

As aforementioned in our previous studies, oxidopamine (also known as 6-hydroxydopamine; 6-OHDA) showed a dose-dependent cytotoxicity against SH-SY5Y cells [21]. 6-Hydroxydopamine (65 µM) was somewhat more cytotoxic at pH 6.5 than at pH 7.4. NRNPs ^{PH} did not exhibit a statistically significant self-cytotoxicity up to ca. 75 µM at both pH conditions (not shown). However, they showed a concentration-dependent protection against 6-OHDA-induced cytotoxicity at both pH values studied and were more efficient at pH 6.5. At pH 7.4, NRNP ^{PH} restored the viability of 6-OHDA treated cells up to about 65% of the control value while at pH 6.5 up to ca. 85% of the control value (Figure 3).
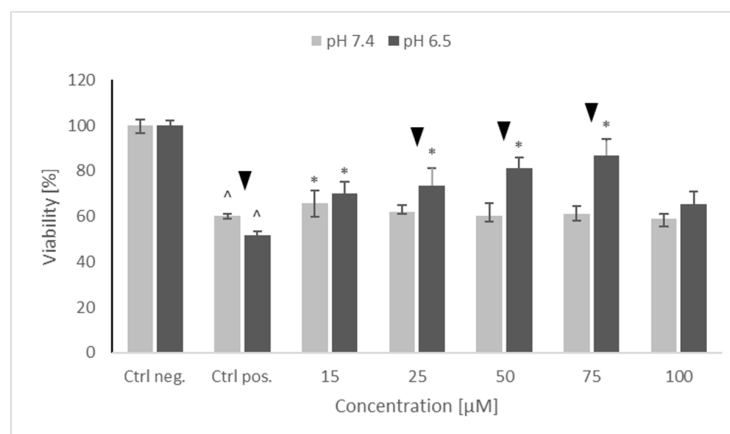
Figure 3. The protective properties of NRNPs ^{PH} against 65 µM 6-hydroxydopamine-induced cytotoxicity for SH-SY5Y cells at pH 7.4 and pH 6.5. Cell viability was estimated with MTT. The whiskers are lower (25%) and upper (75%) quartile ranges. ˆ $p \leq 0.05$, Kruskal–Wallis test vs. the negative control (Ctrl neg.; cells not treated with 6-OHDA), ▼ $p \leq 0.05$, Mann–Whitney U test; differences between the different pH conditions (pH 7.4 vs. pH 6.5), * $p \leq 0.05$, Kruskal–Wallis test vs. positive control (Ctrl pos.; cells treated with 6-OHDA only, without any pretreatment); *n* = 9.

2.3. Intracellular ATP Level

Treatment with 6-OHDA induced a significant drop in the ATP level of the SH-SY5Y cells, more pronounced at pH 6.5 than at pH 7.4. Preincubation with NRNPs ^{PH} partly prevented this drop and, starting from the concentration of 50 µM, the ATP level was

preserved at the same level at both pH values. However, maximal ATP level in the cells pretreated with NRNPs [PH] and challenged with 6-OHDA did not exceed 60% of the level of the negative control (cells not treated with 6-OHDA) (Figure 4).
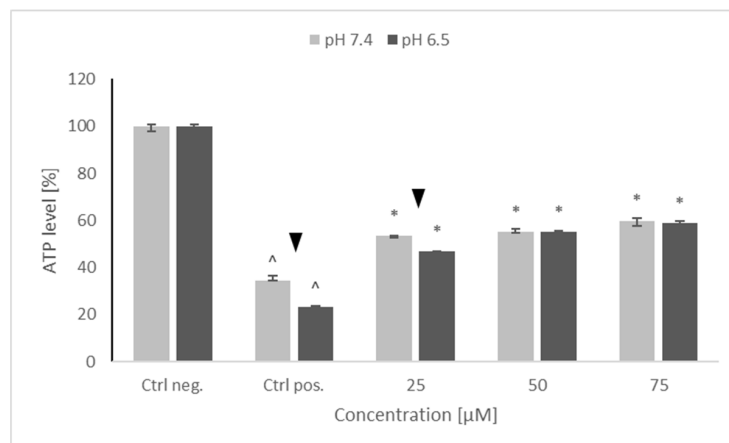
Figure 4. ATP levels after pretreatment of SH-SY5Y cells with NRNPs [PH] and exposure to 6-hydroxydopamine. The whiskers are lower (25%) and upper (75%) quartile ranges. ˆ $p \leq 0.05$, Kruskal–Wallis test vs. the negative control (Ctrl neg.; cells not treated with 6-OHDA),▼ $p \leq 0.05$, Mann–Whitney U test; differences between the different pH conditions (pH 7.4 vs. pH 6.5), * $p \leq 0.05$, Kruskal–Wallis test vs. positive control (Ctrl pos.; cells treated with 6-OHDA only, without any pretreatment); $n = 9$.

2.4. Content of Reduced Glutathione

A substantial increase in GSH content was seen in positive control (cells treated with 6-OHDA only, without any pretreatment). Pretreatment with NRNPs [PH] decreased the GSH content nearly by half in the 25–75 µM concentration range at pH 7.4, and at 25 µM and 50 µM concentrations at pH 6.5. However, at pH 6.5, NRNPs [PH] at a 75 µM concentration did not decrease the GSH content. Furthermore, no difference in the efficacy of nanoparticles was seen between the two pH conditions, except for the 75 µM NRNPs [PH] (Figure 5).
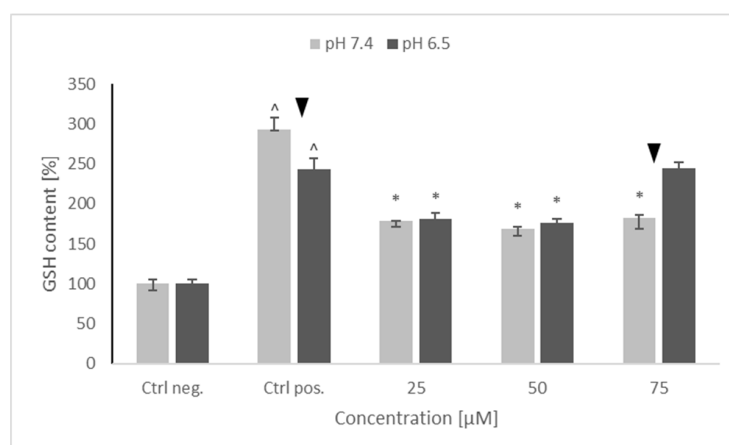
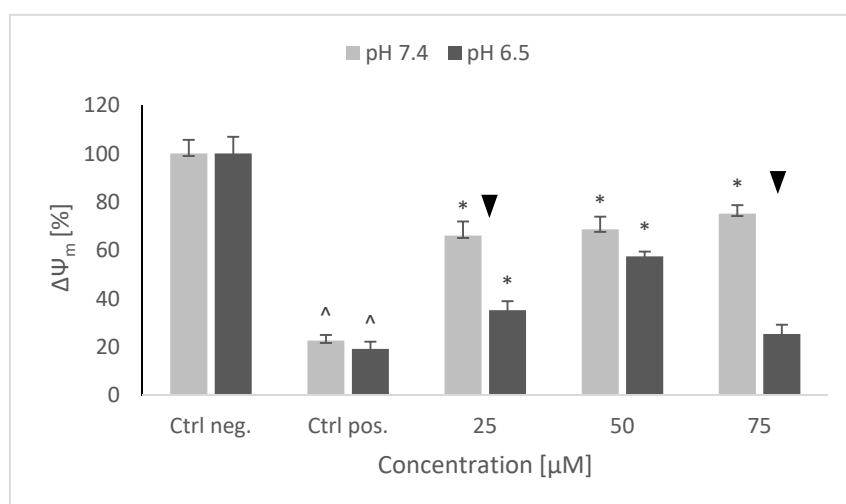**Figure 5.** Glutathione (GSH) content of SH-SY5Y cells after pretreatment with NRNPs [PH] and exposure to 6-hydroxydopamine. The whiskers are lower (25%) and upper (75%) quartile ranges. ˆ $p \leq 0.05$, Kruskal–Wallis test vs. the negative control (Ctrl neg.; cells not treated with 6-OHDA), ▼ $p \leq 0.05$, Mann–Whitney U test; differences between the different pH conditions (pH 7.4 vs. pH 6.5), * $p \leq 0.05$, Kruskal–Wallis test vs. positive control (Ctrl pos.; cells treated with 6-OHDA only, without any pretreatment); $n = 9$.

2.5. ROS Levels Using the Dihydroethidine (DHE) Fluorescent Probe

6-hydroxydopamine caused a significant, up to a 2.5× increase of the ROS level, which was not affected by the cell pretreatment with and NRNPs ^{PH} at both pH values (Figure 6).
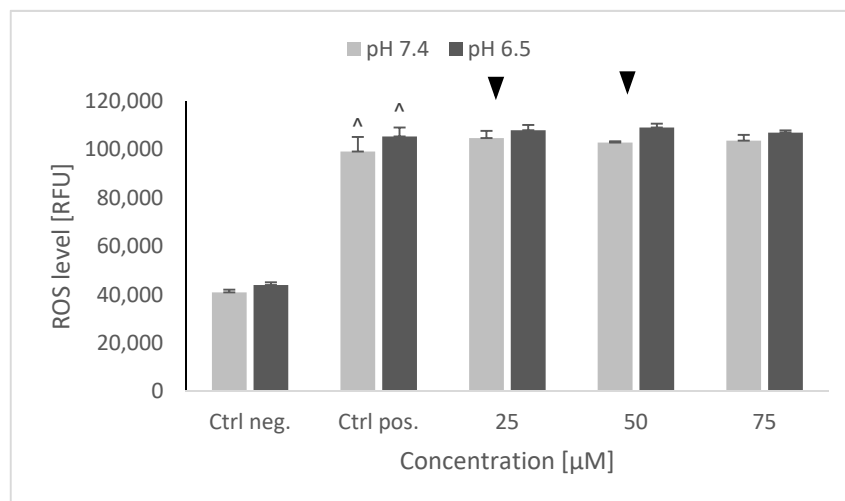
Figure 6. ROS level in SH-SY5Y cells determined using dihydroethidine (DHE) after pretreatment with NRNPs ^{PH} and exposure to 6-hydroxydopamine. The whiskers are standard deviation. ˆ $p \leq 0.05$, Student t-test vs. the negative control (Ctrl neg.; cells not treated with 6-OHDA), ▼ $p \leq 0.05$, paired Student t-test, differences between the different pH conditions (pH 7.4 vs. pH 6.5), (Ctrl pos.; cells treated with 6-OHDA only, without any pretreatment); $n = 3$.

2.6. Mitochondrial Membrane Potential ($\Delta\Psi_m$)

A strong decrease of the mitochondrial membrane potential was observed after 6-OHDA treatment, similar at both pH values, the ratio of red to green fluorescence being lowered by about 80%. NRNPs ^{PH} pretreatment prevented this decrease in a concentration-dependent manner in the whole range of studied concentrations at pH 7.4, and at 25 and 50 μM at pH 6.5. The protective effect was lowered at pH 6.5 (Figure 7).
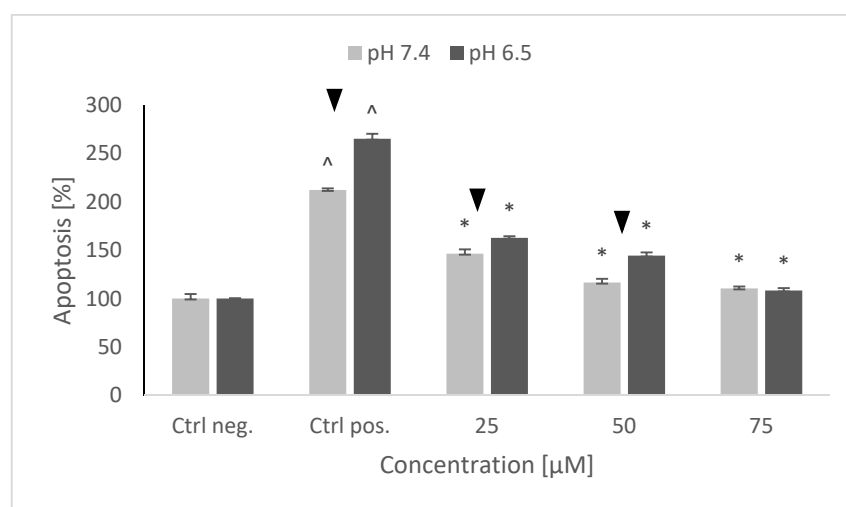

Figure 7. Changes in the mitochondrial potential of SH-SY5Y cells after pretreatment with NRNPs ^{PH} and exposure to 6-hydroxydopamine. The whiskers are standard deviation. ˆ $p \leq 0.05$, Student t-test vs. the negative control (Ctrl neg.; cells not treated with 6-OHDA), ▼ $p \leq 0.05$, paired sample Student t-test, differences between the different pH conditions (pH 7.4 vs. pH 6.5), * $p \leq 0.05$, Student t-test vs. the positive control (Ctrl pos.; cells treated with 6-OHDA only, without any pretreatment); $n = 3$.

2.7. Mitochondrial Mass

6-hydroxydopamine induced a drop in the mitochondrial mass in the SH-SY5Y cells. Pretreatment with NRNPs ^{pH} had a clearly distinct effect on the mitochondrial mass depending on pH. While at pH 7.4 NRNPs ^{pH} caused a further concentration-dependent decrease of the mitochondrial mass, they increased concentration-dependently the mitochondrial mass at pH 6.5 (Figure 8).
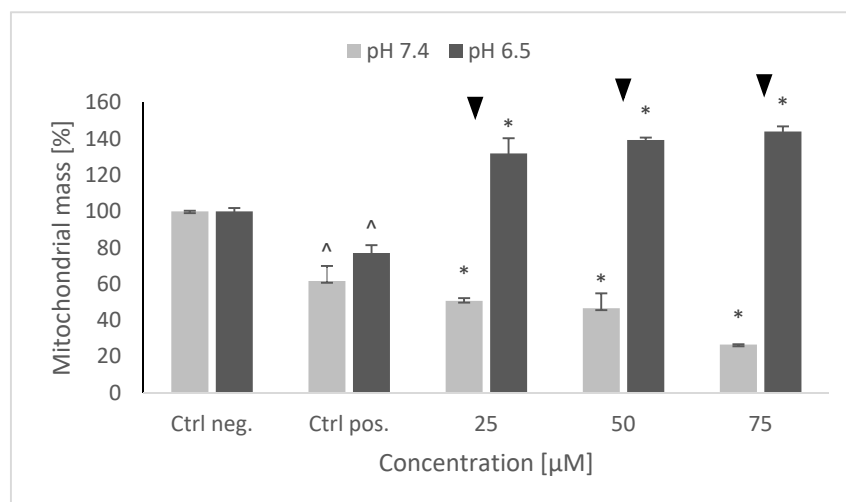
Figure 8. Changes in the mitochondrial mass after pretreatment of SH-SY5Y cells with NRNPs ^{pH} and exposure to 6-hydroxydopamine. The whiskers are standard deviation. ˆ $p \leq 0.05$, Student *t*-test vs. the negative control (Ctrl neg.; cells not treated with 6-OHDA), ▼ $p \leq 0.05$, paired Student *t*-test, differences between (pH 7.4 vs. pH 6.5), * $p \leq 0.05$, Student *t*-test with respect to the positive control (Ctrl pos.; cells treated with 6-OHDA only, without any pretreatment); *n* = 3.

2.8. Prevention of Apoptosis and Necrosis

Treatment of SH-SY5Y cells with 6-OHDA strongly augmented both necrosis and apoptosis. It is not possible to determine the contribution of both cell death types, since the used test allows only for a relative estimation of apoptosis and necrosis levels. Though the increase in the rate of necrosis was higher than that in the rate of apoptosis, it is hard to say what was the absolute level of apoptosis and necrosis in the control preparations (the level of necrosis could be much lower with respect to apoptosis). 6-OHDA induced a higher increase in the rate of apoptosis at pH 6.5 with respect to pH 7.4 and a higher increase in necrosis at pH 7.4 with respect to pH 6.5. Pretreatment with NRNPs ^{pH} decreased the rate of apoptosis in a concentration-dependent manner. Lower concentrations—25 and 50 µM NRNPs ^{pH}—were more effective at pH 7.4 than at pH 6.5, but the efficacy of 75 µM nanoparticles was the same at both pH values (Figure 9).

NRNPs ^{pH} also decreased the rate of necrosis at pH 7.4, but this effect was not concentration-dependent. At pH 6.5, NRNPs ^{pH} were the most effective at the lowest concentration applied (25 µM); the protective effect was lower at higher concentrations (Figure 10).

Figure 9. The level of apoptosis of SH-SY5Y cells after pretreatment with NRNPs pH and exposure to 6-hydroxydopamine. The whiskers are standard deviation. ˆ $p \leq 0.05$, Student *t*-test vs. the negative control (Ctrl neg.; cells not treated with 6-OHDA), ▼ $p \leq 0.05$, paired Student *t*-test, differences between different pH conditions (pH 7.4 vs. pH 6.5), * $p \leq 0.05$, Student *t*-test vs. the positive control (Ctrl pos.; cells treated with 6-OHDA only, without any pretreatment); *n* = 3.
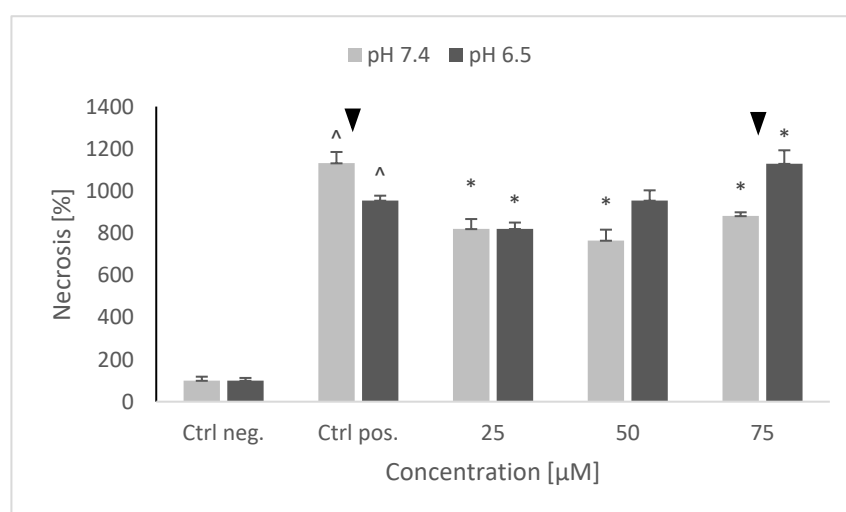
Figure 10. The level of necrosis after pretreatment of SH-SY5Y cells with NRNPs PH and exposure to 6-hydroxydopamine. The whiskers are standard deviation. ˆ $p \leq 0.05$, Student *t*-test vs. the negative control (Ctrl neg.; cells not treated with 6-OHDA), ▼ $p \leq 0.05$, paired Student *t*-test, differences between different pH conditions, * $p \leq 0.05$, Student *t*-test vs. the positive control (Ctrl pos.; cells treated with 6-OHDA only, without any pretreatment); *n* = 3.

3. Discussion

A spectrum of various factors underlies the physiopathology of PD, i.e., genetic factors, impaired signal transduction involved in maintaining mitochondrial homeostasis, impairment of regulation of protein degradation (proteasomal degradation and autophagy) and controlling pathways that help to maintain redox homeostasis [22,23]. Due to the complexity of mechanisms that constitute the basis of all PD characteristics, the understanding of the molecular mechanisms of this disease is far from complete, and its treatment is purely symptomatic and has not been substantially modified for over six decades [1]. Nevertheless, there is a consensus that mitochondrial dysfunction and elevated ROS levels are an integral part of PD pathophysiology, leading to the damage of dopaminergic neurons, thus antioxidants may serve as a useful approach to alleviate PD symptoms [24,25]. Several

cellular models to mimic PD have been proposed, based on the effects of compounds inducing oxidative stress to neuronal cells in vivo; one of the most popular among them employs the catecholaminergic neuroblastoma cell line SH-SY5Y treated with the catecholaminergic neurotoxin 6-OHDA [26,27]. Although the 6-OHDA model does not cover all PD symptoms, it does reproduce the main cellular processes involved in PD. The model has been widely used at physiological pH (7.4). However, since the brain tissue affected by PD has pH lowered to about 6.5 [16], it seemed reasonable to check the protection of SH-SY5Y cells against the effects of 6-OHDA at the lowered pH. NRNPs [PH] seemed to be an appropriate candidate for such protective agent. They are able to cross the blood–brain barrier [20] and reach the brain regions affected by PD. They change their structure in response to the lowering of pH below 7, exposing 4-*N*-linked 2,2,6,6-tetramethylpiperidine-*N*-oxyl redox active residues contained within the hydrophobic shell at higher pH [21,28].

Penetration of NRNPs [PH] into the SH-SY5Y cells strongly depended on pH, showing optimum at pH 6. More NRNPs [PH] penetrated the cells at pH 6.5 than at pH 7.4 (Figure 1). Apparently, unmasking the positive charge of the nanoparticles facilitates their adsorption on the negatively charged cell surface and further penetration of the plasma membrane.

Preincubation of SH-SY5Y cells with NRNPs [PH] (15–75 μM) before exposure to 6-OHDA protected the cells at pH 6.5, whereas the protection at pH 7.4 was negligible (Figure 3). The protection was mainly associated with an inhibition of apoptosis, which occurred at both pH values; however, its rate was higher at pH 6.5 (Figure 9). In order to get an insight into the mechanism of cell protection at pH 6.5, we compared the effect of NRNPs [PH] on selected biochemical parameters of the cells. Even though nanoparticles protected the SH-SY5Y cells against the 6-OHDA-induced drop of ATP levels, this effect did not differ significantly at both pH values. The only exception was the lower protective effect at 25 μM concentration of NRNPs [PH] at pH 6.5 (Figure 4).

Interestingly, 6-OHDA treatment induced an increase rather than a decrease of cellular GSH (Figure 5). This effect has been observed by us previously [21] and is apparently due to the an overcompensative reaction to the initial GSH depletion by 6-OHDA as demonstrated by others [29]. The adaptive increase in the GSH level was prevented to the same extent by NRNPs [PH] at pH 7.4 and pH 6.5, except for a lower effect at pH 6.5, at a 75 μM concentration (Figure 5). The increase in the DHE-detectable ROS level (mainly superoxide) was not affected by preincubation with NRNPs [PH] (Figure 6). Cells were more protected from the mitochondrial depolarization induced by 6-OHDA at pH 7.4 than at pH 6.5 (Figure 7). Only the decrease of mitochondrial mass was prevented in a concentration-dependent manner by NRNPs [PH] at pH 6.5, and it significantly lessened at pH 7.4 (Figure 8).

Positively charged NRNPs [PH] can be expected to accumulate in the most negatively charged site of the cell, i.e., inside mitochondria. Therefore, mitochondrial effects of these particles may be anticipated. Such a localization of NRNPs [PH] may limit or prevent their action outside mitochondria such as scavenging of ROS outside mitochondria.

Mitochondria play several important roles in the cell. Apart from being the main ATP producer and the main source of ROS, they are involved, i.a., in the control of cell cycle, apoptosis, heme, and steroid synthesis [30,31]. All of these processes can be affected by 6-OHDA and, depending on the damage extent, may be critical for cell survival. Although the exact mechanism of SH-SY5Y cell protection against the 6-OHDA cytotoxicity cannot be inferred from this study, the obtained results indicate that stimulation of mitochondrial biogenesis by NRNPs [PH] can evidently prevent the outcomes of the cell survival-limiting damage. Animal experiments are foreseen to check the efficacy of NRNPs [PH] in an in vivo model of PD.

4. Materials and Methods

4.1. Materials and Equipment

The human neuroblastoma cell line SH-SY5Y (ATCC CRL-2266) was obtained from American Type Culture Collection (ATCC, Rockville, MD, USA). Dulbecco's Modified Eagle Medium Nutrient Mixture F-12 (DMEM/F12) without Phenol Red (cat. no. 11039-

021), Dulbecco's Phosphate Buffered Saline $1\times$ with Ca^{2+} and Mg^{2+} ions, cell culture 75 cm^2 flasks (cat. no. 156499), transparent 96-well culture plates (cat. no. 655980) and black (cat. no. 655986) and white (cat. no. 655983) 96-well plates with optical bottoms were purchased from Greiner Bio-One (Kremsmünster, Austria). Fetal bovine serum (FBS, cat. no. 04-001-1A), $10\times$ Trypsin-EDTA solution (cat. no. 03-051-5B), PBS without Ca^{2+} and Mg^{2+} ions (cat. no. 02-023-1A), and Penicillin-Streptomycin solution (cat. no. 03-031-1B) were obtained from Biological Industries (Cromwell, CT, USA).

Tetrahydrofurane (cat. no. 401757), 3,3-diethoxypropanol (cat. no. 273252), chloromethyl-styrene (cat. no. 126136), ethylene oxide (cat. no. 743593), methanesulfonyl chloride (cat. no. 471259), triethylamine (cat. no. 471283), 2-propanol (cat. no. 278475), benzene (cat. no. 401765), chloroform (cat. no. 288306), hexane (cat. no. 296090), *n*-propylamine (cat. no. 240958), sodium sulfate (cat. no. 239313), 1,4-dithiothreitol (cat. no. 111474), 4-amino-2,2,6,6-tetramethylpiperidinyloxy (4-amino-TEMPO; cat. no. 163945) and potassium *O*-ethyldithiocarbonate (cat. no. 820744) were from Merck (Warsaw, Poland). 2,2′-Azo-*bis*-isobutyronitrile was obtained from Nouryon, (Amsterdam, Netherlands). Dialysis membranes, molecular cutoff 2 kD (cat. no. 888-11452) were from Spectrum, New Brunswick, NJ, USA.

The tetrazolium dye 3-(4,5-dimethylthiazol-2-yl)-2,5-diphenyltetrazolium bromide (MTT, cat. no. M2128), Trypan Blue solution (0.4%; cat. no. T8154), 6-hydroxydopamine hydrobromide (6-OHDA) (cat. no. 162957), L-ascorbic acid (cat. no. A0278), acridine orange 10-nonyl bromide (NAO, cat. no. A7847), trichloroacetic acid (TCA; cat. no. T4885), diethylenetriaminepentaacetic acid (DTPA; cat. no. D6518) and *o*-phthaldialdehyde (OPA; P0657) were provided by Sigma Aldrich (St. Louis, MO, USA). CellTiter-Glo® Luminescent Cell Viability Assay (cat. no. G7571) and RealTime-Glo™ Annexin V Apoptosis and Necrosis Assay (cat. no. JA1011) were purchased from Promega (Madison, WI, USA). JC-1 Mitochondrial Membrane Potential Assay Kit was obtained from Abnova (Taiwan, China). PrestoBlue™ Cell Viability Reagent was purchased from ThermoFisher Scientific (Waltham, MA USA).

6-Hydroxydopamine hydrobromide (6-OHDA) (Sigma-Aldrich, cat. no. 162957) was freshly prepared and stabilized with 0.01% L-ascorbic acid, and filtered using 0.22 μm syringe filter for each experiment.

Water was purified with a Milli-Q system (Millipore, Bedford, MA, USA). Measurements of absorbance, fluorescence, and luminescence were carried out with Tecan Spark multimode microplate reader (Tecan Group Ltd., Männedorf, Switzerland).

4.2. Synthesis of Redox Nanoparticles

Acetal-poly(ethylene glycol)-mercapto (acetal-PEG-SH) polymer containing acetyl and mercapto terminals was prepared according to the procedure described by Akiyama et al. [32] with small modifications. Briefly, 15 mL of dry degassed tetrahydrofurane, 148 mg of 3,3-diethoxypropanol, and 186 mg of potassium 3,3-diethoxypropanolate were introduced into a reactor purged with argon and degassed several times to form potassium 3,3-diethoxypropanolate. The mixture was stirred for 15 min and 5.24 mL of ethylene oxide cooled at $-20\,°C$ were introduced via a cooled syringe. The mixture was allowed to react at room temperature (21 °C) for two days. Then, 928 μL of methanesulfonyl chloride and 2.09 mL of triethylamine were added, and the mixture was stirred at room temperature for 6 h. The polymer formed was precipitated with 500 mL of 2-propanol cooled at $-20\,°C$, sedimented by centrifugation ($5000\times g$, 30 min), washed 3 times with cold 2-propanol and freeze-dried with benzene. In addition, 10 mL of dry tetrahydrofurane and 33.6 g of potassium *O*-ethyldithiocarbonate in dry tetrahydrofurane/dimethylformamide (10 mL:5 mL) were successively added to 4.2 g of the polymer and stirred at room temperature for 3 h. The reaction mixture was added with chloroform and washed several times with saturated aqueous solution of NaCl. The organic phase was dried with sodium sulfate, concentrated by evaporation and recovered by precipitation with 500 mL of cold ($-20\,°C$) 2-propanol and centrifugation; this cycle of precipitation/centrifugation was repeated

thrice. Afterwards, the product was freeze-dried with benzene. The yield of the polymer was 3.4 g.

To generate sulphonyl groups, 3.4 g of acetal-PEG ethyldithiocarbonate was added with 719 µL of *n*-propylamine in 15 mL THF. The mixture was stirred at room temperature for 14 h. The product was precipitated in 500 mL of cold (−20 °C) 2-propanol, sedimented by centrifugation (5000× *g*, 30 min), washed with cold 2-propanol and sedimented thrice, and freeze-dried with benzene. To reduce dimers of acetal-PEG-SS-PEG acetal, 3.3 g of the polymer was treated with 1.0 g of 1,4-dithiothreitol in 25 mL of tetrahydrofurane. The product was recovered in 500 mL of cold 2-propanol, sedimented by centrifugation (5000× *g*, 30 min), washed 3 times with cold 2-propanol, and freeze-dried with benzene, yielding 2.7 g of the product (acetal-PEG-SH).

Further synthesis was performed according to Yoshitomi et al. [17]. In addition, 700 mg of acetal-PEG-SH was weighed into a flask, which was then degassed and purged with argon three times. Then, 1.35 mL of chloromethylstyrene, 16 mg of 2,2′-azobisisobutyronitrile and 10 of mL benzene was added to the flask, and polymerization was conducted at 60 °C for 24 h in a water bath. The product was recovered by precipitation with 400 mL of hexane and freeze-dried with benzene, washed three times with diethyl ether to eliminate the PCMS homopolymer, and freeze-dried with benzene. Furthermore, 892 mg of so obtained acetal-PEG-b-PCMS was weighed into a flask, added with 45 mL of a dimethylsulfoxide solution of 4-amino-TEMPO (1.962 g) and allowed for reacting at room temperature with stirring for 5 h. The product was precipitated by addition of 220 mL of cold (−20 °C) 2-propanol and centrifuged (5000× *g*, 30 min). The precipitation–centrifugation cycle was repeated 3 times, and the product was freeze-dried with benzene. In addition, 923 mg of the product was obtained.

For preparation of the core-shell-type nanoparticles from the copolymer, 50 mg of the product was dissolved in 5 mL of dimethylformamide, and the polymer solution was transferred into a preswollen membrane tube (Spectra/Por; molecular-weight cutoff size: 2 kD) and then dialyzed for 24 h against 2 L of water, which was changed three times.

4.3. SH-SY5Y Cell Culture

SH-SY5Y cell line was cultured in DMEM/F12 without phenol red, supplemented with 10% *v/v* heat-inactivated fetal bovine serum (hi-FBS) and 1% *v/v* penicillin and streptomycin solution. Cells were maintained at 37 °C in 5% carbon dioxide and 95% humidity. The cellular morphology was examined under an inverted microscope with phase contrast Zeiss Primo Vert (Oberkochen, Germany), cell viability was estimated by Trypan Blue exclusion test, and cells were counted using a Thoma hemocytometer (Superior Marienfeld, Lauda-Königshofen, Germany).

4.4. Cell Viability Assay

Cell viability was assayed with PrestoBlue or MTT. Human neuroblastoma cells were seeded in 96-well clear plate at a density of 3.5×10^4 cells/well in 100 µL culture medium. After incubation, medium was gently removed by suction and replaced with 100 µL of 1 × PrestoBlue™ Cell Viability Reagent in PBS. After 1-h incubation in a cell culture incubator in the dark, absorbance was read at 570 nm, using 600 nm as a reference wavelength.

Human neuroblastoma cells were seeded in 96-well clear plate at a density of 3.5×10^4 cells/well in 100 µL culture medium. After appropriate incubation time (usually 24 h), medium was gently removed by suction and replaced with cell culture medium brought to appropriate pH or supplemented with appropriate compounds, brought up to appropriate pH. After the exposure, the medium was removed and replaced with 100 µL of 1 × PrestoBlue™ Cell Viability Reagent or 0.5 mg/mL of MTT solution in 1 × PBS with calcium and magnesium ions. In the PrestoBlue method, the cells were incubated in a CO_2 incubator in the dark for 1 h and absorbance was read at 570 nm, using 600 nm as a reference wavelength. In the MTT method, the cells were incubated for 4 h in a CO_2 incubator. Next, 100 µL/well of 2-propanol: HCl (250:1 *v/v*) solution were added to the

cells in order to dissolve formazan crystals and shaken thoroughly for about 20–30 min. Absorbance was measured at 570 nm.

4.5. Treatment of SH-SY5Y Cells with Nanoparticles

For the analysis of protective properties of the NRNPs ^{PH}, cells were seeded as described above in the previous paragraph. After overnight incubation to allow cell adherence, the medium was replaced with 50 µL/well of NRNPs ^{PH} in the medium adjusted with 1 M HCl to appropriate pH. Subsequently to 2-h preincubation with antioxidant, 50 µL/well of 130 µM 6-OHDA were added (final concentration: 65 µM) and then incubated for 24 h. Cells cultured in complete medium served as a negative control, whereas cells treated with 6-OHDA were considered as a positive control.

4.6. Analysis of Penetration of pH-Sensitive NRNPs into SH-SY5Y Cells

Cells from highly confluent T-75 flask were trypsinized, centrifuged (5 min, 900 rpm), and resuspended in 3 mL of medium in four parts, three 250-µL samples for each part. Each part was centrifuged again and the medium was replaced with 250 µL of cell medium of different pH (7.4, 6.5, 6.0 and 5.5, respectively), containing 30 µM NRNPs ^{PH}. Cells were incubated for 6 h. After incubation, the cells were centrifuged, and the supernatant was collected and frozen for further examination. The pellet was washed with 1 mL of PBS and then centrifuged once again. The pellet was suspended in 50 µL/each sample of PBS and frozen. EPR signal intensity of nitroxide was measured.

4.7. Electron Spin Resonance (ESR) Spectroscopy Measurements

ESR signal intensity of nitroxide residues within NRNPs ^{PH} (~15 µL) was measured using microhematocrit capillaries (nonheparinized microhematocrit tubes; 1.55 × 75 mm; Medlab Products, Raszyn, Poland) in a Bruker multifrequency and multiresonance FT-EPR ELEXSYS E580 apparatus (Bruker BioSpin, Billerica, MA, USA). The spectrometer was operated at X-band (around 9.4 GHz). The following settings were used: central field, around 3354.0 G; modulation amplitude, 0.3 G; modulation frequency, 100 kHz; microwave power, 94.64 mW; power attenuation 2.0 dB; scan range, 100 G; conversion time, 25 ms; and sweep time, 25.6 s. The spectra were recorded with 1024 points per scan. The spectra were recorded and analyzed using Xepr 2.6b.74 software. The signal was integrated twice to determine its area and thus the concentration of the radical.

4.8. Analysis of Time-Penetration Axis of pH-Sensitive NRNPs

In order to establish the optimal time of NPs internalization into cells, cells were prepared similarly as above, but cells were resuspended in medium of pH 6.5 and pH 7.4 containing NRNPs ^{PH} and incubated for 3 h, 6 h, 12 h, and 24 h.

4.9. Assessment of Intracellular ATP Level

The intracellular ATP level was estimated using CellTiter-Glo® Luminescent Cell Viability Assay. Cells were seeded into white 96-well plate with optical bottom, cultured and treated as previously described (Section 4.4). Cells were tested after 24 h incubation with 6-OHDA by adding 100 µL of CellTiter-Glo® Reagent to each well. The next steps were performed according to the manufacturer's protocol.

4.10. Content of Reduced Glutathione

The content of reduced glutathione (GSH) was tested using *ortho*-phthalaldehyde (OPA) [33]. SH-SY5Y cells were seeded in a clear 96-well plate at amount of 4×10^4 cells/well in 100 µL culture medium and treated adequately. GSH was measured after 24 h incubation with 6-OHDA. As follows, the medium was aspirated, and cells were washed with PBS (150 µL/well). Afterwards, wells were filled with 60 µL/well of a newly prepared cold lysis buffer (RQB buffer: the solution of 20 mM HCl, 5% TCA, 5 mM

DTPA, 10 mM L-ascorbic acid); next, the plates were agitated at 900 rpm for 5 min and centrifuged at 4000 rpm (5 min).

The lysates were subsequently transferred into two black 96-well plates with black bottom in the amount of 25 μL/well, namely '+NEM' and '−NEM'. Within the first plate '+NEM', 4 μL/well of freshly prepared 7.5 mM NEM in cold RQB buffer were added. Then, 40 μL/well of 1 M phosphate buffer (pH 7.0) were added into both plates and shaken for 5 min at 900 rpm. Next, 160 μL/well of cold 0.1 M phosphate buffer (pH 6.8) and 25 μL/well of newly prepared 0.5% OPA in methanol were pipetted into both plates and shaken at 900 rpm for 30 min. Fluorescence was measured at 355/430 nm. GSH concentration was determined by subtracting the fluorescence of the ('−NEM') plate from the fluorescence of the ('+NEM') plate, and GSH content was calculated with respect to protein content in each well.

4.11. Protein Assay

Protein content was assayed according to Lowry et al. [34].

4.12. Estimation of ROS Levels Using DHE Fluorescent Probe

Cells were handled as described above. Cells were seeded onto black 96-well plates with a clear bottom. The test was performed after 24 h incubation with 6-OHDA. Then, 100 μL/well of freshly prepared DHE working solution in PBS were added; the final concentration of the probe was equaled to 10 μM. The fluorescence was measured immediately at 37 °C, at 475/579 nm for 2 h, at 1 min intervals.

4.13. Evaluation of Changes of Mitochondrial Membrane Potential ($\Delta\Psi_m$)

Changes of mitochondrial membrane potential were evaluated using JC-1 (5,5,6,6-tetrachloro-1,1,3,3-tetraethylbenzimidazolylcarbocyanine iodide) with a Mitochondrial Membrane Potential Assay Kit. In mitochondria with high $\Delta\Psi_m$, JC-1 forms complexes with profound red fluorescence, whereas, in mitochondria that exhibit low $\Delta\Psi_m$ levels, JC-1 persists as monomers and exhibits exclusively green fluorescence.

The cells were seeded into black plates and treated as mentioned before. After 24 h incubation with drugs, the medium was discharged and replaced with $100\times$ diluted JC-1 reagent in complete culture medium and incubated for 30 min in a CO_2 incubator. Next, the plate was centrifuged at 4000 rpm for 5 min. Afterwards, the reagent was aspirated, and cells were washed with 150 μL/well Cell-Based Assay Buffer and centrifuged once more. After removing the supernatant, 100 μL/well of the new buffer was added. Fluorescence was measured at 540/570 nm (red fluorescence) and 485/535 nm (green fluorescence). The results were presented as a green to red fluorescence intensity ratio.

4.14. Mitochondrial Mass Assessment

Cells were seeded at the density of 2×10^5 cells/well onto a 24-well plate and cultured as stated before. Following 24-h exposure to 6-OHDA, the cells were trypsinized, counted, and transferred to separate Eppendorf tubes, and then centrifuged for 6 min at 3000 rpm. Subsequently, the supernatant was discharged, and the cells were washed with 1 mL of PBS and centrifuged again. Afterwards, 1 mL of 10 μM NAO solution in PBS was added into the samples, and incubated for 10 min in a CO_2 incubator at 37 °C. Next, the cells were centrifuged and the pellet was washed with PBS, and resuspended in 300 μL of PBS. Each sample was transferred into a 96-well black plate (100 μL/well; 3 repetitions). Fluorescence was measured at 435/535 nm. The results were determined in relation to the cell count.

4.15. Apoptosis and Necrosis Assay

To examine the type of cell death caused by the treatment, the levels of apoptosis and necrosis were assayed using RealTime-Glo™ Annexin V Apoptosis and Necrosis Assay. Cells were seeded into white 96-well plate with optical bottom, cultured, and treated adequately as stated above. After 24 h, 100 μL of the freshly prepared reagent was added

to each well according to manufacturer's protocol. The fluorescence and luminescence were measured immediately according to the protocol.

4.16. Statistical Analysis

Kruskal–Wallis test or Student *t*-test were performed to estimate the differences between positive control and NRNP [Ph]-treated cells; Mann–Whitney U test or paired sample Student *t*-test were performed to compare effects at different pH. $p \leq 0.05$ was considered statistically significant. Statistical analysis of the data was performed using a STATISTICA software package (version 13.3, StatSoft Inc. 2016, Tulsa, OK, USA, http://www.statsoft.com).

5. Conclusions

Our results demonstrate that NRNPs [pH] can protect SH-SY5Y cells from 6-OHDA induced damage in a cellular model of PD at pH 6.5, which may prevail in the brain in regions affected by PD. This finding may have potential importance for potential applications of NRNPs [pH] in preclinical and perhaps clinical studies.

Author Contributions: M.P. performed the experiments in the cellular system and their statistical evaluation and contributed with reagents/materials/analysis tools as well as participated in the preparation as well as the revision of the manuscript. I.S. carried out EPR measurements and interpreted the data. G.B. participated in the analysis and interpretation of the results; he also participated in the preparation and the revision of the manuscript. I.S.-B. was responsible for the concept of the study, supervision of experimental work, and had an important role in the analysis and interpretation of the results as well as in the preparation and revision of the manuscript. She was also responsible for providing the funding for the study. All authors have read and agreed to the published version of the manuscript.

Institutional Review Board Statement: Not applicable.

Informed Consent Statement: Not applicable.

Data Availability Statement: Data supporting the results of this study shall, upon appropriate request, be available from the corresponding author.

Conflicts of Interest: The authors declare no conflict of interest.

Sample Availability: Samples of the compounds are not available from the authors.

References

1. Armstrong, M.J.; Okun, M.S. Diagnosis and Treatment of Parkinson Disease: A Review. *J. Am. Med. Assoc.* **2020**, *323*, 548–560. [CrossRef] [PubMed]
2. Blanco, E.; Shen, H.; Ferrari, M. Principles of nanoparticle design for overcoming biological barriers to drug delivery. *Nat. Biotechnol.* **2015**, *33*, 941–951. [CrossRef] [PubMed]
3. Sims, C.M.; Hanna, S.K.; Heller, D.A.; Horoszko, C.P.; Johnson, M.E.; Montoro Bustos, A.R.; Reipa, V.; Riley, K.R.; Nelson, B.C. Redox-active nanomaterials for nanomedicine applications. *Nanoscale* **2017**, *9*, 15226–15251. [CrossRef] [PubMed]
4. Nagasaki, Y. Design and application of redox polymers for nanomedicine. *Polym. J.* **2018**, *50*, 821–836. [CrossRef]
5. Guo, X.; Cheng, Y.; Zhao, X.; Luo, Y.; Chen, J.; Yuan, W.E. Advances in redox-responsive drug delivery systems of tumor microenvironment. *J. Nanobiotechnol.* **2018**, *16*, 74. [CrossRef]
6. Jiang, Z.; Thayumanava, S. Disulfide-Containing Macromolecules for Therapeutic Delivery. *Israel J. Chem.* **2020**, *60*, 132–139. [CrossRef]
7. Yang, D.S.; Yang, Y.H.; Zhou, Y.; Yu, L.L.; Wang, R.H.; Di, B.; Niu, M.M. A Redox-Triggered Bispecific Supramolecular Nanomedicine Based on Peptide Self-Assembly for High-Efficacy and Low-Toxic Cancer Therapy. *Adv. Funct. Mater.* **2020**, *30*, 1904969. [CrossRef]

8. Hu, Q.; Katti, P.S.; Gu, Z. Enzyme-responsive nanomaterials for controlled drug delivery. *Nanoscale* **2014**, *6*, 12273–12286. [CrossRef]

9. Sahle, F.F.; Gulfam, M.; Lowe, T.L. Design strategies for physical-stimuli-responsive programmable nanotherapeutics. *Drug Discov. Today* **2018**, *23*, 992–1006. [CrossRef]

10. Gao, W.; Chan, J.M.; Farokhzad, O.C. pH-Responsive nanoparticles for drug delivery. *Mol. Pharm.* **2010**, *7*, 1913–1920. [CrossRef]

11. Deirram, N.; Zhang, C.; Kermaniyan, S.S.; Johnston, A.P.R.; Such, G.K. pH-Responsive Polymer Nanoparticles for Drug Delivery. *Macromol. Rapid Commun.* **2019**, *40*, e1800917. [CrossRef] [PubMed]

12. Sadowska-Bartosz, I.; Bartosz, G. Redox nanoparticles: Synthesis, properties and perspectives of use for treatment of neurodegenerative diseases. *J. Nanobiotechnol.* **2018**, *16*, 87. [CrossRef] [PubMed]

13. Pichla, M.; Bartosz, G.; Sadowska-Bartosz, I. The Antiaggregative and Antiamyloidogenic Properties of Nanoparticles: A Promising Tool for the Treatment and Diagnostics of Neurodegenerative Diseases. *Oxid. Med. Cell. Longev.* **2020**, *2020*, 3534570. [CrossRef] [PubMed]

14. Jankovic, J.; Tan, E.K. Parkinson's disease: Etiopathogenesis and treatment. *J. Neurol. Neurosurg. Psychiatry* **2020**, *91*, 795–808. [CrossRef] [PubMed]

15. Brand, M.D.; Nicholls, D.G. Assessing mitochondrial dysfunction in cells. *Biochem. J.* **2011**, *435*, 297–312, Erratum in **2011**, *437*, 575. [CrossRef] [PubMed]

16. Genoud, S.; Roberts, B.R.; Gunn, A.P.; Halliday, G.M.; Lewis, S.J.G.; Ball, H.J.; Hare, D.J.; Double, K.L. Subcellular compartmentalisation of copper, iron, manganese, and zinc in the Parkinson's disease brain. *Metallomics* **2017**, *9*, 1447–1455. [CrossRef]

17. Yoshitomi, T.; Miyamoto, D.; Nagasaki, Y. Design of core–shell-type nanoparticles carrying stable radicals in the core. *Biomacromolecules* **2009**, *10*, 596–601. [CrossRef]

18. Yoshitomi, T.; Hirayama, A.; Nagasaki, Y. The ROS scavenging and renal protective effects of pH-responsive nitroxide radical-containing nanoparticles. *Biomaterials* **2011**, *32*, 8021–8028. [CrossRef] [PubMed]

19. Vong, L.B.; Nagasaki, Y. Combination Treatment of Murine Colon Cancer with Doxorubicin and Redox Nanoparticles. *Mol. Pharm.* **2016**, *13*, 449–455. [CrossRef]

20. Boonruamkaew, P.; Chonpathompikunlert, P.; Vong, L.B.; Sakaue, S.; Tomidokoro, Y.; Ishii, K.; Tamaoka, A.; Nagasaki, Y. Chronic treatment with a smart antioxidative nanoparticle for inhibition of amyloid plaque propagation in Tg2576 mouse model of Alzheimer's disease. *Sci. Rep.* **2017**, *7*, 3785. [CrossRef]

21. Pichla, M.; Pulaski, Ł.; Kania, K.D.; Stefaniuk, I.; Cieniek, B.; Pieńkowska, N.; Bartosz, G.; Sadowska-Bartosz, I. Nitroxide Radical-Containing Redox Nanoparticles Protect Neuroblastoma SH-SY5Y Cells against 6-Hydroxydopamine Toxicity. *Oxid. Med. Cell. Longev.* **2020**, *2020*, 9260748. [CrossRef] [PubMed]

22. Maiti, P.; Manna, J.; Dunbar, G.L. Current understanding of the molecular mechanisms in Parkinson's disease: Targets for potential treatments. *Transl. Neurodegener.* **2017**, *6*, 28. [CrossRef] [PubMed]

23. Zeng, X.S.; Geng, W.S.; Jia, J.J.; Chen, L.; Zhang, P.P. Cellular and Molecular Basis of Neurodegeneration in Parkinson Disease. *Front. Aging Neurosci.* **2018**, *10*, 109. [CrossRef] [PubMed]

24. Guo, J.D.; Zhao, X.; Li, Y.; Li, G.R.; Liu, X.L. Damage to dopaminergic neurons by oxidative stress in Parkinson's disease (Review). *Int. J. Mol. Med.* **2018**, *41*, 1817–1825. [CrossRef] [PubMed]

25. Trist, B.G.; Hare, D.J.; Double, K.L. Oxidative stress in the aging substantia nigra and the etiology of Parkinson's disease. *Aging Cell* **2019**, *18*, e13031. [CrossRef] [PubMed]

26. Simola, N.; Morelli, M.; Carta, A.R. The 6-hydroxydopamine model of Parkinson's disease. *Neurotox. Res.* **2007**, *11*, 151–167. [CrossRef] [PubMed]

27. Xicoy, H.; Wieringa, B.; Martens, G.J.M. The SH-SY5Y cell line in Parkinson's disease research: A systematic review. *Mol. Neurodegener.* **2017**, *12*, 10. [CrossRef]

28. Yoshitomi, T.; Suzuki, R.; Mamiya, T.; Matsui, H.; Hirayama, A.; Nagasaki, Y. pH-sensitive radical-containing nanoparticle (RNP) for the L-band-EPR imaging of low pH circumstances. *Bioconjug. Chem.* **2009**, *20*, 1792–1798. [CrossRef]

29. Tirmenstein, M.A.; Hu, C.X.; Scicchitano, M.S.; Narayanan, P.K.; McFarland, D.C.; Thomas, H.C.; Schwartz, L.W. Effects of 6-hydroxydopamine on mitochondrial function and glutathione status in SH-SY5Y human neuroblastoma cells. *Toxicol. In Vitro* **2005**, *19*, 471–479. [CrossRef]

30. Annesley, S.J.; Fisher, P.R. Mitochondria in Health and Disease. *Cells* **2019**, *8*, 680. [CrossRef]

31. Nunnari, J.; Suomalainen, A. Mitochondria: In sickness and in health. *Cell* **2012**, *148*, 1145–1159. [CrossRef] [PubMed]

32. Akiyama, Y.; Otsuka, H.; Nagasaki, Y.; Kato, M.; Kataoka, K. Selective synthesis of heterobifunctional poly(ethylene glycol) derivatives containing both mercapto and acetal terminals. *Bioconjug Chem.* **2000**, *11*, 947–950. [CrossRef]

33. Senft, A.P.; Dalton, T.P.; Shertzer, H.G. Determining glutathione and glutathione disulfide using the fluorescence probe *o*-phthalaldehyde. *Anal. Biochem.* **2000**, *280*, 80–86. [CrossRef] [PubMed]

34. Lowry, O.H.; Rosebrough, N.J.; Farr, A.L.; Randall, R.J. Protein measurement with the Folin phenol reagent. *J. Biol. Chem.* **1951**, *193*, 265–275. [CrossRef]

4. **Pichla M**, Bartosz G, Pieńkowska N, Sadowska-Bartosz I. *Possible artefacts of antioxidant assays performed in the presence of nitroxides and nitroxide-containing nanoparticles*. Analytical Biochemistry 2020; 597:113698.

IF$_{2020}$: 2.877; **MNiSW: 70**

Possible artefacts of antioxidant assays performed in the presence of nitroxides and nitroxide-containing nanoparticles

Monika Pichla[a], Grzegorz Bartosz[b], Natalia Pieńkowska[a], Izabela Sadowska-Bartosz[a],**

[a] Department of Analytical Biochemistry, Institute of Food Technology and Nutrition, College of Natural Sciences, Rzeszow University, Zelwerowicza Street 4, 35-601, Rzeszow, Poland
[b] Department of Bioenergetics and Food Analysis, Institute of Food Technology and Nutrition, College of Natural Sciences, Rzeszow University, Zelwerowicza Street 4, 35-601, Rzeszow, Poland

ABSTRACT

Nitroxides and nitroxide-containing nanoparticles (RNP) are excellent antioxidants. However, they have relatively high reduction potentials, which make them behave like oxidants or show little activity in some antioxidant assays. We found that stable nitroxyl radicals (TEMPO and 4-amino-TEMPO) has low reactivity in the test of scavenging of 2,2′-azino-bis(3-ethylbenzthiazoline-6-sulfonic acid) radical (ABTS·). As a result, supplementation of blood plasma with nitroxides may decrease its total antioxidant capacity assayed with ABTS·. Nitroxides oxidize Fe^{2+} and in this way interfere with the ferric-Xylenol Orange assay of peroxides. Nitroxides as well as RNP directly oxidize glutathione and fluorogenic probes used for estimation of reactive oxygen species (ROS) (dihydro-2′7′-dichlorofluorescein diacetate, dihydroethidine and dihydrorhodamine 123) and thus produce artefacts in assays of glutathione and ROS in cell-free and cellular systems. These results point to the necessity of careful interpretation of antioxidant assays concerning nitroxides and RNP or performed in their presence.

1. Introduction

Cyclic nitroxides, also known as aminoxyls or nitroxyls, are stable free radicals stabilized by methyl groups at the α position in six-membered piperidine or five-membered pyrrolidine, pyrroline or oxazolidine ring structures. The methyl groups confer stability to the nitroxide radicals by preventing radical-radical dismutation and limiting access to reactive substances, which can quench free radicals [1]. Nitroxyls have long been utilized as biophysical tools for electron paramagnetic resonance (EPR) spectroscopy as spin probes, e.g. for estimation of membrane [2–4] and cytosol microviscosity [5,6]. Of importance is the possibility of introduction of a nitroxide moiety onto biologically important molecules and use of spin-labeled analogs of membrane phospholipids [3,7,8] or enzyme substrates [9,10]. Covalent spin labeling of macromolecules, especially site-specific, enables getting information about their segmental mobility [11]. Nitroxides are also used as contrast agents in NMR imaging [12].

Nitroxides have also antioxidant properties (including pseudoenzymatic superoxide dismutase activity, reactions with various free radicals, i.a., with products of water radiolysis, inhibition of Fenton reaction and lipid peroxidation as well as protection of proteins from glycoxidation, nitration and oxidation) [13–15]. They have been increasingly frequently studied at the cellular and whole-body levels in the context of protection against oxidative damage, ischemia-reperfusion injury and inflammation, ocular damage, neurodegenerative diseases, in chemoprevention and experimental cancer therapy, radioprotection as well as even weight control [1,16]. Furthermore, nitroxides are non-toxic as well as non-immunogenic for normal cells [16]. Nevertheless, prooxidative properties of nitroxides have been reported due, i.a., to the overproduction of hydrogen peroxide [17].

From the point of view of potential application in therapy, low-molecular-weight nitroxide compounds pose several problems such as nonspecific dispersion in normal tissues, preferential renal clearance and rapid reduction of nitroxide radicals to the corresponding hydroxylamines. Nitroxide radical compounds are also known to show dose-related hypotensive action accompanied by reflex tachycardia, increased skin temperature and seizures [18].

On the basis of nitroxides, redox nanoparticles containing polymer-

* Corresponding author. Department of Analytical Biochemistry, Institute of Food Technology and Nutrition, College of Natural Sciences, Rzeszow University, Rzeszow, Poland.
E-mail addresses: monika.pichla@outlook.com (M. Pichla), gbartosz@ur.edu.pl (G. Bartosz), natalia.pien@gmail.com (N. Pieńkowska), sadowska@ur.edu.pl (I. Sadowska-Bartosz).

List of abbreviations

ABTS˙	2,2′-azino-bis(3-ethylbenzthiazoline-6-sulfonic acid) radical
H₂DCF-DA	dihydro-2,7′-dichlorofluorescein diacetate
DHE	dihydroethidine
DHR123	dihydrorhodamine 123
DMEM + GlutaMax	Dulbecco's Modified Eagle Medium + GlutaMax
DMEM/F12	Dulbecco's Modified Eagle Medium Nutrient Mixture F-12
DMSO	dimethyl sulfoxide
DPBS	Dulbecco's Phosphate Buffered Saline
EPR	electron paramagnetic resonance
FOX	ferrous oxidation-Xylenol Orange
GSH	reduced glutathione
hi-FBS	heat-inactivated foetal bovine serum
NBT	Nitro Blue Tetrazolium
MEHP	Mono-(2-ethylhexyl) phthalate
OPA	*ortho*-phtalaldehyde
PBS	phosphate-buffered saline
RNP	nitroxide-containing nanoparticles
ROS	reactive oxygen species
TBBPA	tetrabromobisphenol A
4-amino-TEMPO	4-amino-2,2,6,6-tetramethylpiperidine-1-oxyl
TEMPO	2,2,6,6-tetramethylpiperidine-1-oxyl

---

bound nitroxide residues have been invented and demonstrated to be more efficient as candidate therapeutic antioxidants than free nitroxides [19,20]. Nitroxide radical-containing nanoparticles show, inter alia, high safety, long blood circulation (half-life of RNP was reported to be 600 min, i.e. 2400-times longer than that of a low-molecular weight nitroxide), magnetic resonance imaging and EPR imaging sensitive character and efficient therapeutic effects in experimental therapy of several diseases such as cerebral and renal ischemia reperfusions, ulcerative colitis and Alzheimer's disease models [21]. Thus, these nanoparticles seem to be promising as new nanotherapeutic materials.

Model studies in cellular and cell-free systems sometimes compare nitroxides with other antioxidants using standard tests and experimental setups. In many cases artefactual results may be obtained due to the specific properties of nitroxides. In this paper, we would like to point to several such cases where atypical behavior of nitroxides may lead to artefacts in antioxidant assays, in order to prevent misinterpretations of experiments involving free nitroxides and RNP. In this study, we used 2,2,6,6-tetramethylpiperidine-1-oxyl (TEMPO) (Fig. 1a) and 4-amino-2,2,6,6-tetramethylpiperidine-1-oxyl (4-amino-TEMPO) (Fig. 1b) and nitroxide radicals-containing redox nanoparticles [RNP; copolymer based on poly(styrene-co-malein anhydride) (Fig. 1c)].

2. Experimental section

2.1. Materials

Xylenol Orange (cat. no. chem*237045902*5g) was obtained from Polish Chemical Reagents (POCh, Gliwice, Poland); phosphate-buffered saline (PBS: 145 mM NaCl, 1.9 mM NaH₂PO₄, 8.1 mM Na₂HPO₄, cat. no. PBS405) was purchased from Lab Empire (Rzeszów, Poland). Dihydrorhodamine 123 (DHR123) (cat. no. D23806), dihydroethidine (DHE) (cat. no. D1168) and dihydro-2,7′-dichlorofluorescein diacetate (H₂DCF-DA, cat. no. D399) were obtained from Thermo Fisher Scientific (Waltham, MA, USA). All other reagents including the nitroxides, 2,2,6,6-tetramethylpiperidine 1-oxyl (TEMPO) and 4-amino-2,2,6,6-tetramethylpiperidine 1-oxyl (4-amino-TEMPO) were purchased from Sigma-Aldrich Corp. (St. Louis, MO, USA) and were of analytical grade. The radical-containing nanoparticles used for the initial experiments were synthesized in our Department according to the protocol described by the group of Prof. Nagasaki [22]. Electron paramagnetic resonance signals were quantified to estimate the amount of nitroxyl radicals in the nanoparticles. They were found to contain 27.6 nitroxyl radical residues per segment (molecular weight of a 7500 g/mol) (Pichla et al., submitted).

4-amino-TEMPO was dissolved in PBS (10 mM stock solution) and filtered using 0.22 μm filters when added to cells. TEMPO was dissolved in dimethyl sulfoxide (DMSO) (50 mM stock solution); the final highest concentration of DMSO in cell media was ≤0.02% and appropriate controls were made for DMSO effects.

Cell culture 75 cm² flasks (cat. no. 156499), transparent (cat. no. 161093) and black (cat. no. 165305) 96-well culture plates were obtained from Thermo Fisher Scientific (Waltham, MA, USA). Other sterile cell culture materials were provided by Nerbe (Winsen, Germany) and NEST Biotechnology (Wuxi, China).

The certified human neuroblastoma cell line SH-SY5Y (ATCC CRL-2266) as well as human lung normal fibroblast cell line [MRC-5 (CCL-171)] were purchased from American Type Culture Collection (ATCC, Rockville, MD, USA). Dulbecco's Modified Eagle Medium Nutrient Mixture F-12 (DMEM/F12) without Phenol Red (cat. no. 11039–021), Dulbecco's Phosphate Buffered Saline 1 × with Ca²⁺ and Mg²⁺ ions, Geltrex™ LDEV-Free Reduced Growth Factor Basement Membrane Matrix (cat. no. A1413202), Dulbecco's Modified Eagle Medium + GlutaMax (DMEM + GlutaMax) (cat. no. 21885–025) and Dulbecco's Phosphate Buffered Saline (DPBS) (cat. no. 14040–117)
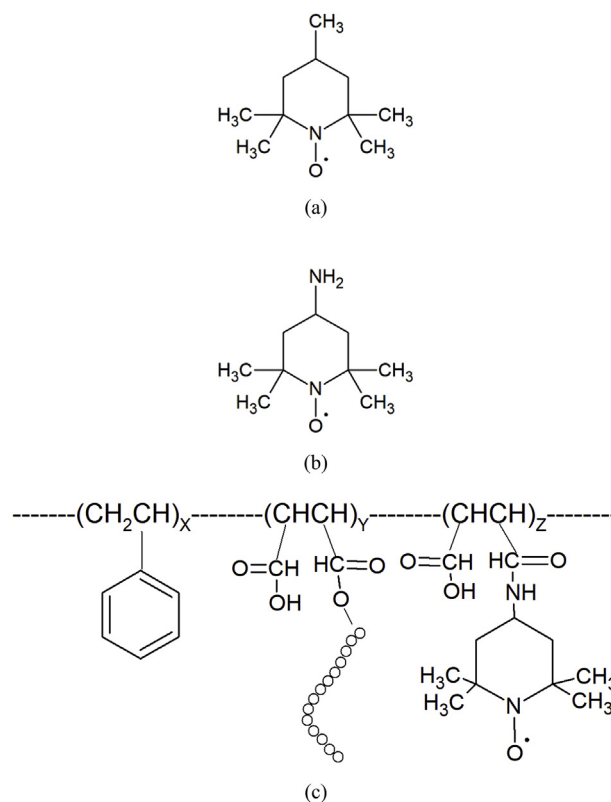

(a)

(b)

(c)

Fig. 1. Structures of studied antioxidant compounds: free nitroxide radicals, 2,2,6,6-tetramethylpiperidine-1-oxyl (TEMPO) (a), and 4-amino-2,2,6,6-tetramethylpiperidine-1-oxyl (4-amino-TEMPO) (b), and nitroxide radicals-containing redox nanoparticles [copolymer based on poly(styrene-co-malein anhydride); RNP] (c).

were obtained from Thermo Fisher Scientific (Waltham, MA, USA). Foetal bovine serum (FBS, cat. no. 04-001-1A), 10 × Trypsin-EDTA solution (cat. no. 03-051-5B), PBS without Ca^{2+} and Mg^{2+} ions (cat. no. 02-023-1A) and Penicillin-Streptomycin solution (cat. no. 03-031-1B) were from Biological Industries (Cromwell, CT, USA). Distilled water was purified using a Milli-Q system (Millipore, Bedford, MA, USA). Fluorometric and absorptiometric measurements were done in a Spark multimode microplate reader (Tecan Group Ltd., Männedorf, Switzerland). All measurements were performed at least in triplicate and repeated at least three times on different preparations.

2.2. Cell cultures

Human neuroblastoma cells were seeded in wells of a 96-well clear plate previously covered with 1% Geltrex™ LDEV-Free Reduced Growth Factor Basement Membrane Matrix (accordingly to the manufacturer's protocol). The neuroblastoma SH-SY5Y cell line was cultured in DMEM/F12 without Phenol Red, supplemented with 10% v/v heat-inactivated foetal bovine serum (hi-FBS) and 1% v/v penicillin and streptomycin solution. SH-SY5Y cells were maintained at 37 °C in 5% carbon dioxide and 95% humidity. Medium was changed twice a week and cells were passaged at about 80% confluence. For all studies, cells up to 14th passage were used.

Human Foetal Lung Fibroblast Cells (MRC-5 Line) were cultured in DMEM + GlutaMax supplemented with 1% v/v penicillin and streptomycin solution and 10% hi-FBS. MRC-5 cells were incubated at 37 °C under 5% carbon dioxide and 95 °C humidity. Fibroblasts were passaged at about 85% confluence.

The cell morphology was examined under an inverted Zeiss Primo Vert microscope with phase contrast (Oberkochen, Germany). Viability was estimated by Trypan Blue exclusion test. Cells were counted using a Thoma hemocytometer (Superior Marienfeld, Lauda-Königshofen, Germany).

2.3. Ethical approval of experiments with human blood

The study was approved by the Bioethics Committee of the University of Lodz (Permit No. KBBN-UŁ/I/3/2013).

2.4. Preparation of human blood plasma

Eight ml of peripheral blood from a healthy donor (lab volunteer, a 42-year-old woman; I. Sadowska-Bartosz) was collected in Citrate Tubes containing 3.2% buffered sodium citrate solution and used within the day of collection. Plasma was obtained by centrifugation at 3000 rpm, at 4 °C for 10 min.

2.5. ABTS˙ scavenging assay

2,2′-Azino-bis(3-ethylbenzthiazoline-6-sulfonic acid) radical (ABTS˙) was prepared by oxidation of ABTS with potassium persulfate [23]. Appropriate amounts of nitroxides (2.5, 5, 7.5, 12.5, 20 and 50 μl of 1 mM stock solution/250 μl) were added to wells of a 96-well microplate containing 200 μl of ABTS˙ solution of absorbance of 1.0 at 734 nm and 0.1 M phosphate buffer, pH 7.0 (up to the total volume of 250 μl). After 10-min incubation at room temperature, decrease of absorbance was measured and compared with analogous decrease of absorbance induced by various amounts of Trolox. Standard curve obtained for the scavenging of Trolox enabled to express the ABTS˙ scavenging activity in mol Trolox equivalents/mol. This method has been used by us previously and was found to be highly reproducible. In this study, longer incubation time with ABTS˙ (10 min) was employed than previously [24].

2.6. Total antioxidant capacity (TAC) of blood plasma

Human blood plasma, obtained from a healthy volunteer, was pretreated with nitroxides (10 and 50 μM) and after 10 min incubation at room temperature, 4 μl of control or nitroxide-pretreated plasma was added to 200 μl of ABTS˙ solution in 0.1 M phosphate buffer, pH 7.0, in a well of a 96-well microplate, diluted so to have absorbance of 1.0 at 734 nm. After 10-min incubation at room temperature, decrease of absorbance was measured and compared with analogous decrease of absorbance induced by Trolox. Standard curve obtained with Trolox enabled to express the ABTS˙ scavenging activity in μM of Trolox equivalents.

2.7. Reaction with fluorogenic probes

Dihydro-2′,7′-dichlorofluorescein diacetate (H_2DCF-DA) (10 μM), dihydroethidine (DHE) (10 μM) or dihydrorhodamine 123 (DHR123) (1 μM) were added to solutions of RNP (10 and 50 μM), 4-amino-TEMPO (100 and 200 μM) and TEMPO (100 and 200 μM) in PBS [final concentration/well]. The probes' fluorescence was measured at excitation/emission wavelengths of 490/529 nm, 475/579 nm and 460/528 nm, respectively, for 120 min in 1 min intervals at 37 ± 0.5 °C, using a TECAN Spark Multiplate Reader. The fluorescence values of oxidation products of the probes over this period were calculated as "area under the curve" (sum of absorbance values recorded during the time of measurement).

The effect of studied nitroxides as well as RNP on the measurement of cellular ROS was studied by addition of freshly prepared H_2DCF-DA probe in PBS (final concentration of 10 μM) to SH-SY5Y cells (3.5×10^4 cells/well of a black 96-well plate with clear bottom) after 2 h preincubation with the nitroxides or RNP. The fluorescence was measured immediately at 37 ± 0.5 °C, at 490/529 nm for 2 h at 1 min intervals. In another experiment, antioxidants were added to MRC-5 fibroblasts grown in wells of a 96-well plate (7.5×10^3 cells/well) and subsequently fluorogenic probes (H_2DCF-DA, DHE as well as DHR123) were added to the final concentration of 5 μM. Fluorescence was measured as described above, without washing off the cells.

2.8. Assay for hydrogen peroxide (H_2O_2) generation

We used the assay described previously [25], based on estimation of H_2O_2 with Xylenol Orange (FOX; ferrous oxidation-Xylenol Orange assay) [26]. Briefly, 1 mM antioxidant (final) was incubated in PBS or in DMEM + GlutaMax cell culture medium at 37 ± 1 °C for 3 h and H_2O_2 generated was determined as follows: to 180 μl samples, 20 μl of Xylenol Orange reagent was added [2.5 mM Xylenol Orange/2.5 mM Mohr's salt ($Fe_2(NH_4)_2SO_4$; purity of 99.997%) in 1.1 M perchloric acid]. After 30-min incubation at room temperature, absorbance of the samples was measured at 560 nm. Catalase (10 μg/ml) was added to an additional set of samples 15 min before the end of incubation in order to check if the reaction product is H_2O_2. We found this assay reliable and reproducible.

2.9. Interaction of nitroxides with Nitro Blue Tetrazolium

100 μM Nitro Blue Tetrazolium (NBT) was allowed to react with nitroxides in PBS for up to 30 min and absorbance at 540 nm (maximum absorbance of formazan) was monitored.

2.10. Reaction with reduced glutathione (GSH)

Glutathione (100 μM) in PBS was reacted with nitroxides or RNP for various time intervals at room temperature. Then, the concentration of GSH was determined with *ortho*-phtalaldehyde (OPA) [27], as described previously [28].

The effect of nitroxides and RNP on intracellular glutathione was

studied by estimation of the content of GSH in neuroblastoma SH-SY5Y cells (4×10^4 cells per well of a 96-well plate) pretreated with these compounds at indicated concentrations for 2 h at 37 °C.

2.11. Statistical analysis

The error bars represent standard deviation. The paired Student's "t" test was performed to estimate differences between supplemented and control samples. Kruskal-Wallis test was also performed to determine differences between antioxidant-treated and non-treated cells in the GSH assay. $P \leq 0.05$ was considered as statistically significant. Statistical analysis of the data was performed using STATISTICA software package (version 13.3, StatSoft Inc. 2016, Tulsa, OK, USA, www. statsoft.com).

3. Results and discussion

Antioxidant can be defined as "any substance that delays, prevents or removes oxidative damage to a target molecule" [29]. Most low-molecular substances act as reductants, reducing free radicals and transient oxidation products of biomolecules. However, the standard reduction potentials of nitroxides are relatively high: apparent standard reduction potentials of TEMPO and 4-amino-TEMPO measured by cyclic voltammetry were 722 and 826 mV, respectively [30]. Therefore, the nitroxides oxidize rather than reduce such species as transition metal ions or ascorbyl radicals although they are able to reduce strongly oxidizing species, including hydroxyl or peroxyl radicals. The steric protection of the nitroxyl group of nitroxides by neighboring methyl groups imposes kinetic limitations on their reactivity. Due to both these facets, nitroxides behave unlike typical antioxidants in some cases.

The most popular assays of antioxidant activity rely on the reduction of test substances such as ABTS˙ and DPPH˙. Nitroxides (TEMPO and 4-amino-TEMPO) showed very low activity in the test of ABTS˙ scavenging. TEMPO as well as 4-amino-TEMPO showed molar activity of 0.069 ± 0.002 mol Trolox/mol and 0.046 ± 0.001 mol Trolox/mol. Apparently, the steric protection of the nitroxyl group seriously limits their reactivity with ABTS˙.

When blood plasma was preincubated with 10 μM and 50 μM nitroxides, its total antioxidant activity estimated by ABTS˙ scavenging, was decreased (Fig. 2). Nitroxides are known to oxidize such compounds as ascorbate and NADH [1,31,32]. A method of the assay of antioxidant capacity of blood plasma dependent on ascorbate, based on the reaction of TEMPO with plasma ascorbate, was proposed [32]. The low reactivity of nitroxides for ABTS˙ in conjunction with oxidation of ascorbate explains the small decrease of the total antioxidant activity of blood plasma (dependent partly on ascorbate) upon preincubation with nitroxides.

Assay of hydrogen peroxide production by nitroxides showed an apparent instantaneous production of H_2O_2 by nitroxides as high absorbance of Xylenol Orange was found in "zero time" samples. The method of determination of peroxide production employed is based on the comparison of the absorbance of a sample added with the Xylenol Orange reagent before and after incubation of an autoxidizable compound for an appropriate time interval. Fe^{2+} present in Xylenol Orange reagent is oxidized by peroxides to Fe^{3+}, which forms a colored complex with Xylenol Orange. The difference between the results for "zero time" and after incubation is a measure of peroxide production during the time of incubation. Small amounts of H_2O_2 were detected when nitroxides were incubated in the DMEM + GlutaMax medium (18.3 ± 6.0 μM for TEMPO, 8.0 ± 3.6 μM for 4-amino-TEMPO). However, nitroxides did not produce detectable amounts of H_2O_2 when incubated in PBS, as estimated by the difference in absorbance of the Fe^{3+}/Xylenol Orange complex before and after incubation, while compounds which do autoxidize generated considerable amounts of hydrogen peroxide also in PBS, in agreement with results of our previous study [25]. Interestingly, high absorbance of the Xylenol Orange

reagent was produced by nitroxides in the "zero-time" samples (absorbances of 1.9–2.1 and similar values after 3 h) while "typical" autoxidizing antioxidants produced absorbance values of 0.12–0.19 for "zero-time" samples and much higher values (1.4–1.8) after 3 h. Instantaneous production of high amounts of hydrogen peroxide by nitroxides in PBS is not feasible and has not been reported by other authors. As the assay is based on the oxidation of Fe^{2+} to and Fe^{3+} by hydrogen peroxide and involves a 30-min incubation of the reaction mixture with the Xylenol Orange reagent, we suspect that the nitroxides oxidize Fe^{2+} during incubation with the reagent. Identical high absorbance values were noted when cell media and nitroxides were added separately to the Xylenol Orange reagent, which supports this conclusion. Incubation of the reaction mixture with 0.1 μg/ml catalase for 10 min, before addition of the FOX reagent to nitroxide solutions in PBS, had no effect on the absorbance measured (Table 1) indicating that the absorbance was not due to the generation of hydrogen peroxide.

Often, antioxidant activity is estimated by the inhibition of generation of ROS, especially in cellular systems. We found that the nitroxides and RNP enhanced the rate of oxidation of three most popular fluorogenic probes used in such assays, H₂DCF-DA, DHE and DHR123 in a cell-free system (Fig. 3).

An apparent interpretation of the results presented in Fig. 3 is that nitroxides produce ROS in PBS. This, however, is hardly possible and the most probable explanation is the direct oxidation of the probes by nitroxides. Oxidation of DHR123 by nitroxides described here may explain our previous results on the protection of DHR123 against oxidation by peroxynitrite by TEMPO. We found a biphasic effect of TEMPO on DHR123 oxidation: protection by low concentrations of the nitroxide followed by loss of protection and increasing oxidation of DHR123 at higher concentrations of TEMPO [14]. Simply, higher TEMPO concentrations could directly oxidize the probe.

Direct oxidation of fluorescent probes used for ROS detection have been postulated for other compounds. H₂DCF-DA was reported to be oxidized directly by heme, hemoglobin, myoglobin and cytochrome *c*, without the intermediacy of ROS [33]. Trolox was also reported to oxidize H₂DCF-DA; this effect was ascribed to direct oxidation of dihydro-DCF, released under slightly alkaline conditions, by the phenoxyl radical of Trolox. Uric acid and another nitroxide, 4-amino-2,2,6,6-tetramethylpiperidine 1-oxyl (TEMPOL) were also observed to oxidize H₂DCF-DA [34]. Mono-(2-ethylhexyl) phthalate (MEHP) and tetrabromobisphenol A (TBBPA) increased the fluorescence of 6-carboxy-2′,7′-dichlorodihydrofluorescein diacetate in the absence of cells, but in the presence of serum as a source of hydrolytic activity, necessary to hydrolyze the ester and liberate the oxidizable 6-carboxy-2′,7′-dichlorodihydrofluorescein. Although autoxidation of MEHP and TBBPA could not be definitely excluded, the most probable explanation was the
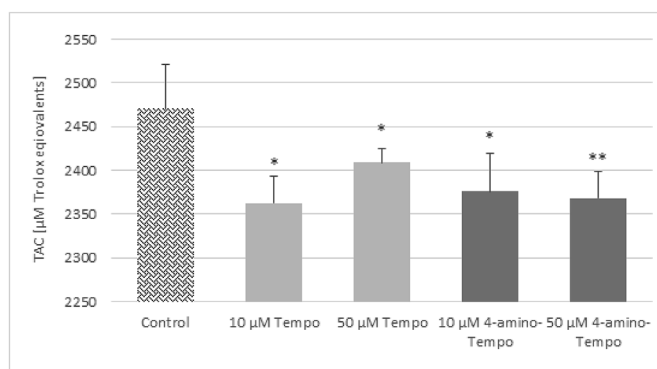

Fig. 2. Effect of nitroxide addition on Total antioxidant capacity (TAC) of blood plasma. Plasma was added with nitroxides to indicated final concentrations and incubated at room temperature for 10 min. Then the plasma was added to ABTS˙ solution in 0.1 M phosphate buffer, pH 7.0, and decrease in ABTS˙ absorbance was measured after next 10 min. P < 0.05, **P < 0.01; n = 6.

Table 1
Absorbance (560 nm) of samples in the FOX assay of hydrogen peroxide generation at time 0 and after 3 h incubation in phosphate-buffered saline (PBS). Concentration of compounds studied: 1 mM. Samples designed "+ *catalase*" were treated with 10 μg/ml catalase for 10 min prior to assay; n = 6.

Compound	Absorbance at time "0"	Absorbance after 3-h incubation in PBS
PBS	0.111 ± 0.002	0.115 ± 0.005
4-amino-TEMPO	2.013 ± 0.027	1.959 ± 0.047
4-amino-TEMPO + catalase		2.058 ± 0.062
TEMPO	1.954 ± 0.029	1.982 ± 0.056
TEMPO + catalase		1.943 ± 0.071
Epigallocatechin gallate	0.185 ± 0.003	1.873 ± 0.065
Quercetin	0.121 ± 0.033	1.393 ± 0.092
Propyl gallate	0.122 ± 0.018	1.684 ± 0.024
Pyrogallol	0.162 ± 0.032	1.572 ± 0.052

direct oxidation of 6-carboxy-2′,7′-dichlorodihydrofluorescein by these compounds [35].

In our opinion, some hydrolysis of H_2DCF-DA occurs spontaneously in aqueous solution or during storage so oxidation can occur even in the absence of any hydrolase. We observed enhancement of 4-amino-TEMPO and RNP oxidation of H_2DCF-DA and DHE (Fig. 3a,**b**); TEMPO increased the oxidation of DHR123, while 4-amino-TEMPO and RNP decreased it (Fig. 3c). It can be concluded from the presented results that 4-amino-TEMPO is more reactive than TEMPO for H_2DCF-DA, while the reverse is true for the reactivity of nitroxides for DHR123. Apparently, the electrostatic factor may condition this difference in reactivity: 4-amino-TEMPO is positively charged at physiological pH, and H_2DCF is charged negatively (which facilitates reaction with the probe), while DHR123 is charged positively (which may hamper the reaction with positively charges 4-amino-TEMPO). RNP oxidized DHE, showing some dose dependence. In the reactions of RNP with H_2DCF-DA and DHR123, antioxidant properties of the nanoparticles (perhaps contributed by the polymer shell) seem to dominate with the increase in RNP concentration and the oxidation of the probes was inhibited with increasing concentration of nanoparticles.

Oxidation of DHR123 was not inhibited by superoxide dismutase (10 μg/ml; not shown) indicating a lack of intermediacy of the superoxide radical. No reduction of NBT took place when this compound was incubated with nitroxides in PBS (not shown) confirming lack of generation of superoxide radical.

When nitroxides were added to fibroblasts and ROS generation was estimated in the cells, a trend for increased oxidation of the probes was noted, reaching statistical significance for TEMPO in the case of H_2DCF-DA (Fig. 4a) and for 4-amino-TEMPO in the case of DHE and DHR123 (Fig. 4b,**c**). RNP inhibited oxidation of the probes (Fig. 4a–c).

However, in an experiment in which the effect of RNP on SH-SY5Y cells treated with selected nitroxides or RNP, RNP and 4-amino-TEMPO produced an increase in the amount of the oxidation product, 5′,7′-dichlorofluorescein (DCF) (Fig. 5a). In Figs. 4 and 5a, the effect of RNP was quite different: in the case of fibroblasts they decreased the rate of probe oxidation, while in SH-SY5Y cells they augmented the oxidation of the probe. The difference may be due to the 2-hr preincubation of SH-SY5Y cells with RNP, which allowed for their penetration into the cells. Fibroblasts were not preincubated with RNP, so they were mostly not present inside the cells where the oxidation of the probe took place.

Increased probe oxidation was found in human fibroblast treated with TEMPO (Fig. 4a) and 4-amino-TEMPO (Fig. 4b and c) and can be attributed to the direct oxidation of the probes by nitroxides. A similar effect [a transient increase in the oxidation of H_2DCF-DA upon addition of higher concentrations of TEMPOL (1–3 mM)] has been reported for mouse lymphoma cells [33].
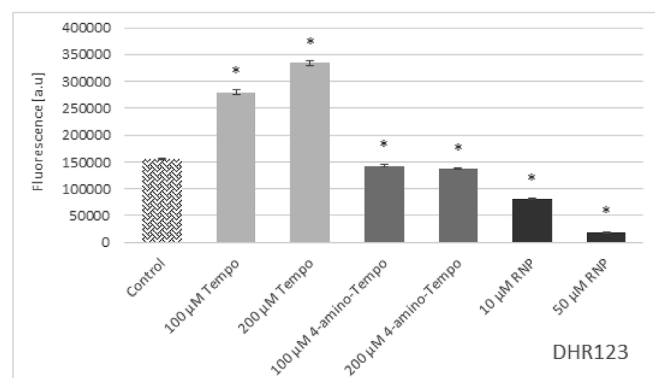
We found small autoxidation of glutathione during 2-h incubation in PBS (Fig. 6). Similar results (autoxidation of GSH during incubation in a cell-free system) have been reported previously [36]. Incubation of
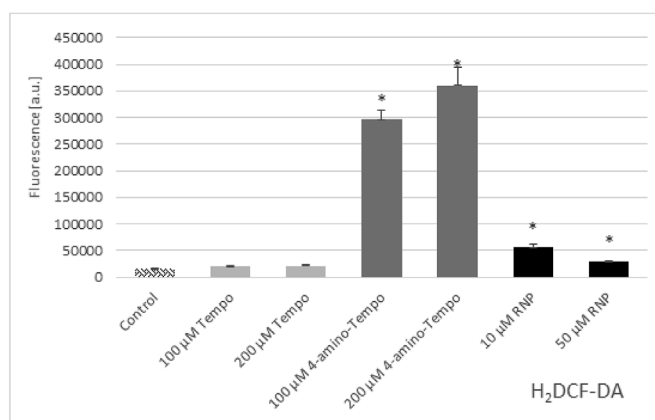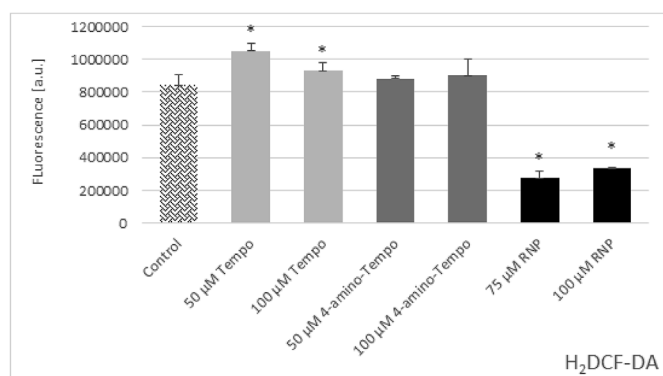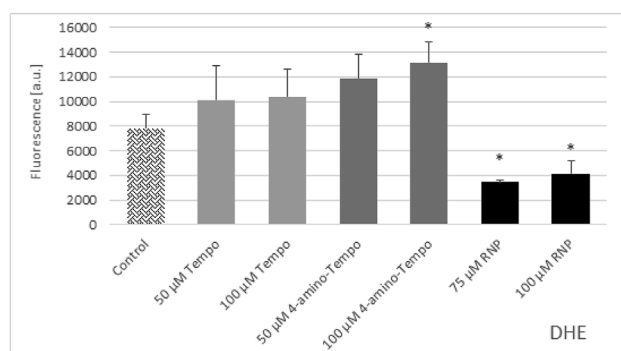

(a)
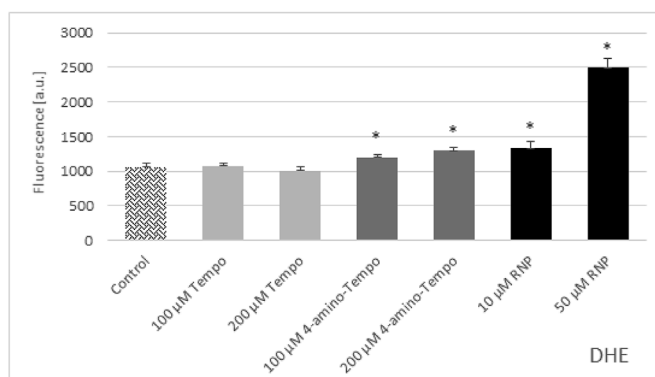
(b)

(c)

Fig. 3. Oxidation of fluorogenic probes: dihydro-2′,7′-dichlorofluorescein diacetate (H_2DCF-DA) (**a**), dihydroethidine (DHE) (**b**) and dihydrorhodamine 123 (DHR123) (**c**) by nitroxides and redox nanoparticles (RNP) in PBS, at room temperature. Probe concentration: 10 μM (H_2DCF-DA and DHE) or 1 μM (DHR123). *$P < 0.05$; n = 9.

glutathione with the nitroxides resulted in a time-and concentration dependent loss of GSH. RNP had an analogous effect (Fig. 6). Nitroxides are known to be able to oxidize thiols, albeit at lower rates [37,38].

In SH-SY5Y cells RNP decreased also GSH level while nitroxides increased it (Fig. 5b). This result is intriguing. We observed an increase in the concentration of GSH in SH-SY5Y cells treated with 6-hydroxydopamine, preceded by a decrease in GSH concentration (Pichla et al., submitted). Such a phenomenon has been observed previously and ascribed to an overcompensatory GSH synthesis caused by oxidant-increased expression of the GSH biosynthesis genes, coding for

(a)

(b)
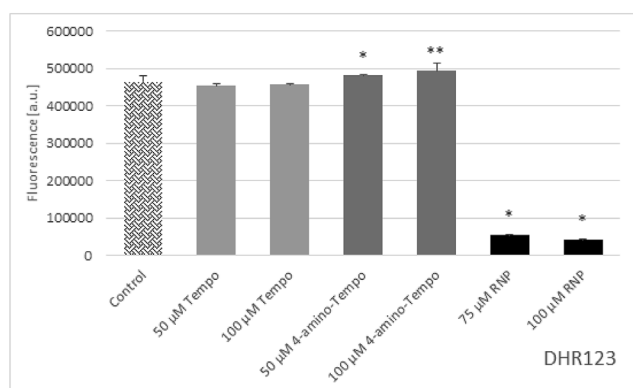
(c)

Fig. 4. Oxidation of fluorogenic probes: dihydro-2′,7′-dichlorofluorescein diacetate (H₂DCF-DA) (**a**), dihydroethidine (DHE) (**b**) and dihydrorhodamine 123 (DHR123) (**c**) in nitroxide-treated fibroblasts. The probes were added to fibroblasts grown in DMEM + GlutaMax medium supplemented with 1% v/v penicillin and streptomycin solution and 10% hi-FBS to a final concentration of 5 μM. The fluorescence was measured for 2 h at 1 min intervals; the values on the plot represent the sum of fluorescence. *$P < 0.05$, **$P < 0.01$; $n = 9$.

glutamate cysteine ligase modifier and catalytic subunits [39]. We suggest that both decrease and increase of GSH in cells treated with nitroxides and RNP reflect different phases of oxidative stress (GSH depletion and its overcompensatory synthesis), faster in the case of free nitroxides.

Thus, our results confirm this reactivity of nitroxides with respect to glutathione and demonstrate it for RNP, and propose explanation for the reported glutathione depletion in nitroxide-treated cells.

Redox nanoparticles are increasingly frequently used in research and proposed to be applied in therapy [19–22,40,41]. Although the

reactivity of nitroxide residues may be lowered when they are hidden inside RNP, eventually they become available to the environment and react like low-molecular weight nitroxides. We found that RNP oxidized fluorogenic probes in the absence of cells (Fig. 3a and b), except for DHR123 (Fig. 3c) and in SH-SY5Y cells (Fig. 5a), reacted with GSH in a cell-free system (Fig. 6) and decreased GSH level in SH-SY5Y cells (Fig. 5b).

Nitroxides and RNP exhibit both antioxidant and prooxidant properties and, depending on system and reaction conditions, one of them may be predominant. Thus, a caution is needed when interpreting results of antioxidant assays concerning or performed in presence of nitroxides and nitroxide-containing nanoparticles since their antioxidant properties may not always be evident or prooxidant artefacts may be introduced.

In summary, nitroxides and RNP can (i) alter redox equilibrium of cells by oxidizing intracellular antioxidants, including GSH, and (ii) introduce artefacts in the assay of oxidative stress markers. Thus, (i) care should be also taken when using nitroxides as biophysical probes because they may modify the redox state of the cells studied and (ii) since, according to Ghezzi's classification of oxidative stress biomarkers [42], ROS level is a "type 0" biomarker, which may be a surrogate marker of diseases, it should be taken into account that nitroxides and RNP may artefactually elevate the measured values of this biomarker.

Author contributions

I. S.-B. was responsible for the concept of the study, design of experiments and supervision of experimental work, performed part of experiments as well as had a leading role in the analysis of the results and preparation of the manuscript. She was also responsible for providing the funding for the study; M. P. performed main part of experiments in the cellular system and their statistical evaluation as well as contributed reagents/materials/analysis tools; G. B. participated in the revision of the manuscript; N. P. took part in the execution of experiments. All authors have read and approved the final manuscript.

Funding sources

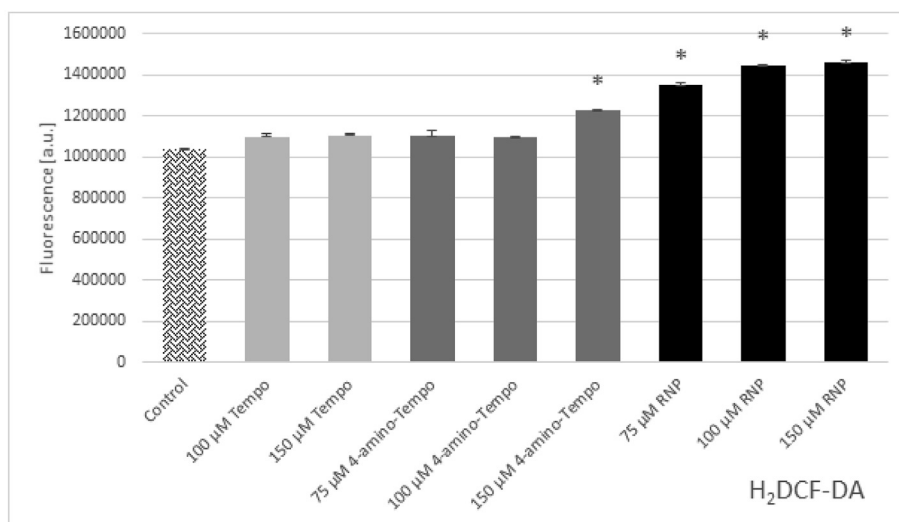### CRediT authorship contribution statement

Monika Pichla: Investigation, Formal analysis, Visualization. **Grzegorz Bartosz:** Writing - review & editing. **Natalia Pieńkowska:** Investigation. **Izabela Sadowska-Bartosz:** Conceptualization, Methodology, Formal analysis, Investigation, Resources, Writing - original draft, Supervision, Project administration, Funding acquisition.

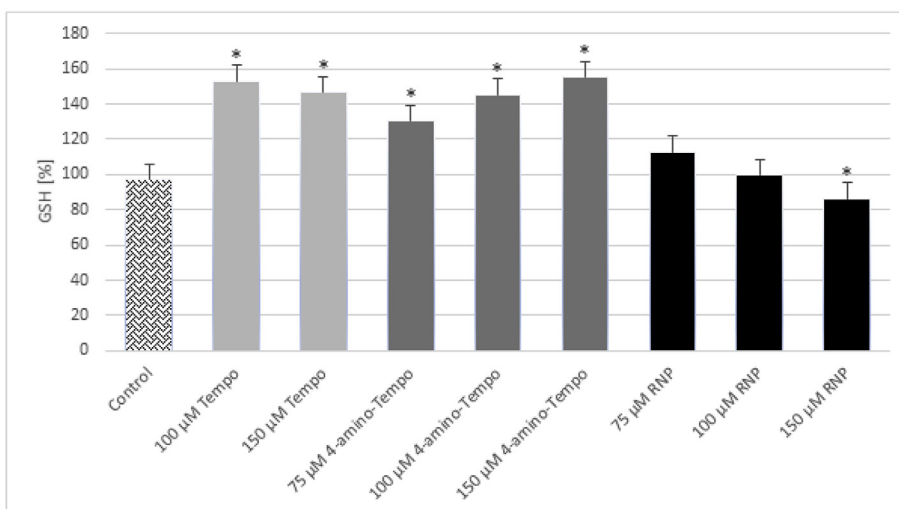### Declaration of competing interest

All authors declare that they have no conflicts of interest with respect to the research, authorship, and/or publication of this article.

Acknowledgments

(a)

(b)

Fig. 5. Effect of nitroxides and redox nanoparticles (RNP) on the fluorescence of dihydro-2′,7′-dichloro-fluorescein diacetate (H$_2$DCF-DA) (**a**) and reduced glutathione (GSH) level (**b**) in SH-SY5Y cells. The cells in DMEM/F12 without Phenol Red, supplemented with 10% v/v heat-inactivated foetal bovine serum (hi-FBS) and 1% v/v penicillin and streptomycin solution were preincubated with nitroxides or redox nanoparticles for 2 h, and added with the probes to a final concentration of 5 μM. The fluorescence was measured for 2 h at 1 min intervals; the values on the plot represent the sum of fluorescence values obtained. GSH was estimated after 1-h incubation with nitroxides or RNP. *P < 0.05; n = 6.
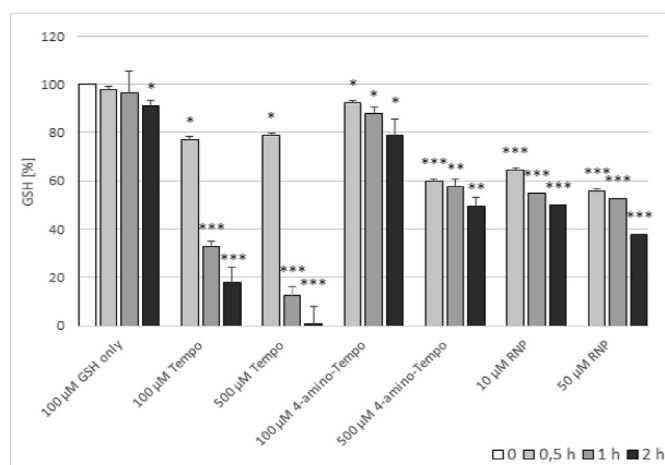
Fig. 6. Oxidation of glutathione (100 μM) by nitroxides and redox nanoparticles in PBS during incubation at room temperature. *P < 0.05, **P < 0.01, ***P < 0.001; n = 6.

References

[1] B.P. Soule, F. Hyodo, K. Matsumoto, N.L. Simone, J.A. Cook, M.C. Krishna, J.B. Mitchell, The chemistry and biology of nitroxide compounds, Free Radic. Biol. Med. 42 (2007) 1632–1650.

[2] S. Schreier, C.F. Polnaszek, I.C. Smith, Spin labels in membranes. Problems in practice, Biochim. Biophys. Acta 515 (4) (1978) 395–436.

[3] W.K. Subczynski, M. Pasenkiewicz-Gierula, J. Widomska, L. Mainali, M. Raguz, High cholesterol/low cholesterol: effects in biological membranes: a review, Cell Biochem. Biophys. 75 (3–4) (2017) 369–385, https://doi.org/10.1007/s12013-017-0792-7.

[4] A.M. Gennaro, Regarding the measurement of microviscosity in lipid bilayers by EPR, Biophys. Chem. 252 (2019) 106223, , https://doi.org/10.1016/j.bpc.2019.106223.

[5] G. Bartosz, W. Leyko, Aging of the erythrocyte. I. Increase in the microviscosity of cell interior as determined by the spin label method, Blut 41 (2) (1980) 131–136.

[6] V.I. Grishchenko, S.K.H. Mezhidov, V.A. Moiseev, O.A. Nardid, [The effect of temperature and concentrations of various substances on the microviscosity of erythrocyte cytosol], Biofizika 40 (1) (1995) 106–109.

[7] S.A. Dzuba, M.E. Kardash, Clustering of spin-labeled cholesterol analog diluted in bilayers of saturated and unsaturated phospholipids, Biochim. Biophys. Acta Biomembr. 1860 (12) (2018) 2527–2531, https://doi.org/10.1016/j.bbamem.2018.09.017.

[8] L. Mainali, M. Pasenkiewicz-Gierula, W.K. Subczynski, Formation of cholesterol bilayer domains precedes formation of cholesterol crystals in membranes made of

the major phospholipids of human eye lens fiber cell plasma membranes, Curr. Eye Res. 45 (2) (2020) 162–172, https://doi.org/10.1080/02713683.2019.1662058.

[9] C.S. Lai, J.Z. Zhang, J. Joseph, Spin-label assay for phospholipase A$_2$, Anal. Biochem. 172 (2) (1988) 397–402.

[10] L.G. Teixeira, L. Malavolta, P.A. Bersanetti, S. Schreier, A.K. Carmona, C.R. Nakaie, Paramagnetic bradykinin analogues as substrates for angiotensin I-converting enzyme: pharmacological and conformation studies, Bioorg. Chem. 69 (2016) 159–166, https://doi.org/10.1016/j.bioorg.2016.10.006.

[11] Y.E. Nesmelov, Protein structural dynamics revealed by site-directed spin labeling and multifrequency EPR, Methods Mol. Biol. 1084 (2014) 63–79, https://doi.org/10.1007/978-1-62703-658-0_4.

[12] F. Hyodo, B.P. Soule, K. Matsumoto, S. Matusmoto, J.A. Cook, E. Hyodo, A.L. Sowers, M.C. Krishna, J.B. Mitchell, Assessment of tissue redox status using metabolic responsive contrast agents and magnetic resonance imaging, J. Pharm. Pharmacol. 60 (8) (2008) 1049–1060, https://doi.org/10.1211/jpp.60.8.0011.

[13] M.C. Krishna, A. Russo, J.B. Mitchell, S. Goldstein, H. Dafni, A. Samuni, Do nitroxide antioxidants act as scavengers of O2-. or as SOD mimics? J. Biol. Chem. 271 (42) (1996) 26026–26031.

[14] I. Sadowska-Bartosz, A. Gajewska, J. Skolimowski, R. Szewczyk, G. Bartosz, Nitroxides protect against peroxynitrite-induced nitration and oxidation, Free Radic. Biol. Med. 89 (2015) 1165–1175.

[15] I. Sadowska-Bartosz, S. Galiniak, J. Skolimowski, I. Stefaniuk, G. Bartosz, Nitroxides prevent protein glycoxidation in vitro, Free Radic. Res. 49 (2015) 113–121.

[16] M. Lewandowski, K. Gwozdzinski, Nitroxides as antioxidants and anticancer drugs, Int. J. Mol. Sci. 18 (2017) pii: E2490.

[17] T. Offer, A. Russo, A. Samuni, The pro-oxidative activity of SOD and nitroxide SOD mimics, Faseb. J. 14 (9) (2000) 1215–1223.

[18] M. Shimizu, T. Yoshitomi, Y. Nagasaki, The behavior of ROS-scavenging nanoparticles in blood, J. Clin. Biochem. Nutr. 54 (3) (2014) 166–173.

[19] Y. Nagasaki, Nitroxide radicals and nanoparticles: a partnership for nanomedicine radical delivery, Ther. Deliv. 3 (2012) 165–179.

[20] I. Sadowska-Bartosz, G. Bartosz, Redox nanoparticles: synthesis, properties and perspectives of use for treatment of neurodegenerative diseases, J. Nanobiotechnol. 16 (2018) 87.

[21] T. Takahashi, A. Marushima, Y. Nagasaki, A. Hirayama, A. Muroi, S. Puentes, A. Mujagic, E. Ishikawa, A. Matsumura, Novel neuroprotection using antioxidant nanoparticles in a mouse model of head trauma, J. Trauma Acute Care Surg. (2020), https://doi.org/10.1097/TA.0000000000002617.

[22] T. Yoshitomi, D. Miyamoto, Y. Nagasaki, Design of core-shell-type nanoparticles carrying stable radicals in the core, Biomacromolecules 10 (2009) 596–601.

[23] R. Re, N. Pellegrini, A. Proteggente, A. Pannala, M. Yang, C. Rice-Evans, Antioxidant activity applying an improved ABTS radical cation decolorization assay, Free Radic. Biol. Med. 26 (1999) 1231–1237.

[24] M. Grzesik, K. Naparło, G. Bartosz, I. Sadowska-Bartosz, Antioxidant properties of catechins: comparison with other antioxidants, Food Chem. 241 (2018) 480–492, https://doi.org/10.1016/j.foodchem.2017.08.117.

[25] M. Grzesik, G. Bartosz, I. Stefaniuk, M. Pichla, J. Namieśnik, I. Sadowska-Bartosz, Dietary antioxidants as a source of hydrogen peroxide, Food Chem. 278 (2019) 692–699.

[26] C.A. Gay, J.M. Gebicki, Perchloric acid enhances sensitivity and reproducibility of the ferric-xylenol orange peroxide assay, Anal. Biochem. 304 (2002) 42–46.

[27] A.P. Senft, T.P. Dalton, H.G. Shertzer, Determining glutathione and glutathione disulfide using the fluorescence probe o-phthalaldehyde, Anal. Biochem. 280 (2000) 80–86.

[28] M. Pichla, J. Sroka, N. Pienkowska, K. Piwowarczyk, Z. Madeja, G. Bartosz, I. Sadowska-Bartosz, Metastatic prostate cancer cells are highly sensitive to 3-bromopyruvic acid, Life Sci. 227 (2019) 212–223.

[29] B. Halliwell, J.M.C. Gutteridge, Free Radicals in Biology and Medicine 4 Clarendon, Oxford, 2007.

[30] M.C. Krishna, D.A. Grahame, A. Samuni, J.B. Mitchell, A. Russo, Oxoammonium cation intermediate in the nitroxide-catalyzed dismutation of superoxide, Proc. Natl. Acad. Sci. U. S. A 89 (1992) 5537–5541.

[31] M. Yamato, K. Kawano, Y. Yamanaka, M. Saiga, K. Yamada, TEMPOL increases NAD (+) and improves redox imbalance in obese mice, Redox Biol 8 (2016) 316–322.

[32] L.L. Piehl, G.B. Facorro, M.G. Huarte, M.F. Desimone, G.J. Copello, L.E. Díaz, E.R. de Celis, Plasmatic antioxidant capacity due to ascorbate using TEMPO scavenging and electron spin resonance, Clin. Chim. Acta 359 (2005) 78–88.

[33] T. Ohashi, A. Mizutani, A. Murakami, S. Kojo, T. Ishii, S. Taketani, Rapid oxidation of dichlorodihydrofluorescin with heme and hemoproteins: formation of the fluorescein is independent of the generation of reactive oxygen species, FEBS Lett. 511 (2002) 21–27.

[34] J.F. Kalinich, N. Ramakrishnan, D.E. McClain, The antioxidant Trolox enhances the oxidation of 2',7'-dichlorofluorescin to 2',7'-dichlorofluorescein, Free Radic. Res. 26 (1997) 37–47.

[35] L.M. Tetz, P.W. Kamau, A.A. Cheng, J.D. Meeker, R. Loch-Caruso, Troubleshooting the production of reactive oxidant species, J. Pharmacol. Toxicol. Methods 67 (2013) 56–60.

[36] N. Hogg, The effect of cyst(e)ine on the auto-oxidation of homocysteine, Free Radic. Biol. Med. 27 (1999) 28–33.

[37] X. Guo, R.A. Mittelstaedt, L. Guo, J.G. Shaddock, R.H. Heflich, A.H. Bigger, M.M. Moore, N. Mei, T.E.M.P.O. Nitroxide, A genotoxic and oxidative stress inducer in cultured cells, Toxicol. Vitro 27 (2013) 1496–1502.

[38] E. Finkelstein, G.M. Rosen, E.J. Rauckman, Superoxide-dependent reduction of nitroxides by thiols, Biochim. Biophys. Acta 802 (1984) 90–98.

[39] M.A. Tirmenstein, C.X. Hu, M.S. Scicchitano, P.K. Narayanan, D.C. McFarland, H.C. Thomas, L.W. Schwartz, Effects of 6-hydroxydopamine on mitochondrial function and glutathione status in SH-SY5Y human neuroblastoma cells, Toxicol. Vitro 19 (4) (2005) 471–479.

[40] T. Mei, A. Kim, L.B. Vong, A. Marushima, S. Puentes, Y. Matsumaru, A. Matsumura, Y. Nagasaki, Encapsulation of tissue plasminogen activator in pH-sensitive self-assembled antioxidant nanoparticles for ischemic stroke treatment - synergistic effect of thrombolysis and antioxidant, Biomaterials 215 (2019) 119–209 2019.

[41] B. Shashni, Y. Nagasaki, Nitroxide radical-containing nanoparticles attenuate tumorigenic potential of triple negative breast cancer, Biomaterials 178 (2018) 48–62.

[42] P. Ghezzi, Environmental risk factors and their footprints in vivo - a proposal for the classification of oxidative stress biomarkers, Redox Biol. 31 (2020) 101442, , https://doi.org/10.1016/j.redox.2020.101442 Jan.